Nature-Based and Engineered Strategies for the Remediation of Nutrients and Emerging Contaminants in Stormwater Runoff

by

Aline Christine Bernegossi

A thesis submitted to the Graduate Faculty of
Auburn University
in partial fulfillment of the
requirements for the Degree of
Master of Science

Auburn, Alabama
August 9, 2025

Keywords: Stormwater runoff, Green infrastructure, Phytotoxicity, 6-PPD-quinone, Nutrient removal, Hybrid geotextile

Approved by

Dr. Shiqiang Zou, Chair, Assistant Professor of Civil and Environmental Engineering
Dr. Michael A. Perez, Associate Professor of Civil and Environmental Engineering
Dr. Jillian Maxcy-Brown, Assistant Professor of Civil and Environmental Engineering

Abstract

Stormwater runoff is a primary pathway for transporting pollutants into aquatic environments, including excess nutrients and pollutants of emerging concern (PECs) such as 6-PPD-quinone (6-PPDq), a toxic transformation product of the tire antioxidant 6-PPD. This study is divided into two parts that explore nature-based and engineered strategies to improve stormwater treatment performance. The first part assessed the phytotoxicity of 6-PPDq through germination bioassays and long-term exposure tests using three species commonly used in green infrastructure: *Rudbeckia hirta*, *Rumex crispus*, and *Trifolium pratense*. Germination assays were conducted at both environmentally relevant (1–100 μg/L) and elevated concentrations (200–3200 μg/L). *R. hirta* and *T. pratense* exhibited high germination rates and increased biomass at the highest concentrations, suggesting a hormetic effect and potential for phytoremediation. *T. pratense* produced up to four times more biomass than *R. hirta*, making it particularly suitable for stormwater applications. A 21-day soil exposure test with *T. pratense* confirmed its tolerance to 6-PPDq, with no significant reductions in growth across concentrations from 100 to 1600 μg/L. The second part evaluated the nutrient removal performance of an iron-modified geotextile as a passive treatment layer in infiltration systems. Three sequential column tests were conducted to compare setups with no geotextile, a standard geotextile, and a modified geotextile. The iron-dosed geotextile achieved up to 50% total phosphorus (TP) removal and improved retention across repeated dosing cycles. While total nitrogen (TN) removal remained modest (< 20%), slight improvements were observed over time. Together, these findings highlight the potential of pairing tolerant native vegetation with enhanced filter media to improve the efficiency of stormwater best management practices (BMPs). This integrated approach offers a scalable and minimally invasive strategy for managing nutrient and contaminant loads in urban runoff, particularly where retrofitting is preferred over full system reconstruction.

Acknowledgments

To God, my greatest guide, for illuminating and blessing my journey.

I would like to express my deepest gratitude to my advisor, Dr. Shiqiang (Nick) Zou, for accepting me as a Master's student and for his continued guidance, encouragement, and support throughout these two years. I am also sincerely thankful to my committee members, Dr. Perez and Dr. Maxcy-Brown, for their time, valuable insights, and contributions to this work.

I am grateful to the members of Dr. Zou's lab, Ao, David, Jiagen, Jason, Zilan, and Najibullah, for making this experience lighter and more enjoyable through their constant support and friendship.

This work was financially supported by the U.S. Environmental Protection Agency (USEPA) and the National Alliance for Water Innovation (NAWI), as well as through my position as a teaching assistant.

I also extend my sincere thanks to the Civil and Environmental Engineering administrative staff at Auburn University, especially Kate and Yury, for their kindness, dedication, and support that made everyday life easier.

To all the Auburn friends who supported me during this journey, Jessica, Lucas, Vivian, Marcus, Monica, Aidan, and Mohammad, thank you for encouraging me and listening when I needed it most. Long-term friends from FORM's, POVO, and LEAA were essential to my growth and motivation. I am also grateful to my cousin Rosane and my godson Arthur, who always knew how to bring me joy and remind me of home. I extend this gratitude to everyone, named or unnamed, who, in any way, contributed to this journey and helped me reach this milestone.

Finally, I dedicate this thesis to my beloved husband, Bruno, for being my partner, friend, and unwavering source of strength throughout every stage of this journey. And to my family, Elione (mamis), José Luis (papis), Agda, and Aninha, for your unconditional love, motivation, and constant support, was the foundation that sustained me, especially during the most challenging moments far from home.

Table of Contents

Abstract 2

Acknowledgments... 3

List of Tables 7

List of Supplementary Material Tables.. 8

List of Figures 9

List of Abbreviations 12

Research Motivation and Scope... 14

Chapter 1. The presence, toxicological effects, and treatment challenges of 6-PPD-quinone in the environment 18

1.1. Tire wear particles and the emergence of 6-PPD-quinone as an environmental concern 18

1.2. Environmental occurrence 23

1.3. Emerging Toxic Effects and Environmental Health Concerns of 6-PPDq....... 28

1.4. Treatment Challenges 31

Chapter 2: Evaluating the resistance of *Rudbeckia hirta*, *Rumex crispus*, and *Trifolium pratense* to germinate in the presence of 6-PPD-quinone. 34

2.1. Introduction.. 34

2.2. Materials and Methods.. 37

2.2.1. Chemicals.. 37

2.2.3. Germination test setup 38

2.2.4. Statistical Analyses 40

2.3. Results.. 41

2.3.1. Germination rate 41

2.3.2. Fresh biomass... 45

2.3.3. Hypocotyl and Radicle lengths 48

2.4. Discussion 50

2.5. Conclusion 53

Chapter 2 - Supplementary Material 55

Chapter 3: Long-Term Exposure Test: Assessing Extended Phytotoxicity in *Trifolium pratense* 57

3.1. Motivation 57

3.2. Materials and Methods 58

3.2.1. Chemicals and other materials 58

3.2.2. Long-term exposure test 59

3.2.3. Growth conditions and endpoints 60

3.2.4. Analysis Methods 62

3.3. Results and Discussions 63

3.4. Conclusion 68

Chapter 4: Nutrient Removal from Stormwater Runoff: Sources, Best Management Practices, and Iron-Modified Treatment Materials 69

4.1. Introduction 69

4.2. Phosphorus and Nitrogen Sources 71

4.3. Nutrient Control through Best Management Practices (BMPs) and Low Impact Development (LID): Processes, Performance, and Limitations. 73

4.4. Iron-enriched materials for nutrient removal 80

Chapter 5: Column Testing of Modified Geotextiles for Nutrient Removal from Stormwater Runoff 84

5.1. Introduction 84

5.2. Materials and Methods 86

5.2.1. Column Design and Material Composition 86

5.2.2. Experimental Setup: Blank and Dosed Conditions 90

5.2.3. Sampling and Analytical Procedures 91

5.3. Results and Discussion 92

5.3.1. Water Quality Parameters: pH, EC, TDS, Turbidity, and Temperature 92

5.3.2. Performance on Phosphorus and Nitrogen removal 101

5.4 Statistical and Comparative Evaluation 106

5.5. Conclusion 111

6. Concluding Remarks and Perspectives 113

7. References 115

List of Tables

Table 1. Reported Environmental Concentrations of 6-PPD-quinone Across Different Matrices and Locations 27

Table 2. 6-PPD-quinone toxicity to aquatic biota and plants. 29

Table 3. Treatment efficiency in removing 6-PPD-quinone 33

Table 4. Number of germinated seeds for *Rudbeckia hirta, Rumex crispus,* and *Trifolium pratense* after 4 and 7 days of exposure to 6-PPD-quinone at environmentally relevant concentrations (1 – 100 µg/L, blue background) and stress level concentrations (200 – 3200 µg/L, orange background). The initial number of seeds was 10. 41

Table 5. Plant water content (%) and dry-to-fresh weight (DW/FW) ratio across 6-PPD-quinone treatments. 65

Table 6. Experimental setup for nutrient removal tests using geotextile columns 90

Table 7. Water quality parameters (pH, electrical conductivity (EC), total dissolved solids (TDS), temperature, and turbidity) for blank test 2. 95

Table 8. Nutrient removal performance by BMP 111

List of Supplementary Material Tables

SM, Table 1: Tukey test p.values comparing Rudbeckia hirta fresh biomass after 7 days of 6-PPD-quinone exposure at non-environmental concentrations (200 – 3200 µg/L) with 95% confidence level. Welch F test in the case of unequal variances: F = 2.585, df = 69.96, p = 0.03331. 55

SM, Table 2: Tukey test p-values comparing Trifolium pratense fresh biomass after 7 days of 6-PPD-quinone exposure at environmentally relevant concentrations (1 – 100 µg/L) with 95% confidence level. Welch F test in the case of unequal variances: F = 4.362, df = 80.39, p = 0.001456..... 55

SM, Table 3: Tukey test p.values comparing Trifolium pratense fresh biomass after 7 days of 6-PPD-quinone exposure at non-environmental concentrations (200 – 3200 µg/L) with 95% of confidence level. Welch F test in the case of unequal variances: F = 4.826, df = 78.91, p = 0.0006685..... 55

SM, Table 4: SM, Table 2: Tukey test p.values comparing Rudbeckia hirta radicle after 7 days of 6-PPD-quinone exposure at non-environmental concentrations (200 – 3200 µg/L) with 95% of confidence level. Welch F test in the case of unequal variances: F = 4.69, df = 67.67, p = 0.009492..... 56

SM, Table 5: Tukey test p.values comparing Trifolium pratense hypocotyl after 7 days of 6-PPD-quinone exposure at environmentally relevant concentrations (1 – 100 µg/L) with 95% confidence level. Welch F test in the case of unequal variances: F = 12.92, df = 79.24, p = 3.402E-09..... 56

SM, Table 6: Tukey test p.values comparing Trifolium pratense hypocotyl after 7 days of 6-PPD-quinone exposure at non-environmental concentrations (200 – 3200 µg/L) with 95% confidence level. Welch F test in the case of unequal variances: F = 12.07, df = 77.28,, p = 1.186E-08..... 56

List of Figures

Figure 1. The emission of tire and road wire particles per capita (kg) per year. 19

Figure 2. Approximate composition of a passenger car tire (by weight). 20

Figure 3. Chemical structures of 6-PPD and 6-PPD-quinone, with molecular formula, molecular weights (g/mol), and log K_{ow}. Data from ITRC (2023). 21

Figure 4. Schematic representation of 6-PPD and 6-PPD-quinone (6-PPDq) environmental dispersion pathways, including typical concentration ranges reported in stormwater runoff, surface water, sediment, and soil. 24

Figure 5. Rudbeckia hirta, Rumex crispus, and Trifolium pratense distribution around the U.S. and Alabama. 36

Figure 6. Germination test setup for Rudbeckia hirta, Rumex crispus, and Trifolium pratense. 39

Figure 8. Mean germination rates (%) of (a) Rudbeckia hirta, (b) Rumex crispus, and (c) Trifolium pratense after 4 and 7 days of exposure to 6-PPDq at environmentally relevant concentrations (1 – 100 µg/L, blue background) and stress level concentrations (200 – 3200 µg/L, orange background). 45

Figure 9. Mean biomass (mg) of (a) Rudbeckia hirta and (b) Trifolium pratense after 7 days of exposure to 6-PPDq at environmentally relevant concentrations (1 – 100 µg/L, blue background) and stress level concentrations (200 – 3200 µg/L, orange background). 47

Figure 10. Mean hypocotyl length (mm, upper panel) and radicle length (mm, lower panel) for (a) Rudbeckia hirta and (b) Trifolium pratense after 7 days of exposure to 6-PPDq at environmentally relevant concentrations (1 – 100 µg/L, blue background) and stress level concentrations (200 – 3200 µg/L, orange background). 49

Figure 11. Seed setup in the substrate. (a) Trifolium pratense seeds; (b) placement depth of approximately 2 cm; (c) two seeds positioned per planting spot. 60

Figure 12. Representative T. pratense leaf morphology. a) Health leaf, b) deformation and asymmetry, and c) chlorosis or localized tissue damage. 61

Figure 13. Trifolium pratense fresh biomass after 21 days exposure to 6-PPD-quinone at environmentally relevant concentrations (100 µg/L, blue background) and stress level concentrations (200 – 1600 µg/L, orange background). 64

Figure 14. Shoot and root lengths of Trifolium pratense after 21 days of exposure to 6-PPD-quinone at environmentally relevant concentrations (100 µg/L, blue background) and stress level concentrations (200 – 1600 µg/L, orange background). 66

Figure 15. Nutrient transportation by stormwater runoff to the receiving water............. 70

Figure 16. Global distribution of phosphorus reserves.. 72

Figure 17. Overview of best management practice types applied for nutrient mitigation in stormwater runoff (n = 30 studies). 78

Figure 18. Geotextile function in best management practices (n = 30 studies)............... 79

Figure 19. Infiltration Trench column test design: a)no geotextile, b)with the standard geotextile layer, and c) with iron-modified geotextile layer. 88

Figure 20. Geotextile placement configurations used in the column tests: standard and modified geotextiles.. 89

Figure 21. Water quality parameters for blank Test 1: a) pH, b) electrical conductivity (EC), c) total dissolved solids (TDS), d) temperature, and e) turbidity.. 94

Figure 22. Influent and effluent pH for the dose Tests 1, 2, and 3. 97

Figure 23. Influent and effluent electrical conductivity (EC) for the dose Tests 1, 2, and 3. 98

Figure 24 .Influent and effluent total dissolved solids (TDS) for the dose Tests 1, 2, and 3. 99

Figure 25 .Influent and effluent temperature for the dose Test 1, 2, and 3.................... 100

Figure 26: Influent and effluentturbidity for the dose tests 1, 2, and 3.......................... 101

Figure 27. Nutrient removal performance over time for a) total phosphorus (TP) and b)total nitrogen (TN) in Blank Test 1... 102

Figure 28. Nutrient removal performance over time for a) total nitrogen (TN) and b) total phosphorus (TP) in Test 1 for NO geo, STD geo, and MOD geo treatments............................ 104

Figure 29. Nutrient removal performance over time for a) total nitrogen (TN) and b) total phosphorus (TP) in Test 2 for NO geo, STD geo, and MOD geo treatments............................ 105

Figure 30. Nutrient removal performance over time for a) total nitrogen (TN) and b) total phosphorus (TP) in Test 3 for NO geo, STD geo, and MOD geo treatments............................ 106

Figure 31. Overall total nitrogen and total phosphorus removal for NO geo, STD geo, and MOD geo treatments in Test 1. 107

Figure 32. Overall total nitrogen and total phosphorus removal for NO geo, STD geo, and MOD geo treatments in Test 2. 108

Figure 33. Overall total nitrogen and total phosphorus removal for NO geo, STD geo, and MOD geo treatments in Test 3. 109

List of Abbreviations

$(NH_4)_2SO_4$	Ammonium Sulfate
6-PPD	N-(1,3-dimethylbutyl)-N-`-phenyl-1,4-benzenediamine
6-PPDq	6-PPDquinone6-PPD-quinone
ANOVA	Analysis of Variance
AOPs	Advanced Oxidation Processes
BMPs	Best Management Practices
CWA	Clean Water Act
DI	Deionized water
DW	Dry Weight
EC	Electrical Conductivity
FW	Fresh Weight
GAC	Granular Activated Carbon
ITRC	Interstate Technology & Regulatory Council
KH_2PO_4	Potassium Phosphate Monobasic
LC-MS/MS	Liquid Chromatograph-tandem Mass Spectrometry
LID	Low Impact Development
Log K_{ow}	Octanol-Water Partition Coefficient
MOD	Modified
NO	No Frabricgeotextile
NTU	Nephelometric Turbidity Unit
PAC	Powdered Activated Carbon

PAHs	Polycyclic Aromatic Hydrocarbons Softeners
PECs	Pollutants of Emerging Concern
PM	Particulate Matter
PMS	Peroxymonosulfate
SD	Standard Deviation
SEM	Standard Error Oof Tthe Mean
STD	Standard
TMDL	Total Maximum Daily Load
TN	Total nitrogen
TP	Total phosphorus
TRWPs	Tire and Road Wear Particles
U.S. EPA	United States Environmental Protection Agency
U.S.	United States
USDA	United States Department of Agriculture
UV	Ultraviolet
WHC	Water Holding Capacity
WWTPs	Wastewater Treatment Plants

Research Motivation and Scope

Stormwater runoff is a complex and dynamic pathway for environmental pollution. As impervious surfaces grow, runoff carries various pollutants, including tire-related transformation products like 6-PPD-quinone (6-PPDq) and nutrients such as phosphorus (P) and nitrogen (N). These pollutants can negatively affect aquatic ecosystems and degrade water quality (Okaikue-Woodi et al., 2020; Tian et al., 2022). Although they originate from different sources, they are all mobilized during storm events, transported by stormwater runoff, persist in natural systems, and are not effectively removed by conventional treatment practices.

This thesis addresses these challenges by evaluating both nature-based and engineered strategies to improve contaminant removal at the source, with an emphasis on increasing the multifunctionality of green infrastructure. The main goal is to identify adaptable components, such as plant species and modified geotextiles, that can be integrated into a variety of best management practices (BMPs) to enhance their ability to manage nutrients and pollutants of emerging concerns in stormwater management systems.

The first part of the thesis (Chapters 1 to 3) focuses on 6-PPDq, a quinone derivative of the tire antioxidant 6-PPD, which is now globally detected in urban stormwater, surface waters, sediments, and soils. Formed during tire wear and atmospheric ozonation, 6-PPDq reaches concentrations capable of causing acute mortality in coho salmon at levels as low as 0.1 µg/L (ITRC, 2023; Nicomel & Li, 2023; Tian et al., 2022). While its ecotoxicity to aquatic organisms is increasingly documented, there is limited knowledge regarding its effects on plants, particularly species used in green infrastructure. To fill this gap, the thesis investigates the phytotoxicity and remediation potential of *Rudbeckia hirta* (U.S. native), *Rumex crispus* (non- native, but naturalized), and *Trifolium pratense* (non-native, but naturalized), using germination, growth, and biomass accumulation as key indicators (Castan et al., 2023; Grasse et al., 2023). As the selected plant species commonly occur along roadsides and can be incorporated into BMP systems, the findings support their use as tolerant native candidates for future evaluation of phytoremediation capacity.

The second part (Chapters 4 and 5) discusses nutrient pollution, a common and ongoing issue in stormwater management. Stormwater runoff nutrients from fertilizer, pet waste, and atmospheric deposition contribute to eutrophication and harmful algal blooms in receiving waters (Hopkins et al., 2017; Paerl et al., 2016). While BMPs, such as bioretention cells and permeable pavements, provide some pollutant control, their removal effectiveness is often inconsistent. To improve treatment capacity, this work investigates the use of a new iron-modified geotextile as a reactive filtration layer in infiltration systems. Through column experiments mimicking an infiltration trench, the study assesses phosphorus and nitrogen removal compared to the standard geotextile and the absence of geotextile, enhancing the functionality of structural BMP components (Luo et al., 2020).

Although these research components focus on different contaminant types, they are connected by a common goal: to develop integrated, multifunctional systems that combine ecological processes with material-based improvements. The nutrient removal study evaluates contaminant capture through engineered media, while the 6-PPDq component identifies plant species capable of tolerating high contaminant exposure for potential integration in green infrastructure. Together, these initiatives help create scalable, resilient BMPs for stormwater management. By addressing key knowledge gaps, one related to the environmental toxicity of a recently prioritized pollutant of emerging concern and the other to innovations in material design for nutrient retention, this thesis supports national efforts to expand green infrastructure (USEPA, 2025a) and contributes to broader strategies for adaptive, treatment-train runoff management (Georgia DNR & EPD, 2016).

Research Objectives and Specific Tasks

To address the challenges outlined above, this thesis is guided by the following research objectives and corresponding tasks outlined in Chapters 2, 3, and 5.

Chapter 2 – Phytotoxicity of 6-PPDquinone in Selected Species for Nature-Based Stormwater Treatment Systems

Research Objective

To evaluate the phytotoxic effects of environmentally relevant and elevated concentrations of 6-PPDquinone (6-PPDq) on plant species commonly used in nature-based stormwater best management practices (BMPs).

Specific Tasks

- Conduct germination assays on *Rudbeckia hirta*, *Rumex crispus*, and *Trifolium pratense* across a concentration gradient of 6-PPDq (1 to 3200 µg/L).
- Assess germination rate, root and shoot length, and biomass to determine dose-response relationships and potential hormetic effects.
- Identify plant species with the highest tolerance and potential for use in phytoremediation systems based on growth performance under contaminant exposure.

Chapter 3 – Long-Term Exposure Test: Assessing Extended Phytotoxicity in *Trifolium pratense*

Research Objective

To investigate the long-term tolerance of *T. pratense* to prolonged exposure to 6-PPDq under soil-based conditions, simulating more realistic environmental scenarios.

Specific Tasks

- Implement a 21-day exposure test using concentrations of 6-PPDq varying from 100 to 1600 µg/L in a controlled soil system.
- Monitor shoot growth, fresh biomass accumulation, and any morphological signs of phytotoxicity throughout the test period.

- Compare results with short-term germination data to evaluate delayed or cumulative effects of 6-PPDq on plant development.

Chapter 5 – Column Testing of Modified Geotextiles for Nutrient Removal from Stormwater Runoff

Research Objective

To assess the nutrient removal performance of a novel iron-dosed geotextile compared to standard geotextile and a no-fabric control in removing phosphorus and nitrogen from stormwater runoff.

Specific Tasks

- Fabricate and install column setups with three treatment conditions: no geotextile (NO), standard geotextile (STD), and modified iron-enriched geotextile (MOD).
- Conduct three sequential column tests under increasing nutrient loads and changing flow conditions to evaluate removal dynamics over time.
- Analyze effluent samples for total phosphorus (TP), total nitrogen (TN), and basic water quality parameters (pH, turbidity, EC, TDS, temperature).
- Determine the statistical significance of treatment effects and compare results with values reported in the literature for traditional BMPs.

Chapter 1. The presence, toxicological effects, and treatment challenges of 6-PPD-quinone in the environment

The following sections explore the environmental distribution of 6-PPD quinone, its toxic effects on biota, and the barriers to its effective removal from water systems.

1.1. Tire wear particles and the emergence of 6-PPD-quinone as an environmental concern

Tire wear and road-associated contaminants have emerged as a significant category of nonpoint source pollution in urbanized watersheds. As vehicles travel over road surfaces, tire treads abrade, releasing complex mixtures of particulate matter that contain various additives and degradation products into the environment. These tire and road wear particles (TRWPs) are now recognized as a major source of microplastic and chemical pollution in stormwater and runoff, with studies estimating that over 1 million metric tons of TRWPs are released annually worldwide Kole et al. (2017). The United States is the largest emitter of TRWPs, with more than 4.5 kg per capita per year. In contrast, Brazil, Japan, and Norway release less than half that amount (Figure 1) (Kole et al., 2017). TRWPs are generated through mechanical abrasion as tires interact with road surfaces during braking, acceleration, and steering. This process releases elongated, often cylindrical particles that can become encrusted with road dust, brake wear, and mineral debris, further increasing their environmental complexity and potential toxicity (Sommer et al., 2018). These particles contribute to microplastic pollution and act as carriers of heavy metals, polycyclic aromatic hydrocarbons (PAHs), and synthetic rubber additives (Sommer et al., 2018).

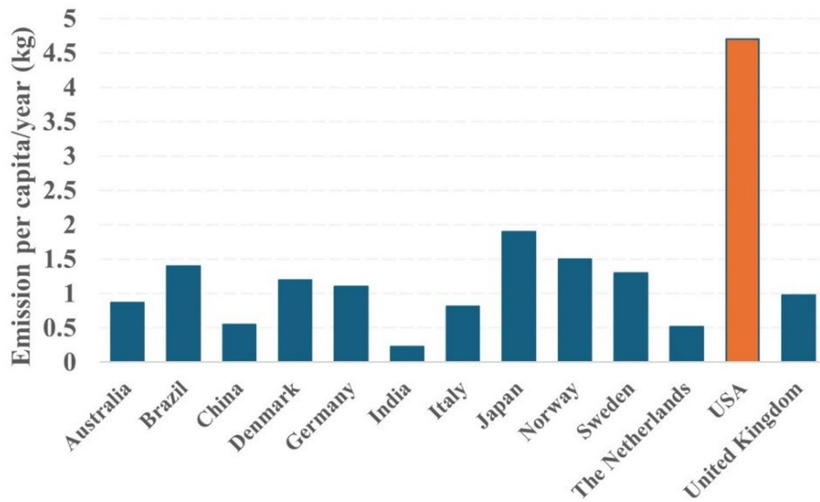

Figure 1. The emission of tire and road wire particles per capita (kg) per year. Data from Kole et al., 2017.

These emissions are driven by increasing transportation demand and vehicle use, with the U.S. exhibiting some of the highest per capita tire wear emissions. Unlike exhaust emissions (e.g., fuel combustion), which have been increasingly regulated over the past few decades, non-exhaust sources, such as tire and brake wear remain largely unregulated and difficult to control, contributing to their continued growth (Sommer et al., 2018). They are expected to remain dominant even with the global transition to electric vehicles (Sommer et al., 2018). Based on volume, tire abrasion particles may account for between 5% and 30% of particulate matter (PM) emissions from road transport in highly trafficked urban areas, making them a significant contributor to particulate pollution near roads (Giechaskiel et al., 2024). Moreover, due to their density, size, and adhesive surface, these particles accumulate in roadside soils and stormwater systems, contributing significantly to terrestrial and aquatic contamination.

The composition of passenger car tires is highly complex, consisting of natural and synthetic rubbers blended with chemical additives and fillers (Sommer et al., 2018). When tires endure physical stress during braking, acceleration, and turning, they release a complex mixture of organic and inorganic compounds. Notably, because many tire additives are not chemically bound to the rubber matrix, they are more likely to leach into the environment during abrasion processes (Sherman et al., 2024). As shown in Figure 2, rubber polymers (e.g., styrene-butadiene rubber and butadiene rubber) make up approximately 45% of a typical tire, while carbon black, silica, and chalk fillers account for 30–35%. Plasticizers and softeners, added to enhance flexibility, represent around 15%. Vulcanizing agents like sulfur and zinc oxide are included at 2–5% to improve elasticity and durability. TRWPs also contain a variety of chemicals, including antioxidants, zinc, extender oils, softeners, and synthetic antioxidants (Halle et al., 2020).

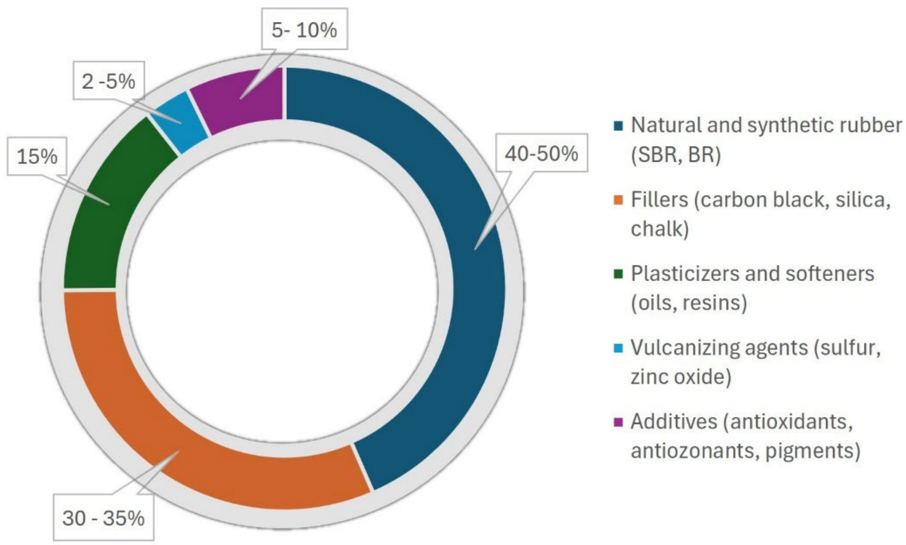

Figure 2. Approximate composition of a passenger car tire (by weight). Adapted from Sommer et al. (2018).

Among the most concerning compounds is N-(1,3-dimethylbutyl)-N'-phenyl-p-phenylenediamine (6-PPD), a rubber antioxidant widely used to enhance tire durability and reduce cracking (Fohet et al., 2023). Notably, up to 10% of the tire's mass may consist of additives such as antioxidants and antiozonants, including 6-PPD, which are not chemically bound to the polymer matrix and can leach into the environment through abrasion and weathering (Sommer et al., 2018). Upon exposure to ozone, 6-PPD transforms into 6-PPD-quinone (6-PPDq), a compound of increasing environmental concern due to its persistence and high toxicity to aquatic organisms (Tian et al., 2022). These characteristics highlight the need to understand the environmental fate of tire-derived compounds released into urban stormwater runoff.

Despite growing awareness of its toxicity, 6-PPD remains indispensable to the tire industry due to its unmatched effectiveness in preventing ozone-induced cracking, resisting thermal degradation, and prolonging tire life under harsh environmental conditions (Wagner et al., 2018). Although research is ongoing to develop safer alternatives, no compound has yet demonstrated equivalent performance while maintaining cost-effectiveness and process compatibility. Moreover, potential replacements must undergo rigorous testing to ensure they do not produce equally harmful transformation products. The development of viable substitutes, therefore, requires a multidisciplinary approach that balances mechanical performance, environmental safety, and industrial scalability (Muller et al., 2025).

The oxidative transformation of 6-PPD to 6-PPDq occurs rapidly in the presence of atmospheric ozone. This reaction happens on road surfaces, in the atmosphere, and during stormwater transport, contributing to the widespread presence of 6-PPDq in urban environments. The physicochemical properties of 6-PPD and 6-PPDq provide insight into their environmental behavior (Figure 3). Their relatively high log K_{ow} values (4.47 for 6-PPD and 3.98 for 6-PPDq) indicate a strong affinity for lipids versus water, suggesting both compounds can accumulate in tissues and biota (Tian et al., 2022). Its low volatility and chemical persistence further contribute to its widespread detection in urban water, sediment, and soil samples (Lane et al., 2024).

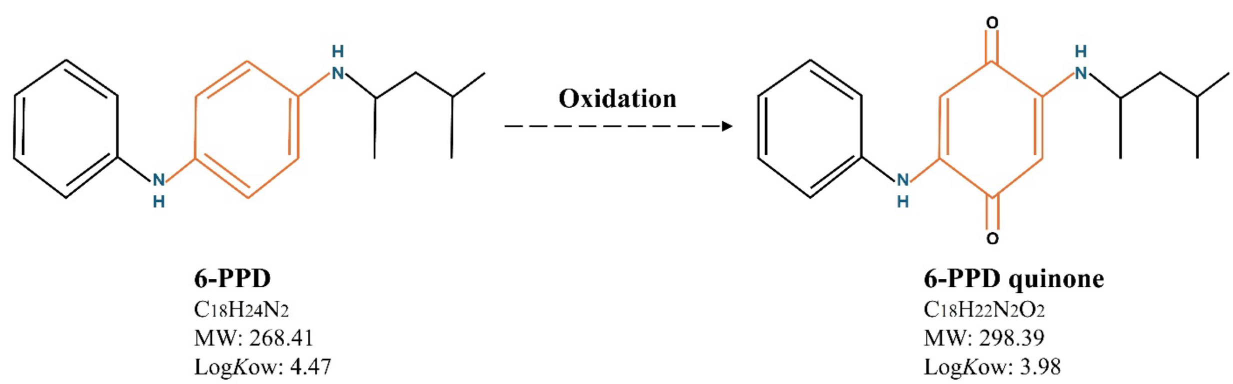

Figure 3. Chemical structures of 6-PPD and 6-PPD-quinone, with molecular formula, molecular weights (g/mol), and log K_{ow}. Data from ITRC (2023).

In addition to their hydrophobicity and strong sorption potential, the environmental fate of these compounds is also influenced by their solubility and ionization properties. Although 6-PPDq is less soluble in water (~38 µg/L) than its precursor 6-PPD (~500–2,000 µg/L), it is fully dissolved at concentrations typically detected in the environment, which facilitates its transport in stormwater and surface waters (ITRC, 2023). Moreover, its reported pK_a of 11.8 indicates that it remains predominantly non-ionized at typical environmental pH values (from 6 to 8), which enhances its lipophilicity, increases bioavailability, and supports its accumulation in organic-rich matrices such as sediments and plant roots (Grasse et al., 2023; Cao et al., 2022). Moderate solubility, chemical persistence, and low volatility contribute to its widespread environmental detection, making it a key target for stormwater runoff treatment and source control efforts.

Both compounds have been detected globally (Y. Jiang et al., 2024) with concentrations reaching up to 19 µg/L in Seattle, Washington, U.S. runoff (Tian et al., 2022) (see Section 1.2 for detailed 6-PPDq occurrence). These compounds are persistent and bioavailable, and can have adverse effects on aquatic ecosystems (Bohara et al., 2024; Y. Jiang et al., 2024). The compound has been linked to Urban Runoff Mortality Syndrome (URMS), a phenomenon responsible for acute mortality in coho salmon (*Oncorhynchus kisutch*) exposed to stormwater during migration (Tian et al., 2022). The LC_{50} for 6-PPDq in sensitive salmonids is reported to be as low as 8 µg/L, with chronic effects such as cardiotoxicity and behavioral impairments observed even at lower concentrations (Grasse et al., 2023; Nicomel & Li, 2023). Detailed ecotoxicological effects of 6-PPDq are described in Section 1.3. Thus, identifying effective removal methods for these pollutants is critical to mitigate their environmental impact.

Phytoremediation is a nature-based strategy that uses plants to remove, degrade, stabilize, or transform pollutants from soil and water through biological and biochemical processes. These mechanisms include phytoextraction (uptake and accumulation in plant tissues), phytodegradation (enzymatic breakdown within the plant), and rhizodegradation (microbial transformation in the root zone) (Aryal, 2024). This low-cost and environmentally friendly approach has shown potential for mitigating a variety of organic and inorganic contaminants in stormwater and urban runoff (Aryal, 2024). However, current research on the phytoremediation of 6-PPDq is limited, particularly regarding plant tolerance, uptake dynamics, and metabolic transformation capacity. Lettuce (*Lactuca sativa*) has demonstrated some capacity to translocate 6-PPD and 6-PPDq from roots to leaves, but most native or stormwater-appropriate species remain untested (Castan et al., 2023).

Despite growing awareness of 6-PPDq's ecotoxicity, most studies have focused on aquatic species. Less is known about its interactions with terrestrial plants, particularly those used in green infrastructure. In this context, this study aims to investigate the tolerance of three plant species commonly found in roadside systems, namely *Rudbeckia hirta*, *Rumex crispus*, and *Trifolium pratense*, when exposed to 6-PPDq, and indicate their suitability for phytoremediation applications. Specifically, the research examines whether (a) germination rate, (b) fresh biomass, and (c) radicle and hypocotyl length are statistically different from control conditions when subjected to a range of 6-PPDq concentrations.

This literature review first introduces tire wear particles and the environmental occurrence of 6-PPD and 6-PPDq. It then addresses 6-PPDq ecotoxicological effects, particularly to aquatic organisms and plants. It then explores the current understanding of phytoremediation potential and concludes with a discussion on in-situ treatment strategies such as bioretention and permeable pavements.

1.2. Environmental occurrence

6-PPD and its oxidation product, 6-PPDq, have been detected across different environmental compartments, including surface water, stormwater runoff, soil, sediment, and even atmospheric particles (Ihenetu et al., 2024). Their widespread occurrence is attributed to the continuous abrasion of tire tread on road surfaces, leading to the release of TRWPs containing unbound chemical additives (Figure 4). These compounds are mobilized primarily by stormwater runoff, especially in urban areas with high traffic density and extensive impervious surfaces.

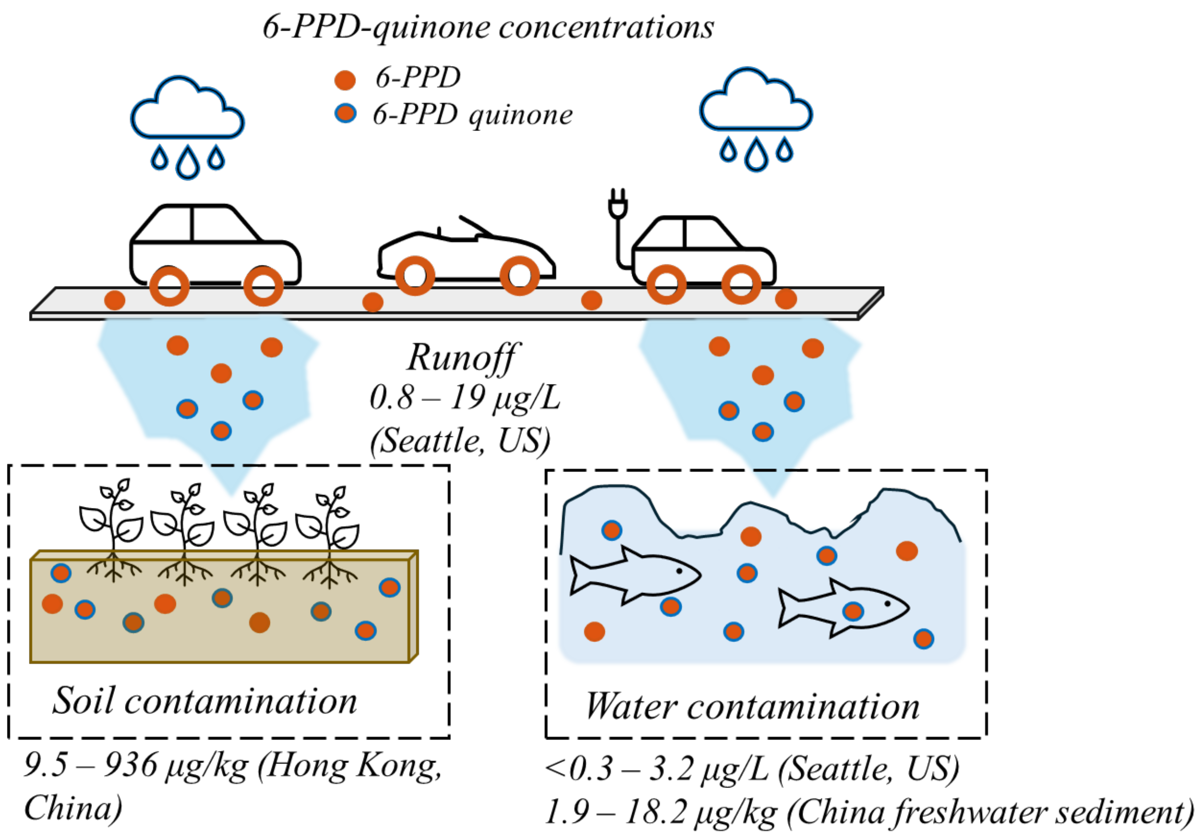

Figure 4. Schematic representation of 6-PPD and 6-PPD-quinone (6-PPDq) environmental dispersion pathways, including typical concentration ranges reported in stormwater runoff, surface water, sediment, and soil. Data from Tian et al. (2022) and Cao et al. (2022).

Stormwater runoff is the dominant transport pathway for 6-PPDq into aquatic systems. These compounds are generated at the road surface during tire abrasion and mobilized by precipitation events. Because 6-PPDq is already present on the surface of road dust and tire particles, the onset of rainfall rapidly transfers the compound into drainage systems. The concentrations of 6-PPDq in runoff and receiving waters are often elevated during and immediately after rainfall, as first-flush conditions mobilize recently deposited TRWPs (Shen et al., 2025; Zeng et al., 2023).

Several studies have quantified 6-PPDq concentrations in runoff and surface water under urban conditions. In Seattle, concentrations of 6-PPDq in roadside stormwater runoff have ranged from 0.8 to 19 µg/L, while in Los Angeles, U.S. values between 4.1 and 6.1 µg/L have been reported (Nicomel & Li, 2023; Tian et al., 2022). These concentrations are of environmental concern, as they often exceed known toxicity thresholds for sensitive aquatic organisms. In ecotoxicity studies, the lethal concentration of 50% (LC_{50}) is defined as the estimated concentration of a compound that causes mortality in 50% of an exposed population within a specific period. For example, the LC_{50} for coho salmon has been estimated at 0.095 µg/L, meaning even trace levels of 6-PPDq can cause mortality (Tian et al., 2022). Traffic density, roadway materials, and storm intensity also affect runoff composition. Y. Jiang et al. (2024) reported stress level concentrations of 6-PPDq in roadside stormwater runoff collected in industrialized and high-traffic regions of China, with strong correlations between road dust concentrations and measured runoff levels. Their mass loading estimates suggest that urban catchments can release several milligrams of 6-PPDq per hectare per storm event, underscoring the cumulative impact of frequent precipitation in dense metropolitan areas.

Beyond roadway drainage, 6-PPDq has also been detected in stormwater ponds, culverts, and detention basins, though often at lower concentrations than in direct runoff, likely due to partial sorption or dilution. Nicomel and Li (2023) synthesized findings from over a dozen field studies and concluded that 6-PPDq is now a globally observed stormwater contaminant, with reported concentrations in runoff from North America, China, Germany, and New Zealand.

While concentrations can spike during the onset of rain events, 6-PPDq remains detectable in baseflow and residual water bodies days after the storm, indicating its moderate persistence in aquatic systems. Its measured half-life in water ranges from 33 hours to over seven days, depending on temperature, pH, and light conditions, allowing its persistence long enough to affect aquatic organisms downstream (Hiki et al., 2021; ITRC, 2023). Therefore, stormwater runoff is a significant conduit for 6-PPDq and a strategic intervention point for environmental mitigation. Source control strategies such as porous pavements, vegetated swales, and bioretention systems have been proposed to intercept runoff before the compound reaches sensitive aquatic habitats.

Surface freshwater concentrations also reflect stormwater runoff inputs. In San Francisco, U.S. concentrations up to 3.5 µg/L have been measured in urban streams, while values of less than 0.3 to 3.2 µg/L were found in Seattle freshwater samples (Tian et al., 2022). These findings confirm the compound's persistence in aquatic systems, where dilution may occur but does not necessarily mitigate its toxic effects.

Soil and sediments near roads and stormwater management structures are long-term reservoirs for 6-PPDq. Roadside soils in Hong Kong, China have shown concentrations ranging from 9.5 to 936 µg/kg, while Japanese road dust samples reached up to 1238 µg/kg (Cao et al., 2022; Y. Jiang et al., 2024). In Guangzhou, China, 6-PPDq concentrations in road dust ranged from below the limit of detection (< 0.11 ng/g) to 1508 ng/g (Deng et al., 2022). Sediment concentrations of 6-PPDq have also been documented in multiple urban environments. In Chinese rivers, sediment levels have reached 1.9–18.2 µg/kg, and in Australian streams such as the Brisbane River, 6-PPDq has been confirmed in bottom sediments (Rauert et al., 2022). Further, sediment samples in the Don River (Canada) revealed concentrations ranging from 21 to 2300 ng/L in overlying waters, with evidence of long-term accumulation (Johannessen et al., 2022). These findings highlight the role of sediment as a long-term reservoir of 6-PPDq, reflecting its low degradability and strong sorption to particulate matter, and indicate that sediment can be a secondary source of contamination over time. To support environmental monitoring efforts, laboratory methods, such as ultrasonication and solvent extraction, have been developed to analyze 6-PPDq in solid and animal matrices (Kuo et al., 2025).

In addition to aquatic and terrestrial matrices, 6-PPDq has been detected in atmospheric particles. Although concentrations are much lower, typically in the pg/m^3 range, this finding suggests the potential for regional transport and dry deposition of the compound, particularly in densely trafficked urban corridors (Cao et al., 2022). Atmospheric presence is likely due to volatilization or abrasion processes that aerosolize fine TRWPs and their additives.

Table 1 summarizes the current known environmental concentrations of 6-PPDq based on recent monitoring studies.

Table 1. Reported Environmental Concentrations of 6-PPD-quinone Across Different Matrices and Locations

Matrix	Concentration Range	Location	Reference
Stormwater runoff	0.8 – 19 μg/L	Seattle, WA, U.S.	Tian et al. (2022)
Stormwater runoff	4.1 – 6.1 μg/L	Los Angeles, CA, U.S.	Tian et al. (2022)
Stormwater runoff	0.4 – 88 ng/L	Brisbane, Australia	Rauert et al. (2022)
Surface freshwater	<0.3 – 3.2 μg/L	Seattle, WA, U.S.	Tian et al. (2022)
Surface freshwater	1.0 – 3.5 μg/L	San Francisco, CA, U.S.	Tian et al. (2022)
Surface freshwater	21 – 2300 ng/L	Don River, Canada	Johannessen et al. (2022)
Freshwater sediment	1.9 – 18.2 μg/kg	Urban rivers, China	Cao et al. (2022)
Sediment	Detected	Brisbane River, Australia	Rauert et al. (2022)
Roadside soil	9.5 – 936 μg/kg	Hong Kong, China	Cao et al. (2022)
Road dust	116 – 1238 μg/kg	Japan	Hiki and Yamamoto (2022)
Road dust	< 0.11 – 1508 ng/g	Guangzhou, China	Chen et al. (2023)
Airborne particles	0.1 – 84 pg/m^3	Chinese megacities	Zhang et al. (2024)
WWTP influent	25 – 105 ng/L	Leipzig, Germany (snowmelt)	Seiwert et al. (2022)

The persistence of 6-PPDq across these matrices and its high detection frequency underscore the need for targeted monitoring and regulation. The USEPA has recognized 6-PPDq as a pollutants of emerging concern and is developing standardized testing methods, such as Method 1634 - Liquid Chromatography–Tandem Mass Spectrometry (LC-MS/MS), to support widespread monitoring in surface and stormwater (EPA, 2024). The widespread and multicomponent distribution of 6-PPDq further justifies integrated source-control strategies, including green infrastructure and phytoremediation, to prevent long-term ecological impacts.

1.3. Emerging Toxic Effects and Environmental Health Concerns of 6-PPDq

The toxicological understanding of 6-PPD and its oxidation product 6-PPD-quinone (6-PPDq) is still evolving, but their potential impacts on both environmental and human health have prompted growing concern. These compounds have been categorized as a contaminant with emerging concern pollutants of emerging concern by the U.S. Environmental Protection Agency (USEPA, 2024a) due to their acute toxicity to aquatic species. The most well-documented case is the mortality of coho salmon at concentrations below 0.1 μg/L, with a proposed freshwater screening level of 8.9 μg/L to protect aquatic biota. More recent data suggest that even environmentally relevant concentrations (1–10 μg/L) can cause sublethal and developmental impacts in early-life stages of sensitive fish species (Dixon & Goh, 2022; Greer et al., 2023; Tian et al., 2022).

Although human toxicity data remain limited, multiple exposure pathways are now recognized, including inhalation, ingestion of contaminated dust or food, and dermal contact (ITRC, 2023). Urban environments, roadways, and playgrounds that utilize recycled tire materials may pose elevated exposure risks. Alarmingly, both 6-PPD and 6-PPDq have been detected in human urine, with detection frequencies ranging from 60% to 100%, indicating widespread and chronic exposure (Ihenetu et al., 2024). Sherman et al. (2024) and Castan et al. (2023) have demonstrated the uptake and translocation of 6-PPD and 6-PPDq in commercial vegetables such as lettuce, with leaf concentrations reaching up to 0.75 μg/g. These findings suggest that crops irrigated or grown near polluted stormwater runoff may act as vectors of human exposure. Moreover, 6-PPDq has been identified in atmospheric particulate matter (PM2.5), and deposition modeling indicates potential for accumulation in the human respiratory tract (N. Jiang et al., 2024). Given the compound's lipophilicity ($\log K_{ow} \approx 4.3$) and potential to cross biological membranes, there is concern that it could reach the central nervous system or cross the placental barrier, although in vivo studies are still lacking (Hu et al., 2023; ITRC, 2023).

Despite these health concerns, most toxicological studies still focus on aquatic species, with fewer investigations on phytotoxicity and the role of vegetation in contaminant uptake (Table

2). These gaps are critical to address, especially considering the potential use of plants in remediation strategies.

Table 2. 6-PPD-quinone toxicity to aquatic biota and plants.

Species	Group	Test Type	LC_{50} (μg/L)	Reference
Salvelinus fontinalis (brook trout)	Fish	Acute	0.59	Brinkmann et al. (2022)
Oncorhynchus mykiss (rainbow trout)	Fish	Acute	1	Brinkmann et al. (2022)
Oncorhynchus kisutch (coho salmon)	Fish	Acute	0.79 ± 0.16	Tian et al. (2022)
Salvelinus fontinalis (brook trout, fry)	Fish	Acute	0.08	Philibert et al. (2024)
Gobiocypris rarus (rare minnow)	Fish	Acute	162 - 201	Di et al. (2022)
Oncorhynchus mykiss (rainbow trout)	Fish	Acute	1.66 - 4.31	Di et al. (2022)
Caenorhabditis elegans (roundworm)	Nematode	Chronic	> 100	Hua et al. (2023b)
Caenorhabditis elegans (roundworm)	Nematode	Chronic	n/a	Hua et al. (2023a)
Daphnia magna (water flea)	Crustacean	Acute	> 100	Hiki et al. (2021)
Hyalella azteca (amphipod)	Crustacean	Acute	> 100	Hiki et al. (2021)
Brachionus koreanus	Rotifer	Chronic	n/a	Maji et al. (2023)
Brachionus calyciflorus	Rotifer	12-day exposure	> 1000	Klauschies and Isanta-Navarro (2022)
Danio rerio (zebrafish, embryos)	Fish	Acute	308.67	Varshney et al. (2022)
Danio rerio (zebrafish, eggs)	Fish	Exposure	n/a	Grasse et al. (2023)
Lactuca sativa (lettuce)	Plant	Uptake/Translocation	n/a	Castan et al. (2023)
Eichhornia crassipes (water hyacinth)	Plant	Growth	< 10	Ge et al. (2024)
Brassica rapa L. ssp. (field mustard)	Plant	Growth	50 - 100	Liu, Yu, Li, et al. (2024)
Trifolium repens L. (white clover)	Plant	Growth	500	Wang et al. (2024)
Chlorella vulgaris (green microalga)	Algae	Growth	200 - 400	Liu, Yu, Shi, et al. (2024)

Although adult salmonids appear less sensitive at environmentally relevant concentrations, early life stages are particularly vulnerable. Dixon and Goh (2022) reported mortality, malformations, and blood-brain barrier disruption in juvenile salmon at concentrations below 10 µg/L. Similarly, Philibert et al. (2024) observed osmorespiratory compromise and altered blood chemistry in brook trout fry exposed to only 0.08 µg/L. Other sensitive species include *Salvelinus fontinalis* and *Oncorhynchus mykiss*, with LC_{50} values ranging from 0.59 to 4.31 µg/L (Brinkmann et al., 2022; Di et al., 2022).

In zebrafish embryos, developmental abnormalities, cardiotoxicity, and reduced swimming velocity were observed at 25 µg/L (Varshney et al., 2022), while Grasse et al. (2023) observed bioaccumulation and biotransformation within 48 hours of exposure. In *Caenorhabditis elegans*, chronic exposure caused lethality, reduced reproduction, increased intestinal permeability, and altered gene expression even at sub-microgram levels (Hua et al., 2023a, 2023b). On the other hand, crustaceans such as *Daphnia magna* and *Hyalella azteca* demonstrated much higher tolerance, with no acute mortality up to 100 µg/L (Hiki et al., 2021).

In addition to aquatic organisms, the toxicity of 6-PPDq extends to soil invertebrates, microorganisms, nematodes, and plants. One of the most concerning developments is its potential for genotoxicity: 6-PPDq has been shown to be mutagenic to the marine amphipod *Parhyale hawaiensis* and weakly mutagenic to bacteria (Botelho et al., 2023). These findings expand the compound's risk profile beyond acute toxicity, raising concerns about DNA damage and long-term ecological impacts.

Despite increasing concern over 6-PPDq's environmental behavior, there remains a critical knowledge gap regarding its phytotoxicity. Laboratory studies have shown that *Eichhornia crassipes* exposed to environmentally relevant concentrations (≤ 10 µg/L) exhibits decreased photosynthetic pigment content and increased oxidative stress, although no significant biomass or root length reductions were observed (Ge et al., 2024). At higher concentrations, however, adverse effects on germination, growth, and fresh weight have been reported for terrestrial and aquatic species, including *Brassica rapa L. ssp.* (50 – 100 µg/L), *Chlorella vulgaris* (200 – 400 µg/L), and *Trifolium repens L.* (500 µg/L) (Liu, Yu, Li, et al., 2024; Wang et al., 2024). Additionally, Castan et al. (2023) demonstrated the uptake and translocation of 6-PPD and 6-PPDq in lettuce leaves at concentrations up to 0.75 µg/g, noting that these compounds remained stable even after partial metabolism. These findings highlight the environmental persistence of 6-PPDq and the potential risk it poses to crop safety, particularly for vegetation used in green infrastructure or cultivated in areas affected by stormwater runoff.

Importantly, this same plant uptake capacity may present an opportunity for phytoremediation and other nature-based strategies to intercept or degrade 6-PPDq before it reaches sensitive aquatic environments. These dual implications, ecotoxicological risk and remediation potential, underline the need for continued toxicological screening, environmental monitoring, and vegetation-based research.

1.4. Treatment Challenges

The mitigation of 6-PPDq in the environment poses an emerging challenge due to its moderate persistence, strong sorption behavior, and toxicity even at microgram-per-liter concentrations. Traditional wastewater and stormwater treatment systems were not designed to target tire-derived contaminants, but recent research identifies promising conventional and nature-based strategies (Nicomel & Li, 2023).

Recent evaluations in conventional wastewater treatment plants (WWTPs) indicate that removing 6-PPDq is highly variable. (Cao et al., 2022) reported partial removal ranges from 16% to 47% across different treatment stages. Moreover, Zhang et al. (2023) reported daily discharge of 6-PPDq ranged from 5.2 to 36 μg/day at Industrial WWTP in Malaysia and 1100 μg/day in Colombo (Sri Lanka), where 50% 6-PPDq removal efficiency was noted. The treatment effectiveness may vary depending on plant design, operational conditions, and the physicochemical characteristics of 6-PPDq. Its limited biodegradability and strong affinity for suspended solids also pose challenges, allowing the compound to bypass traditional biological processes (Chen et al., 2023).

Advanced oxidation processes (AOPs) have shown strong potential for treating 6-PPDq. While degradation was limited under individual treatments with ultraviolet (UV) light (13.3%) or peroxymonosulfate (PMS, 14.1–28.8%), the combined UV/PMS system significantly enhanced removal, achieving 53.4–100% degradation within 120 minutes depending on the PMS-to-6-PPDq ratio, demonstrating high removal efficiency under controlled conditions (Yu et al., 2024). Similarly, granular activated carbon (GAC) and powdered activated carbon (PAC) systems exceeded 80% removal due to strong adsorption to hydrophobic media (Hildebrandt et al., 2024).

Nature-based solutions are gaining attention as effective and sustainable alternatives. Bioretention systems have demonstrated substantial reductions in 6-PPDq concentrations and related toxicity. McIntyre et al. (2023) reported an increase in zebrafish embryo survival from 13% in untreated stormwater runoff to 93% after treatment through bioretention (sand-compost (60:40) with a gravel drainage layer). In a related context, Grasse et al. (2023) investigated the biotransformation of 6-PPDq in zebrafish embryos and found that over 95% of the compound was metabolized within 96 hours of exposure, suggesting a role for endogenous detoxification pathways.

Permeable pavements provide additional benefits by reducing runoff and filtering contaminants through infiltration. Mitchell and Jayakaran (2024) documented the mean mass reduction up to 96% of tire particle mass and 68% of 6-PPDq in stormwater after porous concrete overlaying porous asphalt pavement. These systems promote sorption and potential microbial interactions before pollutants reach the receiving waters.

Recent studies have examined biologically mediated degradation of 6-PPDq, especially using bacteria and fungi. While bacterial degradation by *Streptomyces phaeofaciens* achieved modest removal rates, up to 30% over 30 days in soil and water matrices (Calarnou et al., 2023), the fungal system has shown greater efficiency. *Phanerochaete chrysosporium*, a white-rot fungus, removed over 99% of 6-PPDq in aqueous solution through adsorption and enzymatic catalysis, followed by mineralization of the degradation products (Yu et al., 2025). Despite these progress, no published studies have assessed the use of phytoremediation for 6-PPDq, which presents a significant knowledge gap given the scalability and low cost of plant-based systems. Improving our understanding of plant tolerance, uptake, and transformation capacity is crucial for developing integrated solutions for tire-derived contaminants.-derived contaminants.

The table below summarizes key treatment strategies, their removal efficiency, and supporting references. This growing body of evidence supports the development of hybrid systems combining physical removal, adsorption, and biologically mediated transformation processes.

Table 3. Treatment efficiency in removing 6-PPD-quinone

Treatment Strategy	Matrix	Removal Efficiency (%)	Effect / Performance	Reference
Bioretention	Stormwater	≥ 90%	Eliminated coho salmon embryo survival from 13% to 93%	McIntyre et al. (2023)
Permeable pavement	Stormwater	~68%	52–100 % of potentially leachable 6-PPDq was removed	Mitchell and Jayakaran (2024)
WWTP	Wastewater	16 – 47%	Partial removal, strong partitioning, and low biodegradability	Cao et al. (2023)
WWTP	Wastewater	50%	Efficient removal in Colombo, Sri Lanka	Zhang et al. (2023)
AOP (UV/PMS)	Aqueous	53 – 100%	Highly effective degradation depending on PMS dose under UV activation	Yu et al. (2024)
Microbial biodegradation	Soil slurry	Up to 30%	Partial degradation by *S. phaeofaciens* over 30 days	Calarnou et al. (2023)
Fungal bioremediation	Aqueous	Up 99%	Enzymatic degradation via lignin peroxidase and P450; complete mineralization using *Phanerochaete chrysosporium* over 7 days	Yu et al. (2025)

In conclusion, addressing the environmental risks posed by 6-PPDq requires a multi-faceted approach. While some WWTPs demonstrate high removal under optimal conditions, others offer only partial removal due to the persistence of certain chemicals and their low biodegradability. Advanced oxidation and adsorption systems are promising for centralized treatment, whereas green infrastructure solutions, such as bioretention and permeable pavements, offer effective and lower-cost options for stormwater-dominated contexts. Future research should prioritize scalable biodegradation strategies and validation of treatment technologies under real-world conditions.

Chapter 2: Evaluating the resistance of *Rudbeckia hirta*, *Rumex crispus*, and *Trifolium pratense* to germinate in the presence of 6-PPD-quinone.

To explore the feasibility of phytoremediation strategies for 6-PPD quinone, this chapter examines the resistance of three plant species during early developmental stages

2.1. Introduction

6-PPD-quinone (6-PPDq) is a toxic transformation product derived from the antioxidant N-(1,3-dimethylbutyl)-N′-phenyl-p-phenylenediamine (6-PPD), a chemical widely used in tire manufacturing. As tires wear, particles containing 6-PPD are released into the environment, where exposure to ozone oxidizes them to 6-PPDq (Tian et al., 2022). This contaminant has been increasingly detected in urban stormwater runoff adjacent to roadways (Kolomijeca et al., 2020).

The growing environmental concern regarding 6-PPDq arises from its acute toxicity to several aquatic species, most notably *Oncorhynchus mykiss (*coho salmon), with mortality reported at very low concentrations (< 1μg/L) (Tian et al., 2022). Despite its recognized toxicity in aquatic ecosystems, the behavior and impact of 6-PPDq in terrestrial environments remain largely underexplored.

Phytoremediation, the use of plants to absorb, degrade, or immobilize environmental contaminants, offers a promising nature-based approach for managing stormwater pollution. Its success depends on the ability of selected plant species to germinate, establish, and grow in contaminated environments (Aryal, 2024; Vangronsveld et al., 2009). However, limited studies are available on the phytotoxicity of 6-PPDq and plant species' tolerance, particularly during critical early plant development, such as germination and seedling establishment. To address this gap, it is crucial to investigate species with potential for growth in environments affected by pollutants of emerging concerns such as 6-PPDq, especially those already adapted to urban or disturbed settings.

In this context, *Rudbeckia hirta* (Black-Eyed Susan), *Rumex crispus* (Curly Dock), and *Trifolium pratense* (Red Clover) were selected for evaluation based on their ecological relevance, observed presence in the southeastern U.S. (Figure 5), and potential applicability in green infrastructure exposed to stormwater runoff. Although no published studies yet report the phytoremediation of 6-PPDq using *R. hirta, R. crispus,* or *T. pratense*, all three species have demonstrated the ability to accumulate or tolerate heavy metals in contaminated environments. For example, *T. pratense* has been identified as a promising bioindicator that accumulates Cr, Ni, and Pb with high bioconcentration and translocation factors in urban soils (Cakaj et al., 2023). *Rumex crispus* has been used in the remediation of Cd-contaminated soils, demonstrating both tolerance and uptake capacity (Aryal, 2024). Additionally, controlled studies growing *R. hirta* in soils spiked with Cd, Zn, Pb, and Cu revealed resilience and potential for restoration in contaminated soils (Miles & Parker, 1979).

Rudbeckia hirta is a native perennial herbaceous plant widely distributed across Alabama and the southern U.S.. It is well-adapted to disturbed soils, grasslands, roadsides, and low-maintenance landscapes, displaying high resilience to drought and moderate salinity. Its fibrous root system and deep taproot make it a valuable candidate for erosion control and infiltration-based stormwater applications, where root stability and tolerance to environmental stressors are critical (Keener, 2025a; U.S. Department of Agriculture, 2024a).

Rumex crispus, on the other hand, is an introduced perennial forb typically regarded as a cosmopolitan weed, but it is frequently found colonizing roadside soils and drainage ditches in Alabama and other southern states. Its adaptability to a wide range of soil conditions, including compacted or nutrient-poor substrates and its long taproot, allows it to survive in heavily disturbed urban environments. Its documented presence in roadside stormwater runoff catchments suggests a high tolerance to pollutants and potential utility in passive treatment zones (Keener, 2025b; U.S. Department of Agriculture, 2024b).

Trifolium pratense is a nitrogen-fixing legume commonly used in forage production, cover cropping, and bioretention designs. It is a biennial or short-lived perennial that produces high-quality biomass and grows well in fine- to medium-textured soils with moderate fertility. Its ability to improve soil quality through nitrogen fixation, combined with a fibrous root system and shade tolerance, has made it a preferred species for vegetated filter strips and stormwater bioretention cells (Keener, 2025c; U.S. Department of Agriculture, 2008). In addition, *T. pratense* has demonstrated rapid establishment and high survival rates in managed green infrastructure.

Together, these three species represent a functionally diverse group, offering a combination of tolerance to roadside stressors, ecological relevance in Alabama landscapes, and compatibility with low-impact development practices. Their selection enables the investigation of contaminant resistance and uptake mechanisms in stormwater-impacted soils, particularly for tire-derived compounds such as 6-PPDq.

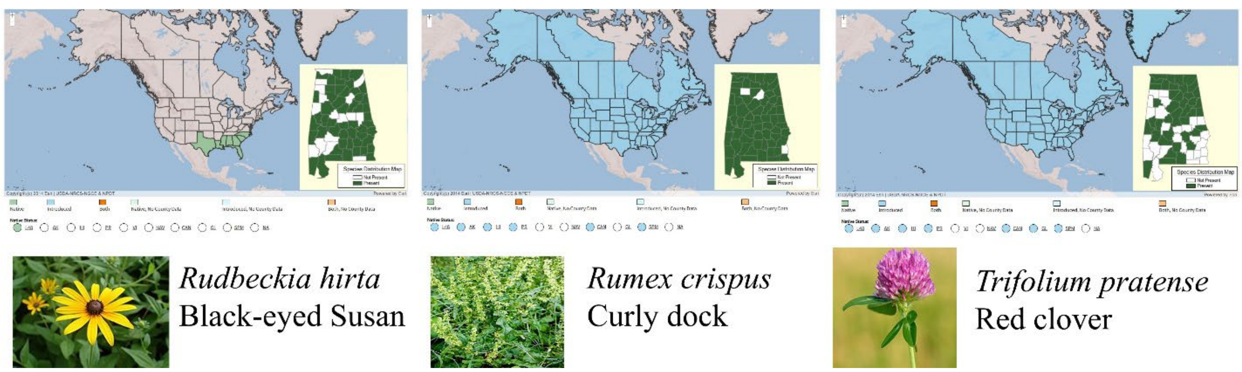

Figure 5. Rudbeckia hirta, Rumex crispus, and Trifolium pratense distribution around the U.S. and Alabama. Images from (Keener, 2025a, 2025b, 2025c; U.S. Department of Agriculture, 2008, 2024a, 2024b).

This study evaluates the resistance of *R. hirta, R. crispus,* and *T. pratense* to 6-PPDq exposure by assessing germination rates, root and shoot lengths, and fresh biomass production. Germination tests effectively assess plant tolerance during early development, where the radicle represents initial root growth and the hypocotyl indicates shoot elongation. This work provides insights into the potential of these species for future phytoremediation applications targeting 6- PPDq contaminated runoff. The findings will support the development of effective, nature-based solutions to improve urban stormwater quality.

2.2. Materials and Methods

The following subsections describe the materials, chemical reagents, experimental setup, and analytical procedures used to conduct the germination and growth tests.

2.2.1. Chemicals

The contaminant used in this study was N-(1,3-Dimethylbutyl)-N′-phenyl-p-phenylenediamine quinone (6-PPDq, CAS# 2754428-18-5). The 6-PPDq analytical standard was purchased from HPC Standard Inc. (Atlanta, Georgia, U.S.) and stored at 4ºC until use. To prepare the stock solution, 1.6 mg of 6-PPDq was accurately weighed using an Ohaus Pioneer™ analytical balance and dissolved in 5 mL of acetonitrile (≥ 99.8%, HPLC grade, ThermFisher, Geel, Belgium). The solution was homogenized for 30 s using an ultrasonic homogenizer (Symphony™, VWR, China) to ensure complete dissolution.

Working solutions were prepared by serial diluting the stock solution in acetonitrile to achieve the following concentrations of 10, 25, 50, 100, 200, 400, 800, 1600, and 3200 µg/L.

2.2.2. Seeds preparation

Rudbeckia hirta, R. crispus, and *T. pratense* seeds were purchased from SeedVille U.S. (Canton, Ohio, U.S.) and stored at room temperature (21 ± 2 ºC), in a dark, dry location until use.

For the germination experiments, seeds were exposed to one control treatment, and ten treatment concentrations of 6-PPDq, which were divided into two groups: (1) five environmentally relevant concentrations (1, 10, 25, 50, and 100 µg/L); and (2) five stress level concentrations (200, 400, 800, 1600, and 3200 µg/L). The control test consisted of deionized (DI) water with 1%

acetonitrile (v/v). In all subsequent figures, environmentally relevant concentrations are presented with a blue background, and elevated.

To ensure that all treatments contained identical solvent content, 50 µL of the corresponding stock solution was diluted in 4950 µL of DI water for each test solution. For example, to prepare 5 mL of a 1 µg/L test solution, 50 µL of the 1 µg/L work solution was diluted in 4950 µL of DI water. As a result, all test solutions (1 to 3200 µg/L) contained 1% acetonitrile (v/v). Test solutions were freshly prepared and used immediately.

2.2.3. Germination test setup

The germination tests were conducted under laboratory conditions at Auburn University (Auburn, AL, U.S.), maintained at 21 ± 2°C in complete darkness. The germination test was conducted following USEPA – OPPTS 850.4200 guidelines (USEPA, 1996) to evaluate the resistance of *R. hirta* and *R. crispus to 6-PPDq.* This method is a standardized and accepted approach for assessing phytotoxicity. It allows controlled and repeatable conditions and provides insights into plant responses to contaminants.

For each species, ten seeds were placed in individual glass Petri dishes containing qualitative filter paper (Cytiva Whatman^{TM}, Grade 4, 0.21 mm thick) as the growth substrate. Each treatment (control and the ten different 6-PPDq concentrations) was tested in triplicate, resulting in 30 seeds per treatment (n = 30) (Figure 6). In total, 33 Petri dishes were prepared for each plant species. For each treatment, 1 mL of the corresponding 6-PPDq test solution was pipetted onto the filter paper to ensure complete saturation. For the control treatment, 1 mL of DI water containing 1% acetonitrile (v/v) was also pipetted onto the filter paper.

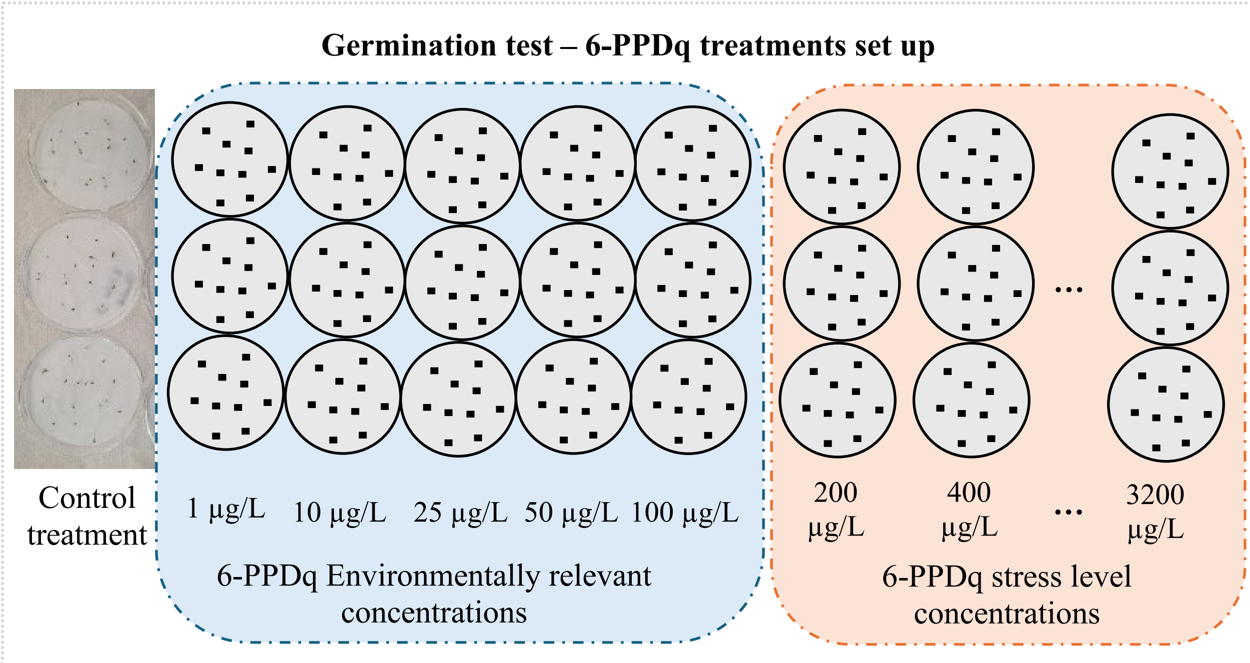

Figure 6. Germination test setup for Rudbeckia hirta, Rumex crispus, and Trifolium pratense. The diagram illustrates the layout used for a single plant species. Each concentration treatment includes three replicates for the control and 6-PPDq treatments: five environmentally relevant concentrations (1 – 100 µg/L, blue background) and five stress level concentrations (200 – 3200 µg/L, orange background).

The experiment was conducted over a 7-day period. In addition, on day 4, 1 mL of DI water was added to each replicate to maintain moisture levels. Under optimal conditions, germination of *Rudbeckia hirta*, *Rumex crispus*, and *Trifolium pratense* typically begins within 3 to 7 days (Keener, 2025a, 2025b, 2025c; U.S. Department of Agriculture, 2008, 2024a, 2024b). Therefore, the observation period used in this study aligns with standard germination expectations, allowing assessment of both early and delayed responses to 6-PPD quinone exposure. After 7 days of exposure, germinated seedlings were carefully removed from the Petri dishes using tweezers, placed on millimeter paper, and photographed for measurement. Radicle and hypocotyl lengths (mm) were quantified using ImageJ software. Fresh biomass was determined individually by weighing each plant on an analytical balance (Ohaus PioneerTM).

The germination tests were considered valid when at least 65% of the seeds germinated in the control group, following the USEPA (1996) guideline. Damaged or non-viable seeds were excluded from the germination counts to ensure accuracy. In addition to this general validity criterion, a stricter internal benchmark was adopted to evaluate species tolerance to 6-PPDq. Specifically, a species was considered a viable phytoremediation candidate only if germination rates remained ≥ 65% not only in the control but also across treatments containing 6-PPDq. A drop below this threshold in any concentration was interpreted as a sign of phytotoxicity.The dependent variables—germination rate (%), radicle and hypocotyl lengths (mm), and fresh biomass weight (mg)—were analyzed quantitatively and presented as mean values with corresponding standard errors (SEM) plotted against the tested 6-PPDq concentrations.

2.2.4. Statistical Analyses

This study hypothesized that *R. hirta, R. crispus,* and *T. pratense* possess tolerance to 6-PPDq exposure and could potentially be used in phytoremediation systems for stormwater runoff. To test this hypothesis, the following null hypothesis were evaluated: a) the germination rate (%) of *R. hirta, R. crispus,* and *T. pratense* exposed to 6-PPDq is statistically greater than or equal that of the control (Ho_g); b) the fresh biomass (mg) of seedlings exposed to 6-PPDq is statistically equal to that of control (Ho_{fb}); and c) the radicle and hypocotyl lengths (mm) of seedling exposed to 6-PPDq are statistically equal to those of the control (Ho_l).

For each plant species and each concentration group (control, environmentally relevant, and stress level concentrations), the data were first tested for normality using the Shapiro-Wilk if the results were normally distributed, a one-way analysis of variance (ANOVA) was performed to determine whether statistically significant differences existed across treatments, followed by Tukey test for pairwise comparisons. If the data were not normally distributed, the non-parametric Kruskal-Wallis test was applied, followed by Dunn`s post hoc test to identify significant differences between specific treatments. All statistical analyses were performed in PAST software (version 1.68), with a confidence level of 95% (Hammer et al., 2001).

For each dependent variable, the null hypothesis (Ho_g, Ho_l, Ho_{fb}) was evaluated based on the *p*-values obtained from the statistical analyses. When $p < 0.05$, the null hypothesis (Ho) was rejected, indicating that the 6-PPDq significantly affected at least one treatment and influenced germination, growth, or biomass. In such cases, post-hoc tests were used to identify which concentration differed significantly from the other concentration. On the other hand, if the $p > 0.05$, the null hypothesis (Ho) was accepted, indicating no statistically significant effect of 6- PPDq on the germination, growth, or fresh biomass of *R. hirta, T. pratense,* and *R. crispus*.

2.3. Results

This section presents the results of the germination and growth assays conducted to assess the phytotoxic effects of 6-PPDq on the selected species. Findings are organized by plant response variables and concentration levels.

2.3.1. Germination rate

Germination counts were recorded on days 4 and 7 to evaluate early seedling emergence and assess potential delays or inhibition due to 6-PPD quinone exposure. Table 4 presents the number of germinated seeds observed in each replicate across all treatments and species, including environmentally relevant and stress level concentrations. This dataset provides the basis for calculating the mean germination rates (%) and standard error, which are presented graphically in the following figures for comparative assessment across treatments and species.

Table 4. Number of germinated seeds for Rudbeckia hirta, Rumex crispus, and Trifolium pratense after 4 and 7 days of exposure to 6-PPD-quinone at environmentally relevant concentrations (1 – 100 µg/L, blue background) and stress level concentrations (200 – 3200 µg/L, orange background). The initial number of seeds was 10.

6-PPDq (µg/L)	Number of germinated seeds of *R. hirta*						Number of germinated seeds of *R. crispus*						Number of germinated seeds of *T. pratense*					
	Day 4			Day 7			Day 4			Day 7			Day 4			Day 7		
	R1	R2	R3	R1	R2	R3	R1	R2	R3	R1	R2	R3	R1	R2	R3	R1	R2	R3
0	10	8	8	10	9	9	10	8	9	10	10	10	10	10	10	10	10	10
1	10	10	7	10	10	10	7	6	5	9	7	6	8	10	10	9	10	10
10	8	9	10	9	10	10	8	8	7	9	9	9	10	10	10	10	10	10
25	7	8	10	10	10	10	7	7	4	7	8	4	10	10	9	10	10	10
50	8	10	9	8	10	10	7	7	9	7	7	10	10	10	10	10	10	10
100	4	9	8	6	9	10	5	6	4	5	6	5	10	10	10	10	10	10
200	7	8	7	9	8	8	8	5	7	9	5	7	10	9	10	10	9	10
400	8	10	7	10	10	9	5	7	9	6	7	9	10	8	10	10	10	10
800	10	10	10	10	10	10	9	8	4	10	8	4	10	10	10	10	10	10
1600	10	7	6	10	10	6	7	10	8	7	10	9	10	8	10	10	8	10
3200	7	8	5	8	9	6	8	7	19	9	10	10	9	10	9	10	10	10

Figure 7 shows the germination rates (%) of *R. hirta*, *R. crispus,* and *T. pratense* seeds after 4 days (light green bars) and 7 days (dark green bars) of exposure to 6-PPDq. The control group, which was not exposed to 6-PPDq but contained 1% acetonitrile to match solvent concentrations, was included as the reference for all statistical comparisons.

Overall, the germination test met the general validity criterion defined by USEPA (≥ 65% germination in the control) for all plant species (Fig. 7). However, in this study, an internal validation approach was adopted to identify species resistant to 6-PPDq. Specifically, a species was considered a viable candidate for phytoremediation only if germination in the presence of 6-PPDq remained comparable to the control (≥ 65%). Although *R. crispus* met the control germination threshold (Fig. 7b), its significantly lower germination rates at several 6-PPDq concentrations indicated a toxic response; thus, the species was considered unsuitable under the established criteria for this experiment.

For *R. hirta* (Fig. 7a), germination remained above 80% on day 4 for both the control and all environmentally relevant 6-PPDq concentrations, except at 100 µg/L. Kruskal-Wallis analysis indicated no significant effect of 6-PPDq exposure on germination rate at either day 4 ($p = 0.8061$) or day 7 (p = 0.3618). Although slightly lower germination and greater variability were observed at the stress level concentrations (e.g., 76.7 ± 7.2% at 3200 µg/L), these differences were not statistically significant ($p = 0.1491$ for day 4 and p = 0.1072 for day 7).

For *R. crispus* (Fig. 7b), control germination reached 90% on day 4 and 100% on day 7. Under environmentally relevant 6-PPDq concentrations, germination ranged from 50% (at 100 μg/L) to 76.7% (at 50 μg/L), while at stress level concentrations, rates ranged from 66.7% (at 200 μg/L) to 83.3% (at 1600 and 3200 μg/L). No consistent dose-response trend was observed, with greater variability occurring at lower concentrations. The Kruskal-Wallis test indicated that 6-PPDq significantly affected *R. crispus* germination at environmentally relevant concentrations ($p = 0.0291$ for day 4 and $p = 0.0322$ for day 7). At the same time, no significant effects were observed at stress level concentrations ($p = 0.5068$ for day 4 and $p = 0.122$ for day 7). Dunn's post hoc test revealed that germination rates at 1, 25, and 100 μg/L were significantly lower than the control ($p < 0.05$). For *T. pratense*, germination rates remained high across all treatments (Fig. 7c). On day 4, germination exceeded 90% for all environmentally relevant concentrations (1–100 μg/L), with the lowest value observed at 1 μg/L. By day 7, all treatments reached 100% germination, indicating full germination capacity regardless of 6-PPDq exposure. Kruskal-Wallis analysis showed no significant effect of 6-PPDq on germination rates at either environmental or stress level concentrations (environmental concentrations: $p = 0.5133$ for day 4 and p = 0.5735 for day 7; stress level concentrations: $p = 0.4159$ for day 4 and p = 0.5133 for day 7).

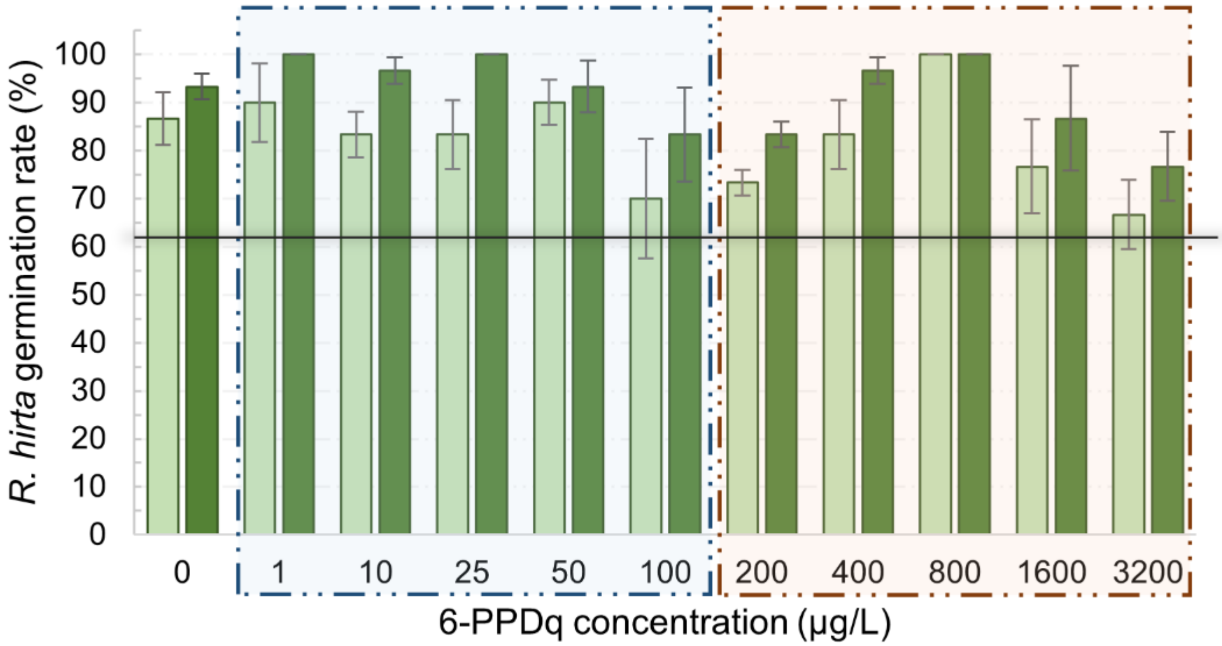

(a) *R. hirta*

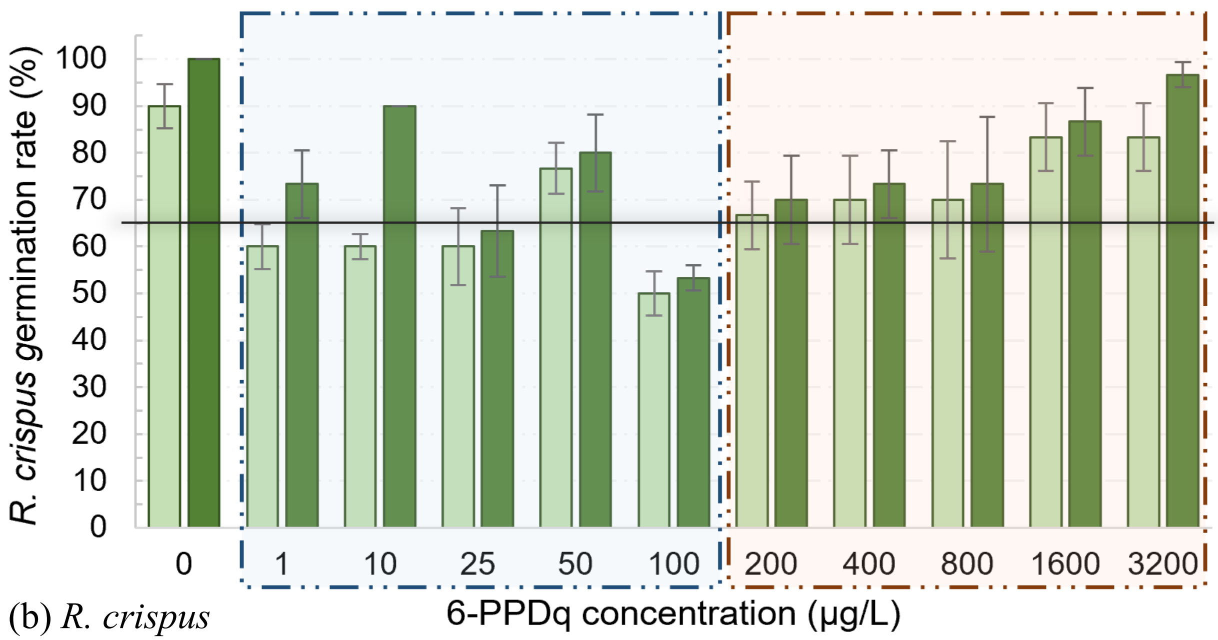

(b) *R. crispus*

Figure continued on the next page

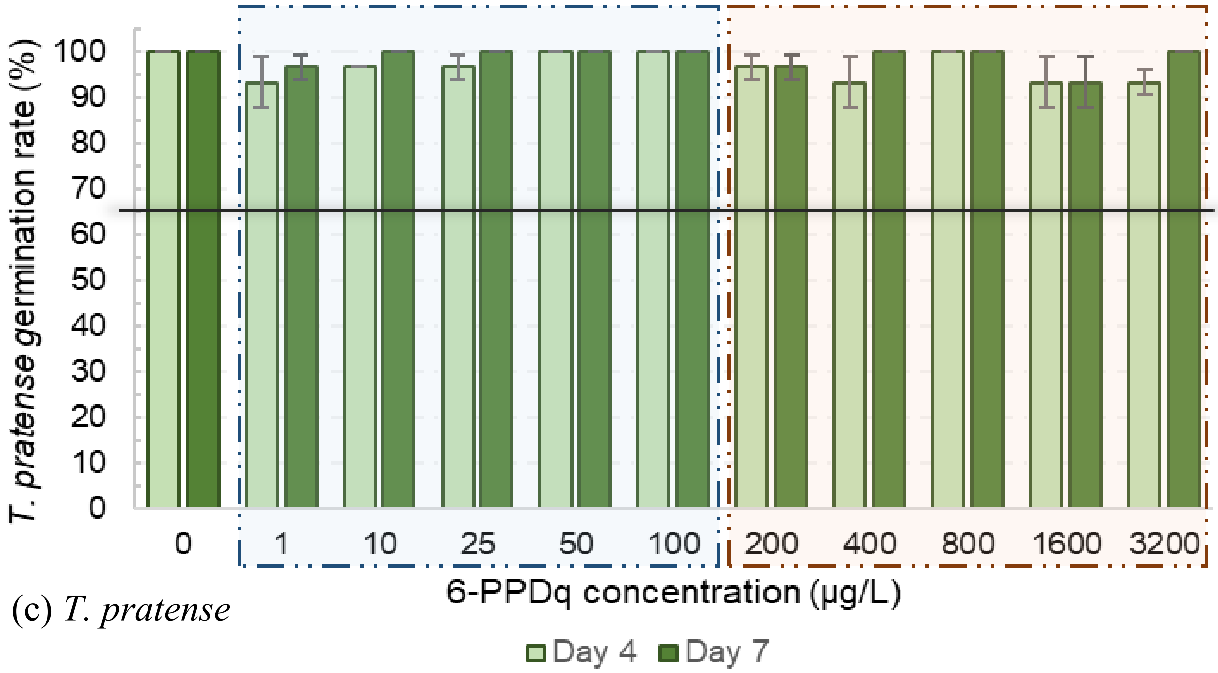

(c) *T. pratense*

Figure 7. Mean germination rates (%) of (a) Rudbeckia hirta, (b) Rumex crispus, and (c) Trifolium pratense after 4 and 7 days of exposure to 6-PPDq at environmentally relevant concentrations (1 – 100 µg/L, blue background) and stress level concentrations (200 – 3200 µg/L, orange background). The control group (no 6-PPDq exposure; 1% acetonitrile) is included for baseline comparison. Light green bars represent germination on day 4; dark green bars represent germination on day 7. Error bars represent standard error. The horizontal black line represents the minimum 65% germination threshold required to validate the test.

2.3.2. Fresh biomass

Overall, the fresh biomass remained relatively consistent across most 6-PPDq concentrations for *R. hirta* (Fig. 8a). In the control treatment, the average fresh biomass was 3.18 ± 0.17 mg. Under environmentally relevant 6-PPDq concentrations, biomass ranged from 2.76 ± 0.24 mg at 25 µg/L to 3.38 ± 0.25 mg at 200 µg/L. At stress level concentrations, biomass ranged from 3.07 ± 0.26 mg at 400 µg/L to 4.31 ± 0.30 mg at 3200 µg/L.

Within the environmentally relevant concentration range, one-way ANOVA analysis indicated no significant effect of 6-PPDq on fresh biomass ($p = 0.3035$), suggesting no clear phytotoxic effect under these conditions. However, at elevated 6-PPDq concentrations, a statistically significant effect on biomass was observed (*p* = 0.0017), indicating that some concentrations altered the fresh biomass compared to the control or other treatments. Tukey's post hoc test showed that exposure to 3200 µg/L resulted in significantly higher biomass than the control (p = 0.0298), with an average increase of 1.13 mg. Interestingly, this concentration also corresponded to one of the lowest germination rates observed for *R. hirta*. Detailed statistical analysis for these comparisons is provided in the Supplementary Material (SM, Table 1).

For *T. pratense* (Fig. 8b), fresh biomass exhibited variability across treatments. Still, it remained relatively high even at elevated 6-PPDq concentrations. At environmentally relevant concentrations, the control group exhibited an average biomass of 15.2 mg. In comparison, biomass values ranged from 19.2 mg at 1 µg/L, 17.2 mg at 10 µg/L, and 16.3 mg at 25 µg/L. Although no consistent dose-response trend was observed, one-way ANOVA indicated a statistically significant difference across these treatments (*p* = 0.0129). Dunn's post hoc test showed that 1 µg/L resulted in significantly higher biomass than the control (*p* = 0.0034), suggesting that very low concentrations of 6-PPDq may influence early biomass accumulation in *T. pratense*. At stress level concentrations, biomass ranged from 14.9 mg at 3200 µg/L to 18.7 mg at 200 µg/L. One-way ANOVA also indicated statistically significant differences among these treatments (*p* = 0.0107). Dunn's post hoc test revealed that biomass at 3200 µg/L was significantly higher than at 800 µg/L (*p* = 0.0327), with an average increase of 3.8 mg. Interestingly, while biomass remained high, this concentration also corresponded to one of the lowest germination rates observed for *T. pratense*. These findings suggest that *T. pratense* is capable of maintaining biomass production under 6-PPDq exposure, but its biomass response may not directly correlate with germination performance. Detailed statistical analysis is provided in SM, Table 2 and SM, Table 3.

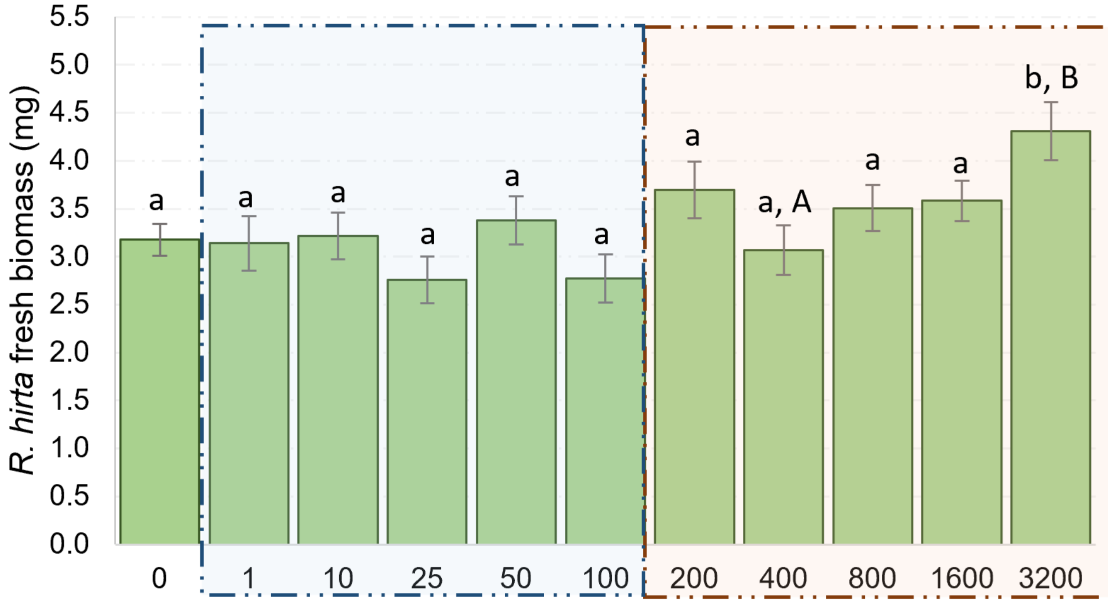

(a) *R. hirta*

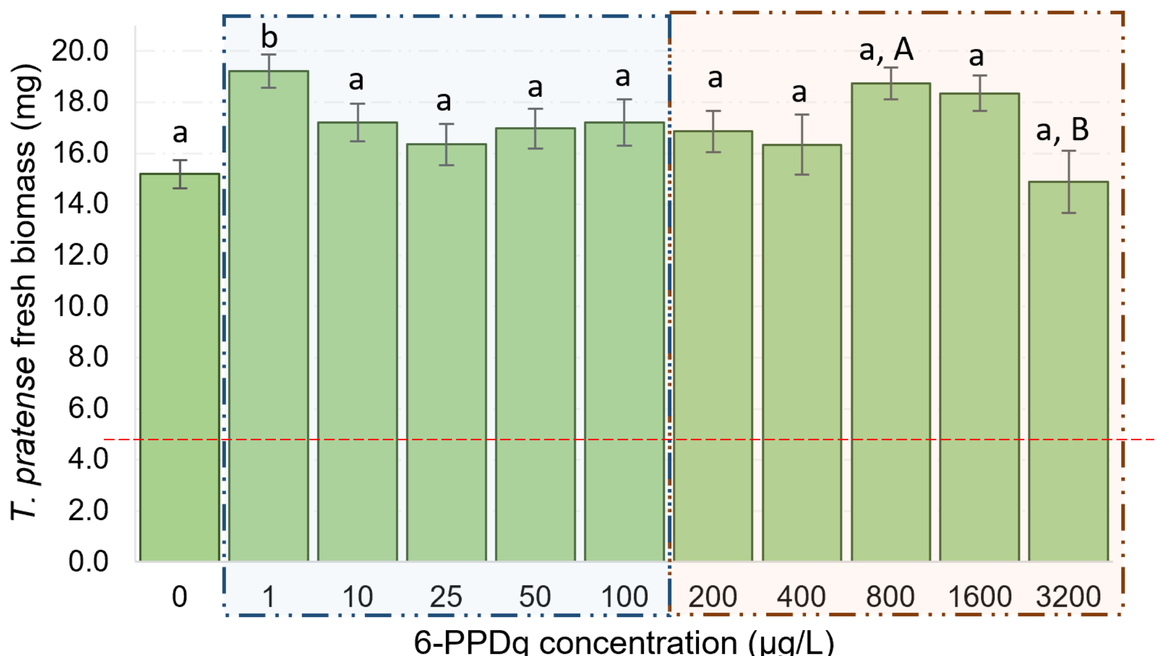

(b) *T. pratense*

Figure 8. Mean biomass (mg) of (a) Rudbeckia hirta and (b) Trifolium pratense after 7 days of exposure to 6-PPDq at environmentally relevant concentrations (1 – 100 µg/L, blue background) and stress level concentrations (200 – 3200 µg/L, orange background). The control group (no 6-PPDq exposure; 1% acetonitrile) is included for baseline comparison. Error bars represent the standard error. Different lowercase letters indicate significant differences compared to the control, while uppercase letters indicate significant differences between 6-PPDq concentrations according to Tukey`s test. The red horizontal line in (b) indicates the highest biomass value recorded for R. hirta, included for comparative scale.

2.3.3. Hypocotyl and Radicle lengths

For *R. hirta*, the control treatment had a mean hypocotyl length of 7.76 ± 0.66 mm. Under environmentally relevant 6-PPDq concentrations, hypocotyl length ranged from 8.47 ± 0.98 mm (100 µg/L) to 10.11 ± 0.88 mm (10 µg/L). At stress level concentrations, hypocotyl length ranged from 8.58 ± 0.81 mm (400 µg/L) to 10.57 ± 0.87 mm (200 µg/L) (Fig. 9a). Although some variation was observed, one-way ANOVA indicated no statistically significant differences in hypocotyl length for either environmentally relevant concentrations (p = 0.4153) or stress level concentrations (p = 0.1050). Thus, 6-PPDq exposure did not significantly affect hypocotyl elongation in *R. hirta*.

For radicle length, the control treatment showed an average length of 7.58 ± 0.70 mm. At environmentally relevant concentrations, radicle lengths ranged from 10.03 ± 1.13 mm (10 µg/L) to 11.78 ± 1.27 mm (1 µg/L). At stress level concentrations, radicle lengths ranged from 10.73 ± 1.31 mm (200 µg/L) to 14.13 ± 1.40 mm (800 µg/L) (Fig. 9a). In environmentally relevant concentrations, significant differences were detected (p = 0.1349, one-way ANOVA). However, at stress level concentrations, significant differences emerged (p = 0.0138, one-way ANOVA). Tukey's post hoc test revealed that 800 µg/L and 3200 µg/L treatments produced significantly longer radicles compared to the control (p = 0.0103 and p = 0.0251, respectively). Detailed p-values can be found in SM, Table 4.

For *Trifolium pratense*, the control treatment exhibited a mean hypocotyl length of 29.6 ± 4.64 mm. At environmentally relevant concentrations, hypocotyl lengths ranged from 35.6 ± 7.84 mm (10 µg/L) to 39.9 ± 7.05 mm (100 µg/L). Under stress level concentrations, hypocotyl lengths ranged from 32.9 ± 16.1 mm (3200 µg/L) to 39.6 ± 6.2 mm (800 µg/L) (Fig. 9b). One-way ANOVA indicated statistically significant differences in the hypocotyl lengths at both environmentally relevant ($p = 1.38\ 10^{-5}$) and stress level concentrations (p = 0.0025). Tukey's post hoc test revealed that all environmentally relevant concentrations (1–100 µg/L) resulted in significantly longer hypocotyls compared to the control ($p < 0.05$, SM, Table 5), while stress level concentrations of 800 and 1600 µg/L also showed significantly greater hypocotyls than the control ($p < 0.05$; SM, Table 6). For radicle length, the control showed a mean of 33.59 ± 8.62 mm. Under environmentally relevant concentrations, radicle lengths ranged from 30.80 ± 13.60 mm (25 µg/L) to 35.84 ± 10.9 mm (1 µg/L). For stress level concentrations, radicle lengths ranged from 27.70 ± 13.56 mm (400 µg/L) to 37.03 ± 10.55 mm (800 µg/L) (Fig. 9b). Despite the variability observed, no statistically significant effects were detected in radicle length for either environmentally relevant (p = 0.5987) or stress level concentrations (p = 0.0553).

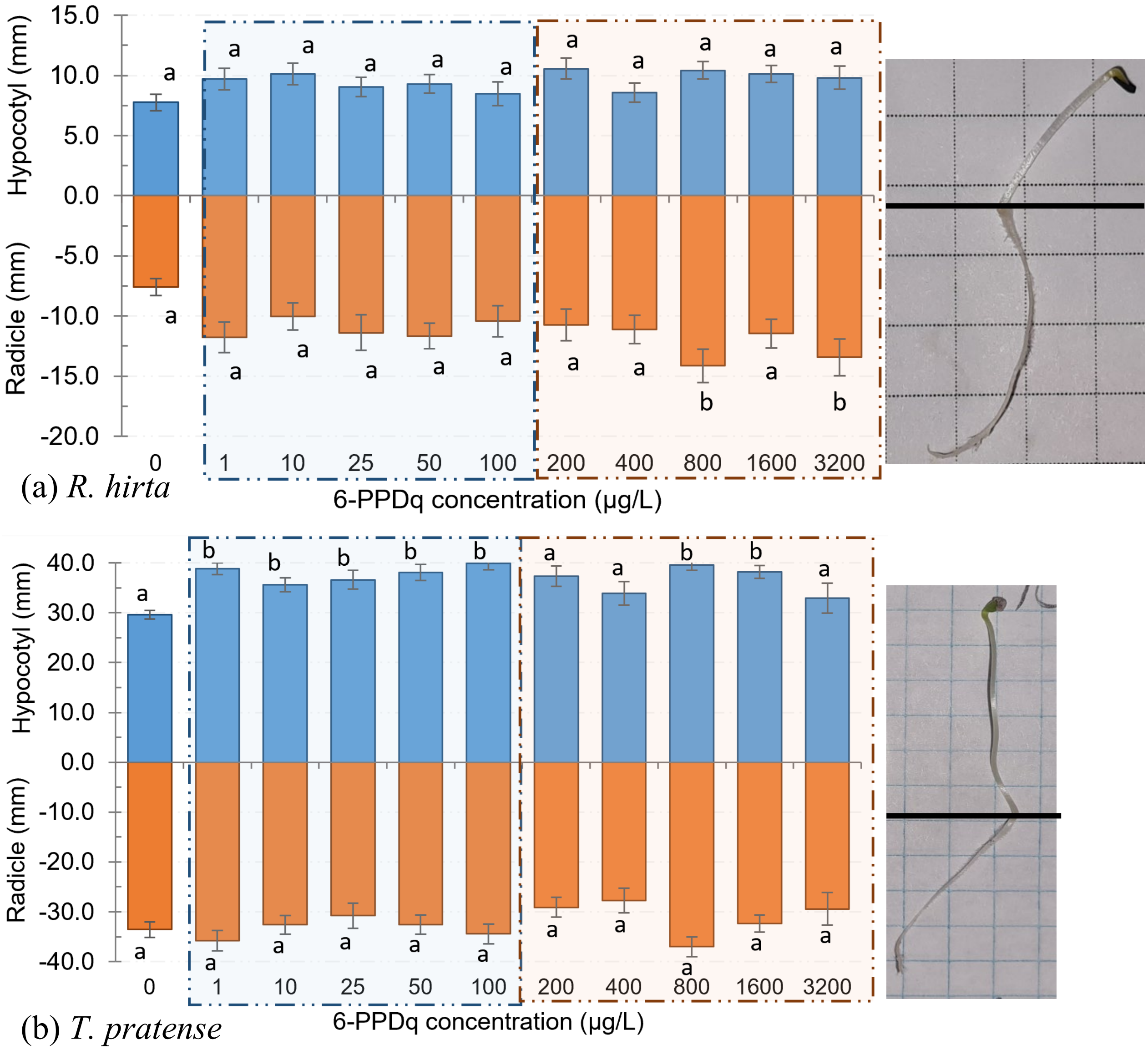

Figure 9. Mean hypocotyl length (mm, upper panel) and radicle length (mm, lower panel) for (a) Rudbeckia hirta and (b) Trifolium pratense after 7 days of exposure to 6-PPDq at environmentally relevant concentrations (1 – 100 µg/L, blue background) and stress level concentrations (200 – 3200 µg/L, orange background). The control group (no 6-PPDq exposure; 1% acetonitrile) is included for baseline comparison. Error bars represent the standard error. Different lowercase letters indicate statistically significant differences from the control according to Tukey`s test. An

illustrative image of a seedling placed on graph paper is included alongside the panel to clarify the measurement approach. The black horizontal line separates the hypocotyl (above) and radicle (below).

2.4. Discussion

The identification of plant species capable of tolerating and potentially remediating pollutants of emerging concerns, such as 6-PPDq, is critical for developing effective nature-based stormwater treatment solutions. The present study provides novel evidence of species-specific responses to 6-PPDq exposure in *R. hirta, T. pratense*, and *R. crispus*, offering insights into their potential application in phytoremediation systems targeting tire-derived pollutants.

Among the three species tested, *R. hirta* demonstrated consistent tolerance to 6-PPDq exposure. Germination rates remained above 80% across all environmentally relevant concentrations (1-100 µg/L), with no statistically significant reduction even at stress level concentrations. This result suggests a strong capacity for successful establishment under 6-PPDq-contaminated conditions, which are typically found in urban stormwater runoff. Fresh biomass, radical length, and hypocotyl length remained stable at environmentally relevant concentrations. At the highest concentration tested (3200 µg/L), biomass significantly exceeded that of the control, suggesting a possible compensatory growth response to chemical stress. A similar trend was observed for radicle length at stress level concentrations (800 and 3200 µg/L). Such compensatory responses have been previously reported in species exposed to environmental contaminants Ge et al. (2024). The ability of *R. hirta* to sustain germination, growth, and biomass accumulation under chemical stress reinforces its potential as a phytoremediation species for use in bioretention cells, bioswales, and vegetated filters in urban environments (Yan et al., 2020).

Similarly*, T. pratense* maintained high germination rates, achieving 100% germination by day 7 across all concentrations, including elevated levels up to 3200 µg/L. The absence of significant inhibitory effects during germination reflects a strong tolerance to early-stage chemical stress, reinforcing this species' known resilience and its established role in ecological restoration and green infrastructure (Wahdan et al., 2021). Low concentrations of 6-PPDq (1 µg/L) led to significantly higher biomass accumulation compared to the control, while biomass remained relatively stable across higher concentrations, even up to 3200 μg/L. This suggests that *T. pratense* may exhibit a hormetic response, where low-level exposure to stress induces enhanced growth. Similar trends have been observed in other species exposed to 6-PPDq and related tire-derived contaminants, such as *Brassica rapa* L. (Liu, Yu, Li, et al., 2024). The ability of *T. pratense* to sustain biomass production under both low and high 6-PPDq concentrations reinforces its resilience and suitability for phytoremediation. Additionally, all 6-PPDq treatments led to longer hypocotyls than the control, reinforcing its adaptability. Given its nitrogen-fixing properties and frequent use in ecological restoration, *T. pratense* emerges as another strong candidate for green infrastructure systems (Wahdan et al., 2021). Hypocotyl length was significantly enhanced across all environmentally relevant and stress level concentrations, with no clear dose-response pattern. The consistent promotion of hypocotyl elongation suggests an adaptive growth mechanism in response to chemical exposure. In contrast, despite some observed variability, radicle length remained statistically unchanged across all concentrations. These results indicate that while shoot elongation may serve as a plastic growth response to stress, root growth appears more stable and resistant to 6-PPDq exposure in *T. pratense*. Conversely, Wang et al. (2024) reported radicle inhibition for *Trifolium repens L.* exposed to tire wear particles, emphasizing that species-specific tolerance mechanisms play a significant role.

In contrast, *R. crispus* met the minimum germination threshold in the control group but failed to maintain ≥ 65% germination in several treatments, particularly at environmentally relevant concentrations. This reduction indicates phytotoxic sensitivity to 6-PPDq and supports its exclusion as a candidate for phytoremediation in this context. The significant reduction in germination observed at 1, 25, and 100 μg/L suggests that *R. crispus* is more sensitive to 6-PPDq during the germination phase. Although *R. crispus* is known for its adaptability to disturbed soils and its tolerance to heavy metals (Zhang et al., 2020), these findings indicate that its germination is vulnerable to synthetic organic contaminants such as 6-PPDq. This sensitivity likely limits its utility for phytoremediation applications targeting tire-derived pollutants.

The ability of plants to tolerate and grow in the presence of pollutants of emerging concerns such as 6-PPDq is a crucial first step in developing effective phytoremediation strategies. Both *R. hirta* and *T. pratense* demonstrated robust tolerance to 6-PPDq during early growth stages, making them promising candidates for phytoremediation systems offering a low-cost, nature-based solution to mitigate tire-derived pollutants like 6-PPDq (Zhang et al., 2020). Their ability to maintain germination, accumulate biomass, and sustain shoot and root development under chemical stress is a critical trait for long-term survival and functional efficiency in engineered ecosystems (Yan et al., 2020). When integrated into green stormwater infrastructure, such as bioretention cells, constructed wetlands, or vegetated swales, these species can enhance pollutant retention while delivering co-benefits like erosion control and biodiversity support (Lapointe et al., 2022; Pilon-Smits, 2005).

However, tolerance alone does not guarantee effective phytoremediation. Long-term effectiveness also depends on a plant's ability to uptake, translocate, transform, or degrade those compounds into less toxic forms. If this transformation does not occur, the maintenance frequency should be established based on the plant's average lifespan to ensure timely removal of contaminants from the site, along with the safe disposal of biomass in landfills or through incineration. If species like *R. hirta* and *T. pratense* primarily accumulate 6-PPDq without metabolizing or transforming it, harvested biomass may become a secondary source of pollution, if not properly managed. Previous studies have reported translocation of 6-PPDq into edible plant tissues, such as lettuce leaves (Castan, Sherman et al. 2023, Hämmerle, Sherman et al. 2024). In such cases, appropriate post-harvest management practices, such as regular replacement, safe disposal, and solid waste controls, become essential to minimize environmental risks (Pilon-Smits 2005).

Future studies should expand on this foundational work by evaluating the uptake, accumulation, and transformation capacity of *R. hirta* and *T. pratense* for 6-PPDq under controlled and field conditions. In particular, determining whether these species can actively degrade 6-PPDq or sequester it will be critical for assessing long-term risk and maintenance requirements. Additionally, pairing tolerant plant species with microbial consortia or soil amendments may enhance contaminant degradation, as previously demonstrated for other xenobiotic compounds (Sharma et al., 2022). Field-scale validation is also needed to assess how hydrologic conditions, seasonal variability, and maintenance regimes affect the performance of vegetated stormwater systems under real-world runoff scenarios (Revitt, 2004). Incorporating species such as *R. hirta* and *T. pratense* into nature-based solutions may offer an affordable, sustainable, and multifunctional approach to mitigating the environmental impacts of tire wear particles and their transformation products in urban stormwater runoff.

2.5. Conclusion

Using a standardized germination assay, this study evaluated the resistance of *R. hirta, R. crispus*, and *T. pratense* to the tire-derived contaminant 6-PPDq. While *R. crispus* failed to meet the minimum germination threshold, *R. hirta* and *T. pratense* demonstrated high tolerance across a wide range of concentrations. In both species, germination rates, biomass accumulation, and hypocotyl or radicle elongation were either maintained or enhanced in response to 6-PPDq exposure. Interestingly, *T. pratense* showed increased biomass and shoot growth even at very low contaminant levels. This suggests a possible hormetic response, consistent with a biphasic effect in which low doses stimulate and high doses inhibit growth.

The results suggest that *R. hirta* and *T. pratens*e are promising candidates for future phytoremediation systems targeting runoff contaminated by tire-derived chemicals. Their proven resistance under controlled conditions supports their implementation in stormwater green infrastructure. However, further research is needed to assess their uptake capacity and degradation potential of 6-PPDq, as the accumulation without transformation could present long-term environmental risks. Establishing best practices for plant maintenance, harvest frequency, and safe biomass disposal will be essential to ensure these species' safe and effective application in real-world scenarios.

These results can be useful for transportation agencies and municipalities considering *R. hirta* or *T. pratense* for roadside stormwater management projects and green structures to improve water quality. Other states where *R. hirta* is a native plant with high occurrence and easy growth, such as Texas, Louisiana, Mississippi, and Georgia, can also use this species in runoff treatments if it shows phytoremediation capacity.

Given its remarkable performance under 6-PPDq exposure, *Trifolium pratense* emerged as a particularly promising species for future phytoremediation applications. The consistent germination success, enhanced biomass production, and signs of possible hormesis at low concentrations warrant further investigation under more realistic or prolonged exposure scenarios. Building upon these initial findings, the next chapter focuses specifically on *T. pratense*, aiming to deepen our understanding of its long-term physiological responses, potential for contaminant uptake and transformation, and practical feasibility in phytoremediation systems targeting tire-derived pollutants.

Chapter 2 - Supplementary Material

SM, Table 1: Tukey test p.values comparing Rudbeckia hirta fresh biomass after 7 days of 6-PPD-quinone exposure at non-environmental concentrations (200 – 3200 µg/L) with 95% confidence level. Welch F test in the case of unequal variances: F = 2.585, df = 69.96, p = 0.03331.

	0	**200**	**400**	**800**	**1600**	**3200**
0		0.7031	0.9995	0.9279	0.8511	**0.02978**
200	2.035		0.4959	0.9947	0.9996	0.5946
400	0.4528	2.486		0.7843	0.6654	**0.01109**
800	1.367	0.756	1.84		0.9999	0.2381
1600	1.653	0.4473	2.12	0.3144		0.3616
3200	4.343	2.274	4.801	3.129	2.793	

SM, Table 2: Tukey test p-values comparing Trifolium pratense fresh biomass after 7 days of 6-PPD-quinone exposure at environmentally relevant concentrations (1 – 100 µg/L) with 95% confidence level. Welch F test in the case of unequal variances: F = 4.362, df = 80.39, p = 0.001456.

	0	**1**	**10**	**25**	**50**	**100**
0		**0.0034**	0.4122	0.8863	0.5504	0.4064
1	5.282		0.4295	0.0893	0.3056	0.4353
10	2.672	2.633		0.9666	0.9999	1
25	1.536	3.759	1.136		0.9917	0.9649
50	2.368	2.934	0.3037	0.832		0.9999
100	2.685	2.619	0.0132	1.149	0.3169	

SM, Table 3: Tukey test p.values comparing Trifolium pratense fresh biomass after 7 days of 6-PPD-quinone exposure at non-environmental concentrations (200 – 3200 µg/L) with 95% of confidence level. Welch F test in the case of unequal variances: F = 4.826, df = 78.91, p = 0.0006685.

	0	**200**	**400**	**800**	**1600**	**3200**
0		0.7819	0.944	0.0618	0.1445	0.9999
200	1.846		0.9986	0.6813	0.8597	0.6428
400	1.284	0.5724		0.4089	0.6257	0.8644
800	3.964	2.084	2.68		0.9997	**0.03275**
1600	3.469	1.626	2.207	0.4264		0.08469
3200	0.3266	2.17	1.611	4.29	3.789	

SM, Table 4: SM, Table 2: Tukey test p.values comparing Rudbeckia hirta radicle after 7 days of 6-PPD-quinone exposure at non-environmental concentrations (200 – 3200 µg/L) with 95% of confidence level. Welch F test in the case of unequal variances: F = 4.69, df = 67.67, p = 0.009492.

	0	**200**	**400**	**800**	**1600**	**3200**
0		0.5072	0.3313	**0.01031**	0.2517	**0.02509**
200	2.462		0.9999	0.6345	0.9987	0.72
400	2.868	0.3023		0.7362	1	0.8097
800	4.832	2.188	1.958		0.8526	1
1600	3.087	0.5594	0.272	1.648		0.8984
3200	4.426	1.996	1.772	0.03161	1.491	

SM, Table 5: Tukey test p.values comparing Trifolium pratense hypocotyl after 7 days of 6-PPD-quinone exposure at environmentally relevant concentrations (1 – 100 µg/L) with 95% confidence level. Welch F test in the case of unequal variances: F = 12.92, df = 79.24, p = 3.402E-09

	0	**1**	**10**	**25**	**50**	**100**
0		**0.000171**	**0.04126**	**0.009525**	**0.000642**	**1.86E-05**
1	6.381		0.6096	0.8784	0.9992	0.9959
10	4.175	2.242		0.9967	0.8206	0.2944
25	4.858	1.564	0.6833		0.9754	0.5887
50	5.917	0.5141	1.742	1.059		0.9522
100	7.103	0.7163	2.964	2.286	1.237	

SM, Table 6: Tukey test p.values comparing Trifolium pratense hypocotyl after 7 days of 6-PPD-quinone exposure at non-environmental concentrations (200 – 3200 µg/L) with 95% confidence level. Welch F test in the case of unequal variances: F = 12.07, df = 77.28,, p = 1.186E-08

	0	**200**	**400**	**800**	**1600**	**3200**
0		0.08368	0.5976	**0.003155**	**0.0228**	0.8168
200	3.797		0.8828	0.9028	0.9964	0.7068
400	2.267	1.549		0.2641	0.6114	0.9993
800	5.316	1.475	3.049		0.9946	0.1335
1600	4.465	0.697	2.238	0.7585		0.3976
3200	1.753	2.027	0.4952	3.518	2.706	

Chapter 3: Long-Term Exposure Test: Assessing Extended Phytotoxicity in *Trifolium pratense*

Following the short-term germination tests presented in Chapter 2, *Trifolium pratense* was selected for further evaluation due to its superior performance under 6-PPDq exposure. Among the three tested species, *T. pratense* consistently exhibited the highest germination rates across all treatments and demonstrated higher fresh biomass accumulation compared to *Rudbeckia hirta*. These results indicate a higher potential for resilience and contaminant uptake, supporting its use in the long-term exposure test to assess extended phytotoxic effects under more realistic exposure durations.

3.1. Motivation

While initial germination and early growth assays offered valuable insights into the short-term tolerance of *T. pratense* to 6-PPDq, these tests mainly focus on early-stage responses. They may miss delayed or cumulative effects that develop under prolonged exposure. Considering the persistence of 6-PPDq in soils and its ongoing input from stormwater runoff, assessing plant performance beyond germination is crucial to understanding its long-term ecological impact and the practicality of using *T. pratense* in phytoremediation systems. Therefore, this chapter introduces a standardized 21-day soil exposure test designed to evaluate the sustained effects of 6-PPDq on growth parameters and morphological integrity of *T. pratense* under environmentally relevant conditions. This longer timeframe allows for the detection of subtle phytotoxic responses, physiological stress, and developmental limitations that might not be apparent in short-term trials, ultimately facilitating a more thorough evaluation of plant resilience and its potential application in green infrastructure.

3.2. Materials and Methods

The following subsections describe the materials, chemical preparation, experimental design, soil characteristics, and analytical procedures adopted for the 21-day exposure test. Particular attention was given to ensuring consistency in soil treatment, irrigation, and light conditions to isolate the effects of 6-PPDq on *T. pratense*.

3.2.1. Chemicals and other materials

6-PPDq (CAS# 2754428-18-5) was purchased in solid form from HPC Standards Inc. and stored at 4 °C. Stock solutions were prepared in HPLC-grade acetonitrile (CAS# 75-05-8, ≥ 99.9%). A stock solution of 6-PPDq was prepared by dissolving 0.8 mg of the compound in 5 mL of HPLC-grade acetonitrile, yielding a concentration of 0.16 g/L (160,000 µg/L). From this, 2 mL were used to prepare the 1600 µg/L treatment solution (final volume of 200 mL), and 2 mL were used to generate sequential 1:1 dilutions to obtain intermediate solutions of 800, 400, 200, and 100 µg/L, each subsequently diluted to 200 mL with deionized water, maintaining a final solvent concentration of 1% (v/v) in all treatments. All stock solutions were freshly prepared and homogenized using an ultrasonic homogenizer before use.

The species used in this study was *Trifolium pratense* (red clover), selected based on the best results in biomass production in the germination test. Seeds were purchased in SeedVille and stored in a dry, dark location at room temperature until they were used.

3.2.2. Long-term exposure test

This study aimed to assess the phytotoxicity of 6-PPDq in *T. pratense* through a standardized soil exposure test based on adaptations from ISO 11269-2:2012 and the EPA's OCSPP 850.4800 guidelines. Six nominal concentrations were prepared: 100, 200, 400, 800, and 1600 µg/L. Each treatment comprised six pots: five containing plants and one without plants to evaluate natural degradation. A control group with no 6-PPDq exposure (but with plants) was included. A total of 36 experimental units were established.

Each pot (400 mL volume, non-toxic plastic) was filled with 150 grams of a commercial soil substrate specifically designed for indoor plant cultivation. Before contamination, the commercial soil was air-dried in an oven at 35 ± 2 °C for 48 to 96 hours, depending on the thickness of the soil layer. To ensure homogeneity, the soil was thoroughly mixed at least three times per day throughout the drying process. The soil was spread in a thin layer and homogenized daily during drying to prevent temperature gradients and ensure uniform water loss. This controlled drying step was employed to prevent microbial activity and ensure the accurate calculation of the water volume required for contamination. After drying, the soil was sieved through a 4 mm mesh to remove all fragments and ensure homogeneity.

To ensure homogeneity, the soil contamination was conducted before potting by mixing the soil thoroughly with 6-PPDq in a heavy-duty polyethylene bag. Contamination solutions (180 mL per treatment) were prepared as described in Section 3.2.1 and added to 900 g of soil (6 × 150 g) to achieve a final soil moisture of 20% w/w, equivalent to approximately 70% of the soil's Water Holding Capacity (WHC), following ISO 11269-2 Annex C. After thoroughly mixing 180 mL of contaminant solution into 900 g of dried soil, the resulting 1080 g of moist soil was divided evenly into six test pots by weighing 180 g of the mixture per pot.

Ten seeds of *T. pratense* were sown per pot, approximately 2 cm below the soil surface (Fig 11). After germination, only five seeds were maintained, totaling 25 viable seeds per treatment concentration, as recommended for statistical robustness.

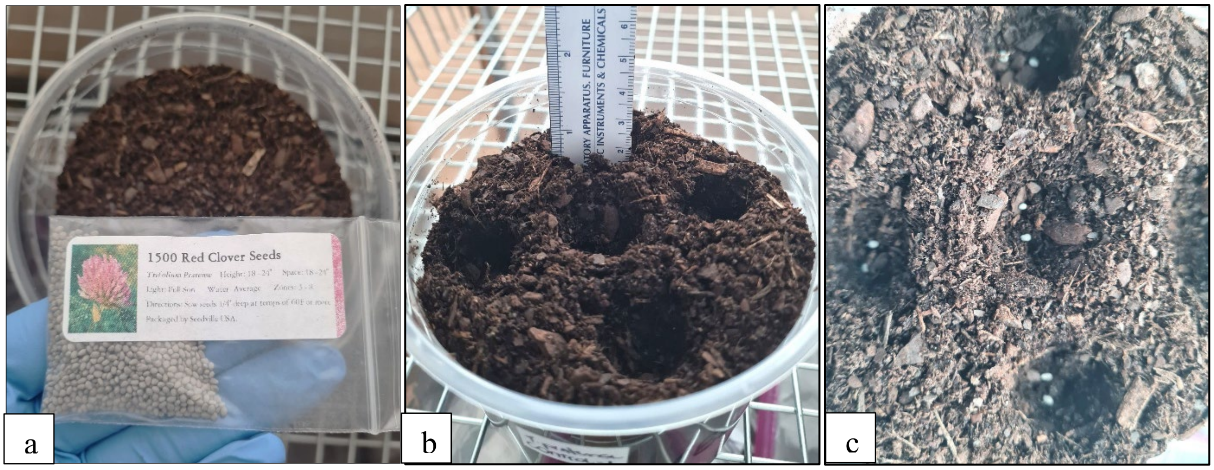

Figure 10. Seed setup in the substrate. (a) Trifolium pratense seeds; (b) placement depth of approximately 2 cm; (c) two seeds positioned per planting spot.

3.2.3. Growth conditions and endpoints

All pots were maintained in a controlled indoor environment under artificial grow lights emitting predominantly purple/orange wavelengths (LED, full spectrum for plant growth), with a photoperiod of 16 h:8 h light-dark regulated by an automatic timer. The temperature was maintained at 22 ± 2 °C. Irrigation with deionized (DI) water was performed three times a week, and the temperature and air humidity were recorded each time the plants were randomly repositioned to minimize any effects from light intensity or tray location. DI water was used to avoid background contamination and ensure consistency across replicates. However, it is acknowledged that DI water does not fully reflect the ionic composition or chemical complexity of natural waters, such as stormwater or shallow soil water, which may influence the mobility of 6-PPD quinone and plant physiological responses. No additional fertilizers were applied to prevent interference from confounding nutrient effects.

The experiment was conducted over 21 days, starting from the day the seed was placed. Seedling emergence was monitored three times a week (Mondays, Wednesdays, and Fridays), allowing for the removal of excess germinated seeds. Seedling emergence and growth were monitored regularly to assess potential phytotoxic effects of 6-PPDq. The following endpoints were recorded: germination rate (%), shoot height (cm), fresh biomass (mg), and dry biomass (mg).

These parameters were measured at test termination. The roots were gently washed, and the plants were separated into shoots and roots. Fresh biomass (FW) was recorded immediately using an analytical balance. Plant tissues were oven-dried at 35°C for 72 h to remove residual moisture and ensure consistent dry biomass (DW) measurements. Water content (%) was calculated using the gravimetric formula:

$$Water\ content\ (\%) = \left(\frac{FW-DW}{FW}\right) * 100 \qquad \textit{Equation 1}$$

The DW/FW ratio was also determined for each sample as an indicator of tissue hydration status. Additional endpoints and qualitative observations were recorded to complement standard measurements. Following USEPA (2012) Guidelines, seedlings were regularly inspected for visible symptoms of phytotoxicity. Signs of deformation and asymmetry, as well as visible discoloration and localized tissue damage, were recorded (Figure 11). These observations, although qualitative, support the interpretation of quantitative endpoints and enhance the ecological relevance of the test. Additionally, root-to-shoot ratios were derived from measured lengths and biomasses, providing further insight into the differential effects of 6-PPDq on plant development under soil exposure conditions.

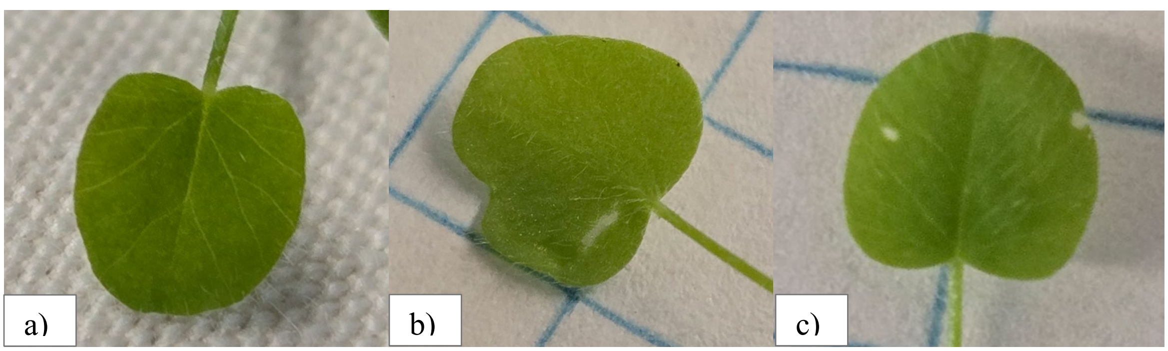

Figure 11. Representative T. pratense leaf morphology. a) Health leaf, b) deformation and asymmetry, and c) chlorosis or localized tissue damage.

3.2.4. Analysis Methods

This study hypothesized that *T. pratense* exhibits tolerance to 6-PPDq after long-term exposure and could potentially be utilized in phytoremediation systems for stormwater runoff. To test this hypothesis, the following null hypothesis were evaluated: a) the germination rate (%) of *T. pratense* exposed to 6-PPDq is statistically greater than or equal to that of the control (Ho_g); b) the fresh biomass (mg) of seedlings exposed to 6-PPDq is statistically equal to that of control (Ho_{fb}); and c) the lengths (cm) of seedling exposed to 6-PPDq are statistically equal to those of the control (Ho_l).

The data were first tested for normality using the Shapiro-Wilk test for each concentration group. If the results were normally distributed, a one-way analysis of variance (ANOVA) was performed to determine whether statistically significant differences existed across treatments, followed by a Tukey test for pairwise comparisons. If the data were not normally distributed, the non-parametric Kruskal-Wallis test was applied, followed by Dunn`s post hoc test to identify significant differences between specific treatments. All statistical analyses were performed using PAST software (version 1.68), with a 95% confidence level (Hammer et al., 2001).

For each dependent variable, the null hypothesis (Ho_g, Ho_l, Ho_{fb}) was evaluated based on the *p*-values obtained from the statistical analyses. When $p < 0.05$, the null hypothesis (Ho) was rejected, indicating that the 6-PPDq significantly affected at least one treatment and influenced germination, growth, or biomass. In such cases, post-hoc tests were used to identify which concentration differed significantly from the control. On the other hand, if the $p > 0.05$, the null hypothesis (Ho) was accepted, indicating no statistically significant effect of 6-PPDq on the germination, growth, or fresh biomass of *T. pratense*.

3.3. Results and Discussions

After thinning, all treatments maintained five seedlings per pot throughout the experiment. Final counts confirmed 100% germination across all treatments, indicating no apparent effect of 6-PPDq on emergence. Each germinated seedling developed between 2 and 4 true leaves, resulting in a total leaf count per pot ranging from 62 to 87. Localized leaf-level abnormalities, such as irregular curvature, a glossy surface, and visible signs of chlorosis or tissue damage (e.g., discoloration spots and uneven pigmentation), were observed in a small number of plants: two leaves in the control group, three leaves at 100 µg/L, and one leaf each at 200, 400, and 800 µg/L of 6-PPDq. Despite these indications of morphological stress or developmental abnormalities, the overall occurrence was below 10%, suggesting that these symptoms likely represent natural variation among seedlings rather than a response to 6-PPDq exposure.

The fresh biomass of *T. pratense* was quantified at day 21. Mean biomass ranged from 19.08 mg to 23.09 mg across treatments, with the highest average observed at 800 µg/L (Figure 13). The control group (0 µg/L) exhibited a mean fresh weight of 19.52 mg (SEM = 1.23), while the lowest biomass mean occurred at 1600 µg/L (19.08 mg, SEM = 1.31). Despite the observed variability, statistical analysis using one-way ANOVA indicated no significant difference in biomass means across treatments ($F = 1.203$, $p = 0.3106$). Interestingly, although not statistically significant, a slight increasing trend in biomass was observed at moderate doses (200 and 800 µg/L), which may suggest a hormetic effect where low to intermediate contaminant levels mildly stimulate growth.

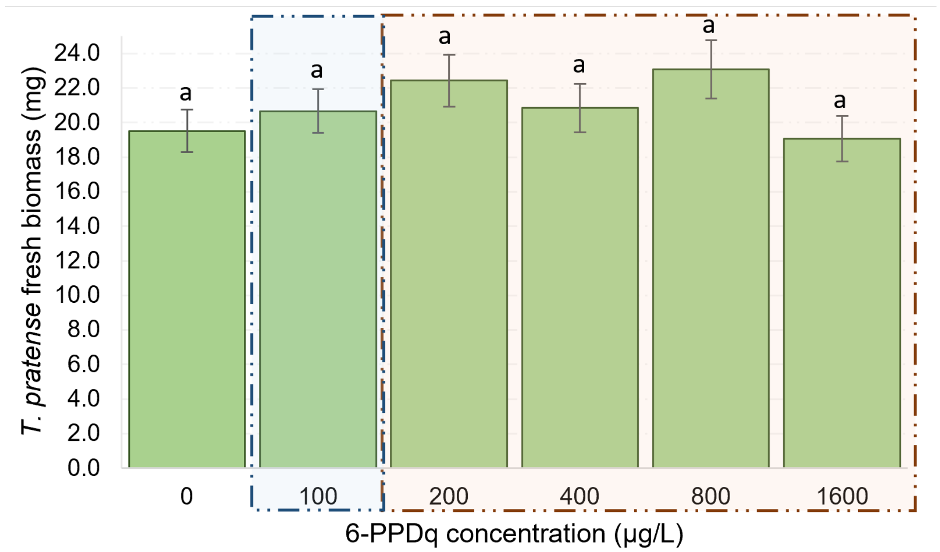

Figure 12. Trifolium pratense fresh biomass after 21 days exposure to 6-PPD-quinone at environmentally relevant concentrations (100 µg/L, blue background) and stress level concentrations (200 – 1600 µg/L, orange background). Same lowercase letters indicate no significant differences in fresh biomass between 6-PPD quinone treatments and the control.

Importantly, a visual inspection of the plants toward the end of the experiment revealed signs of wilting and chlorosis in several pots. These symptoms were particularly notable in treatments with reduced root mass, suggesting that excess moisture may have impaired oxygen availability and consequently limited root development. A post hoc substrate moisture analysis indicated gravimetric moisture contents of 4%, 13%, 8%, 7%, 8%, and 7% for the control, 100, 200, 400, 800, and 1600 µg/L 6-PPDq treatments, respectively. While moisture levels below 10% are generally not associated with saturated conditions, the elevated reading of 13% in the 100 µg/L treatment may reflect localized water retention sufficient to induce hypoxic stress. This aligns with findings by (Yamauchi et al., 2018), who notes that poor drainage and excess water can create oxygen-limited conditions in the root zone, even in seemingly well-drained substrates. These results highlight the need for improved moisture control in long-term soil-based phytotoxicity tests, recommending real-time monitoring and better drainage strategies to support root development.

The water content (%) and dry-to-fresh weight ratio (DWDW/FWW) of *T. pratense* tissues remained within expected physiological ranges across all 6-PPDq treatments (Table 5). The water content varied from 93.9% (at 1600 µg/L) to 94.7% (at 800 µg/L), and DW/FW ratios ranged from

0.0528 to 0.0606. The slightly higher water content observed at 800 µg/L, along with the corresponding lower DW/FW ratio (0.0528), may indicate a minor osmotic adjustment that enhances water uptake or retention. However, given the absence of significant effects on fresh biomass or aerial length, these changes are more likely the result of natural variability rather than an adaptive response to 6-PPDq. Herbaceous species such as *T. pratense* typically maintain water content values above 90%, especially in actively growing shoots. This high water content reflects strong cell turgor and active metabolism, indicating hydration levels close to full turgidity (100% relative water content or zero water deficit) (Spomer, 1985). The DW/FW ratios around 0.05 are also an indicator that tissue hydration was physiologically adequate.

Table 5. Plant water content (%) and dry-to-fresh weight (DW/FW) ratio across 6-PPD-quinone treatments.

6-PPDq concentration (µg/L)	Water content (%)	DW/FW
0	94.5%	0.0545
100	94.2%	0.0585
200	94.0%	0.0601
400	94.3%	0.0574
800	94.7%	0.0528
1600	93.9%	0.0606

The shoot length of *Trifolium pratense* seedlings was evaluated as an indicator of aerial growth. Mean shoot lengths ranged from 3.54 cm in the control group (0 µg/L) to 4.09 cm at 800 µg/L, with small variations across all treatments (Figure 14). The maximum mean shoot length was recorded at 800 µg/L, while the lowest was observed in the control and at 1600 µg/L (3.56 cm). Despite observable differences in individual values, statistical tests indicated no significant effect of 6-PPDq concentration on aerial length ($p = 0.2661$, one-way ANOVA). Although the mean shoot length peaked slightly at 800 µg/L, the increase was not statistically supported and may reflect random variability or a weak hormetic effect, as previously observed in fresh biomass.

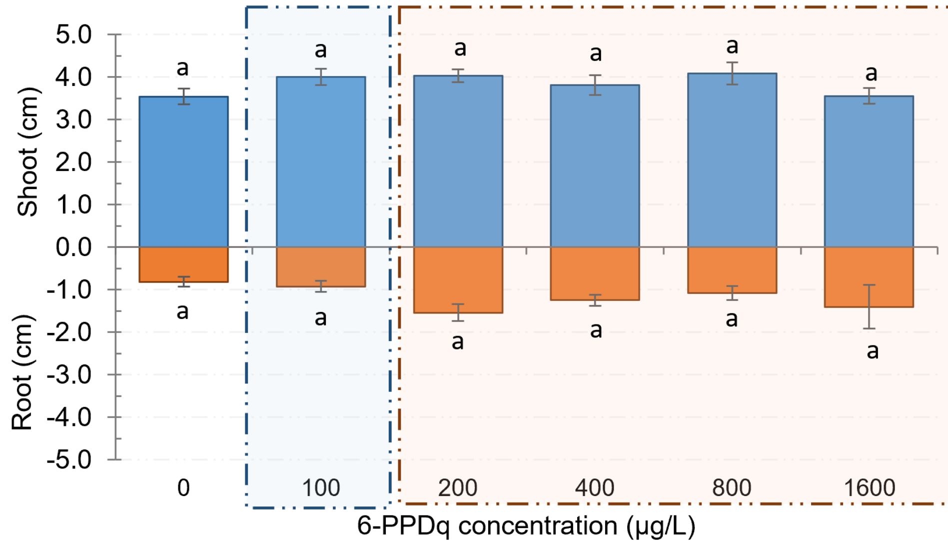

Figure 13. Shoot and root lengths of Trifolium pratense after 21 days of exposure to 6-PPD-quinone at environmentally relevant concentrations (100 µg/L, blue background) and stress level concentrations (200 – 1600 µg/L, orange background). Same lowercase letters indicate no significant differences in shoot and root lengths between 6-PPD quinone treatments and the control.

The average root length in the control group was 0.81 cm, and values for the treatments ranged from 0.92 cm (100 µg/L) to 1.54 cm (200 µg/L). Although 200 µg/L showed the highest mean root length, this increase was not consistent across concentrations and did not follow a dose-response trend. Statistical analysis using one-way ANOVA revealed no significant difference in root length across treatments ($p = 0.5376$). However, absolute root growth across all treatments, including the control, was limited, with mean lengths remaining below 1.6 cm. These low values suggest an environmental constraint on root development, likely linked to excess substrate moisture. Toward the end of the experiment, widespread wilting, chlorosis, and poor root establishment were observed; these symptoms are consistent with hypoxic stress, which reduces oxygen availability in the root zone and impairs cellular respiration. Given these conditions, part of the variability observed in shoot growth may also be attributed to non-chemical stressors, as restricted root development likely constrained water and nutrient uptake.

Previous studies have shown that root elongation is often more sensitive to environmental stressors than aerial growth (Yamauchi et al., 2018). In this experiment, the disproportionately low root development compared to aerial length supports the hypothesis that excess moisture was the dominant limiting factor. Given the sensitivity of root growth to both biotic and abiotic stressors, future phytotoxicity assays involving *T. pratense* should focus on improving drainage, moisture monitoring, and maintaining aerobic soil conditions. These adjustments are crucial to ensure that early growth responses accurately represent chemical toxicity rather than issues caused by waterlogging or compaction.

While *T. pratense* showed resilience to 6-PPDq during early development (as discussed in Chapter 2), its long-term response under chronic exposure remains uncertain. After 21 days, there were no statistically significant decreases in fresh biomass, shoot length, or root elongation at various 6-PPDq concentrations. These findings might indicate genuine chemical tolerance, but environmental factors could also influence them.

Nonetheless, it is notable that even under suboptimal conditions, *T. pratense* maintained stable physiological parameters and water content levels indicative of tissue hydration and viability. This finding aligns with prior studies in *Brassica rapa*, where exposure to 6-PPDq caused oxidative stress and inhibited root growth in a dose-dependent manner (Liu, Yu, Li, et al., 2024), contrasting with the more consistent response observed here. Additionally, studies such as those by Castan et al. (2023) have shown that lettuce plants can uptake and translocate 6-PPDq into their aboveground tissues, raising questions about whether *T. pratense* might act similarly, even without visible signs of stress.

Up to now, no peer-reviewed research has assessed *T. pratense's* ability to uptake, translocate, or metabolize 6-PPDq or similar organic compounds. However, as a perennial legume with an extensive root system and common use in restoration efforts, *T. pratense* might show physiological traits suitable for phytoremediation if it can actively absorb contaminants. This point is important: while tolerance is beneficial, it does not mean the plant can perform phytoremediation unless it can also remove or modify contaminants in the environment.

Given the increasing detection of 6-PPDq in urban soils and stormwater runoff (Nicomel & Li, 2023) research should investigate whether *T. pratense* can accumulate and detoxify this compound. Additionally, combining *T. pratense* with microbial communities or rhizosphere amendments may enhance its transformation abilities, as demonstrated in other contaminant systems (Sharma et al., 2022).

3.4. Conclusion

This chapter evaluated the long-term effects of chronic exposure to the tire-derived contaminant 6-PPDq on *T. pratense*, focusing on fresh biomass accumulation, shoot growth, and root elongation. No statistically significant differences were observed among treatments across any of the measured endpoints. Fresh biomass showed a slight, non-significant increase at intermediate concentrations, while shoot length remained relatively stable throughout the exposure gradient. Root length was consistently low, even in the control group, indicating that environmental stress, particularly excess moisture, likely had a significant impact on plant performance.

The limited variation in biomass and shoot development, along with the absence of a clear dose–response relationship, suggests that 6-PPDq did not induce acute phytotoxicity under the tested conditions. Although no adverse effects could be directly attributed to the contaminant, the experiment revealed critical environmental limitations that should be addressed in future trials to facilitate greater plant development and to evaluate the contaminant's uptake and translocation capacity. Optimizing moisture conditions, improving drainage, and ensuring adequate aeration are essential for reliably assessing plant responses in soil-based phytotoxicity assays.

Therefore, consistent with the results observed in the germination test, *T. pratense* also demonstrated resilience under prolonged exposure and suboptimal conditions. This reinforces its potential as a candidate for use in GI and BMPs aimed at improving stormwater treatment performance.

Chapter 4: Nutrient Removal from Stormwater Runoff: Sources, Best Management Practices, and Iron-Modified Treatment Materials

Nutrient pollution in stormwater runoff remains a persistent environmental challenge. This chapter reviews the primary sources of nutrient contamination, the mechanisms and performance of existing stormwater runoff management systems, and explores the application of iron-modified treatment materials as a strategy to enhance phosphorus and nitrogen removal.

4.1. Introduction

Urbanization significantly disrupts the natural hydrological cycle by replacing permeable landscapes with impervious surfaces such as asphalt and concrete. These surfaces prevent infiltration and evapotranspiration, leading to increased volume and speed of stormwater runoff. This allows pollutants, including nutrients such as nitrogen (N) and phosphorus (P), to be transported into water bodies (Hopkins et al., 2017; Jurczak et al., 2019). The presence of nutrient-rich runoff has become one of the main causes of declining water quality in urban catchments worldwide (USEPA, 2025b).

Phosphorus and nitrogen, although essential for primary productivity in aquatic ecosystems, can become detrimental in excess. Their accumulation leads to eutrophication, marked by accelerated algal and cyanobacterial blooms, oxygen depletion, and ecological degradation in both freshwater and coastal zones (Dodds et al., 2008; Paerl et al., 2016). In the United States, harmful algal blooms (HABs) have become a growing public health and ecological concern. Notably, in the year 2020 alone, fifteen states voluntarily reported 372 harmful algal bloom events, including 95 cases of human illness and at least 102,071 cases of animal illness, being a single event responsible to affect at least 100,000 fish and other marine animals (CDC, 2024). Even one episode of heavy rainfall over impervious surfaces can mobilize significant nutrient loads derived from fertilizer residues, pet waste, atmospheric deposition, and decomposing organic matter (Figure 15) (Wang et al., 2023).

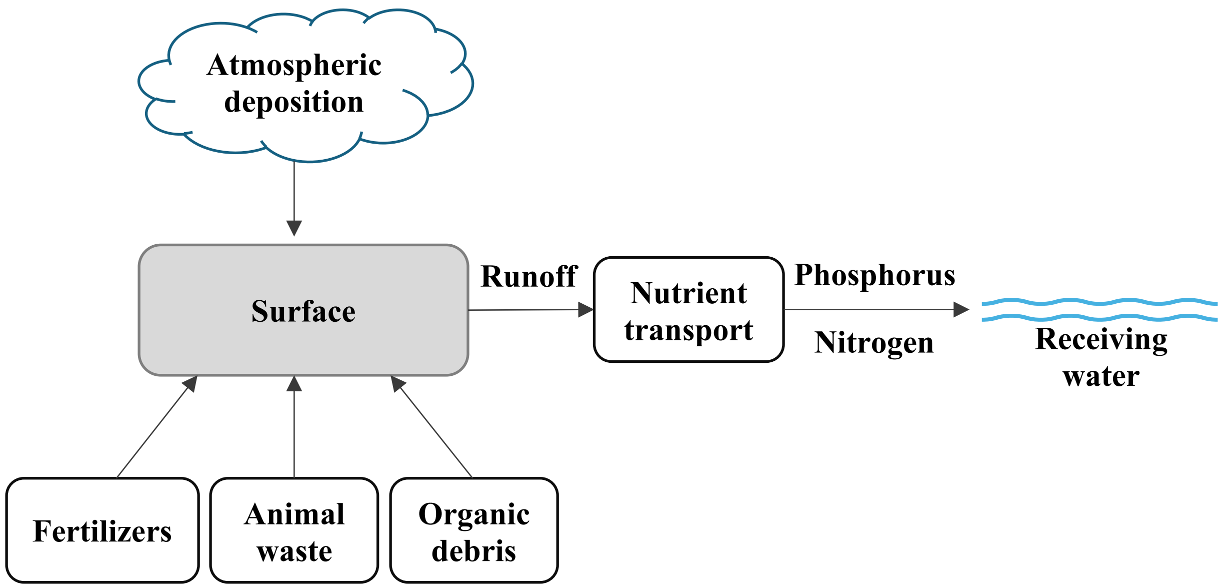

Figure 14. Nutrient transportation by stormwater runoff to the receiving water.

In many urbanized regions, conventional stormwater management systems, including curbs and gutters, pipelines, and detention basins, primarily focus on flood mitigation and lack provisions for treating or removing nutrients before discharge (Francis & Yang, 2020). Consequently, nutrient pollution originating from stormwater runoff has become a major environmental challenge, especially considering the implications of climate change and the increasing extent of impervious surfaces (Moazzem et al., 2024). To mitigate these challenges, stormwater management has evolved to incorporate green infrastructure strategies through Best Management Practices (BMPs) and Low Impact Development (LIDs), including rain gardens, infiltration trenches, vegetated swales, bioretention cells, and permeable pavements. These systems are designed to simulate pre-development hydrological conditions through retention, infiltration, and evapotranspiration, while also enhancing water quality through filtration and biochemical processes (Batalini de Macedo et al., 2021; USEPA, 2024b).

Among the emerging innovations in BMPs and LIDs is the strategic integration of engineered geotextiles and filter media specifically modified to enhance nutrient removal performance, as investigated in Chapter 5. While geotextiles have traditionally served as structural separators in systems like bioretention cells and infiltration trenches, recent research has explored their potential as reactive treatment layers. When amended with materials such as iron, aluminum, or biochar, these geotextiles can adsorb phosphorus, promote denitrification, and function as active filtration components rather than passive structural barriers (Li & Davis, 2016; Luo et al., 2020).

In this context, the integration of modified geotextiles into infiltration-based BMPs represents a promising approach to address urban nutrient pollution. This chapter reviews the sources of nitrogen and phosphorus in urban environments, assesses the effectiveness of traditional BMPs in mitigating nutrient loads, and examines emerging engineered materials designed to improve stormwater treatment. Additionally, Chapter 5 presents the results of a modified geotextile column test, which supports advances in scalable and sustainable stormwater management solutions.

4.2. Phosphorus and Nitrogen Sources

Phosphorus is a finite and non-renewable resource, essential to global food security due to its role in crop fertilization. However, its availability is limited by geopolitics. Approximately 85% of the world's phosphate reserves are concentrated in just eight countries, with Morocco and Western Sahara holding nearly 67% of the world's known phosphate supply (Figure 16) (U.S. Geological Survey, 2023). In the United States, active phosphorus mining occurs at ten mines across four states: Florida, North Carolina, Idaho, and Utah (U.S. Geological Survey, 2023).

Mining operations typically involve land disturbance by removing surface layers to access phosphate-rich formations, followed by beneficiation processes such as flotation, washing, and chemical treatment to produce usable fertilizer or phosphoric acid (Rout et al., 2023). Although post-mining land reclamation is required, it often takes several years to restore ecological function and control pollutant discharge.

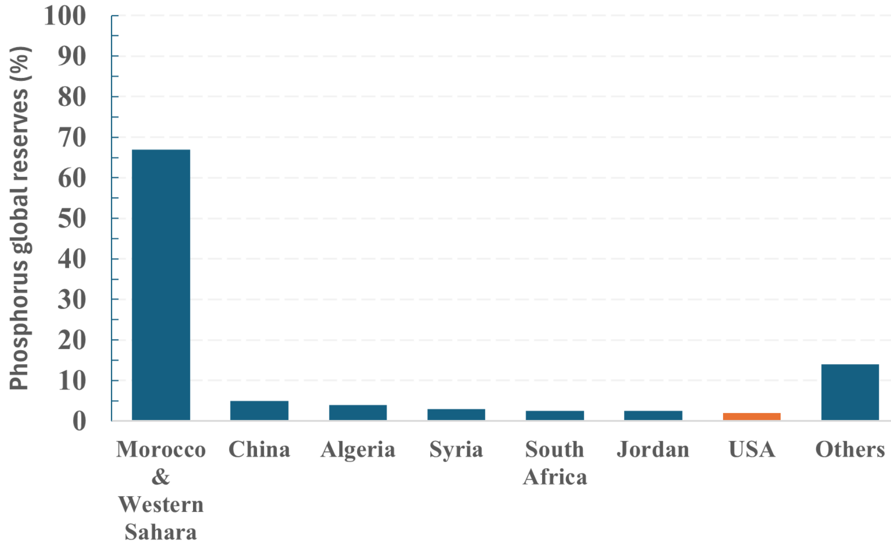

Figure 15. Global distribution of phosphorus reserves. Data from U.S. Geological Survey (2023).

Global phosphorus demand continues to increase. In 2024, the U.S. alone utilized approximately 20 million metric tons of marketable phosphate, with nearly 95% directed toward fertilizer and animal feed supplement production (U.S. Geological Survey, 2023). Worldwide, phosphorus fertilizer consumption exceeds 46 million tons annually, fueling food production for a growing population. However, an estimated 80% of this applied phosphorus is ultimately lost to the environment via leaching, surface runoff, or erosion from agricultural lands and urban areas (Cordell et al., 2009; Rout et al., 2023). These losses contribute significantly to freshwater eutrophication and coastal hypoxia, particularly in watersheds with intensive agriculture and rapid urbanization. As phosphorus has no known substitute in agriculture, resource recovery and reuse strategies are an urgency of capturing and recycling lost phosphorus to ensure long-term food security and protect water quality (Cordell et al., 2009).

Nitrogen, although abundant in the atmosphere as dinitrogen gas (N_2), is unavailable to most organisms in this inert form. To become biologically accessible, nitrogen must be converted into reactive forms such as ammonium (NH_4^+) and nitrate (NO_3^-), either through biological nitrogen fixation or industrial processes. Synthetic nitrogen fertilizers have significantly enhanced global food production; however, they have also introduced substantial environmental burdens, particularly when reactive nitrogen is lost to the environment (Cai et al., 2025). In urban and suburban areas, nitrogen enters stormwater runoff from lawn fertilizers, pet waste, vehicle emissions, atmospheric deposition, and leaking septic systems (Yang & Lusk, 2018).

Nitrogen undergoes a suite of biogeochemical transformations, including ammonification (conversion of organic nitrogen to ammonium), nitrification (oxidation of ammonium to nitrate under aerobic conditions), and denitrification (reduction of nitrate to nitrogen gases under anoxic conditions). These pathways regulate nitrogen availability and mobility but are sensitive to oxygen availability, pH, redox potential, and microbial community structure (Mosley et al., 2022; Smith, 2003). Nitrate, in particular, is highly soluble and prone to leaching through soils and into groundwater or surface runoff, contributing to eutrophication, harmful algal blooms, and hypoxia (Mosley et al., 2022).

Phosphorus and nitrogen are the two most critical nutrients associated with water quality degradation in urban catchments. Unlike point-source discharges, these nutrients typically originate from diffuse sources, are episodic, and are often linked to rainfall-driven mobilization of accumulated residues on impervious surfaces, requiring integrated management strategies to ensure effective control and mitigation (Hopkins et al., 2017). These biogeochemical dynamics emphasize the complexity of managing diffuse nutrient pollution in stormwater. While traditional BMPs provide only partial retention of nitrogen and phosphorus, engineered solutions, such as iron-enhanced filter media, biochar, and modified geotextiles, are increasingly used to promote sorption, precipitation, or biological transformation. These materials provide scalable opportunities to enhance the nutrient removal capacity of infiltration systems and promote sustainable watershed management.

4.3. Nutrient Control through Best Management Practices (BMPs) and Low Impact Development (LID): Processes, Performance, and Limitations.

Managing stormwater nutrients in urban areas increasingly depends on a combination of traditional engineering techniques and nature-based solutions. In this context, BMPs include various structural and non-structural strategies aimed at controlling water volume and improving stormwater runoff quality. Among these, LID is a relatively new, ecologically focused subset of

BMPs. It prioritizes decentralized, small-scale interventions designed to mimic natural hydrology through infiltration, evapotranspiration, and on-site treatment (Georgia DNR & EPD, 2016).

Structural BMPs consist of physical structures designed to intercept and treat runoff, such as bioretention cells, constructed wetlands, infiltration trenches, permeable pavements, and green roofs (Batalini de Macedo et al., 2021; Francis & Yang, 2020). Non-structural BMPs, on the other hand, focus on source control methods, such as fertilizer management, education programs, land-use planning, and other policies. While both approaches are important, structural BMPs are particularly effective at capturing and removing nutrients either at the runoff source or where it accumulates.

One prominent structural BMPs is the bioretention system, which has gained widespread use and research attention for its multifunctionality and adaptability to different urban environments. They usually consist of vegetated basins filled with engineered media, including sand, compost, and soil blends, that support infiltration, microbial activity, and sorption. When stormwater flows into these systems, nutrients such as phosphorus and nitrogen are either filtered through the soil, adsorbed onto particles, absorbed by plants, or transformed by microbial processes. Under ideal conditions, these systems have shown removal efficiencies of up to 92% for total phosphorus (TP) and 80% for total nitrogen (TN) (Ali et al., 2021; Luo et al., 2020). However, nutrient removal performance can vary significantly depending on site-specific factors related to media composition, vegetation, moisture levels, and loading rates. Nitrate removal, in particular, remains challenging because of its high solubility and the prevalence of aerobic conditions in many systems, which favor nitrification over denitrification. Studies indicate that systems without anoxic zones or sufficient carbon may even release nitrate (Ali et al., 2021).

Permeable pavements are a common BMP that serves a dual purpose: they support vehicle loads while allowing stormwater to infiltrate into subsurface layers. Their effectiveness in nutrient removal depends primarily on the design of these layers, including the type of aggregate, the filter media, and whether amendments such as geotextiles are incorporated. Studies report that phosphorus levels can be reduced by 30% to 80%, with outcomes influenced by system maturity, rainfall intensity, and retention time. Liu et al. (2020) observed that structural variations, particularly thicker sub-base layers, enhanced nutrient retention by extending contact time and storage. Similarly, Razzaghmanesh and Borst (2019) reported median reductions in total phosphorus of up to 65% in a long-term field study of three permeable pavement types. However, nitrate removal was consistently low or negative, especially under highly aerobic conditions lacking carbon inputs. These findings align with those of Collins et al. (2008), who compared four permeable pavement designs and found that although all reduced runoff volumes and peak flows significantly, water retention characteristics varied depending on joint fill and base storage capacity.

Constructed wetlands mimic natural wetland environments to improve stormwater treatment through sedimentation, plant uptake, microbial transformation, and chemical sorption. These systems are generally effective at retaining 40 – 50% total phosphorus and total nitrogen due to sediment retention and sorption, but nitrate removal tends to be inconsistent unless anoxic conditions are maintained (Georgia DNR & EPD, 2016). Vegetated swales, filter strips, and bioswales provide additional options for decentralized treatment by slowing runoff and promoting infiltration and nutrient uptake through plants and soils. However, like constructed wetlands, they have limited capacity for nitrate removal (Barrett, 2005).

Comprehensive analyses by Barrett (2005); Yu et al. (2013) and (Yu et al., 2013) show that wet ponds and constructed wetlands usually outperform other BMPs in nutrient removal because of longer retention times and anaerobic zones, achieving up to 80% phosphorus and 50% nitrogen removal. However, their use is limited by land availability and maintenance costs. Conversely, dry detention basins, though common, are less effective at reducing nutrients because they lack treatment media and have short residence times. Hopkins et al. (2017) highlighted that distributed BMPs, such as multiple small bioretention systems, are more successful at lowering peak flows and nutrient levels than centralized detention systems.

Green roof systems consist of vegetated layers installed on top of building surfaces, mainly functioning to retain rainfall and decrease peak runoff, while also providing thermal, ecological, and aesthetic benefits (Mihalakakou et al., 2023). From a water quality perspective, green roofs can reduce nutrient loading by slowing runoff and allowing partial retention or uptake by plants and substrate. However, their nutrient removal performance varies greatly and can sometimes be counterproductive, especially during the early stages of operation. Several studies have noted nutrient leaching, particularly of phosphorus and nitrogen, caused by the wash-off of excess nutrients from newly installed growing media or fertilizers used to establish vegetation (Akther et al., 2021; Marín et al., 2023). Over time, this leaching generally decreases as nutrients are depleted or stabilized, and under certain conditions, green roofs may become nutrient sinks, depending on the media composition, vegetation type, and local hydrometeorological conditions (Akther et al., 2021). Extensive green roofs with shallow media typically have lower retention capacity than intensive systems, which can support more diverse vegetation and deeper substrates. Although their nutrient reduction efficiency may not match other BMPs such as constructed wetlands or bioretention cells, green roofs offer distributed treatment benefits and valuable co-benefits in urban areas with limited space (Marín et al., 2023).

Despite its broad implementation, several persistent challenges continue to undermine BMP effectiveness. Seasonal temperature variation affects microbial activity and plant uptake, particularly during cold periods when denitrification slows. Maintenance practices are also critical to sustaining performance. These involve sediment removal, vegetation upkeep, and periodic replacement of the filter media, yet they are often applied inconsistently. Long-term studies reveal that phosphorus removal efficiency declines over time as sorption sites become saturated (Francis & Yang, 2020). Moreover, design limitations and the absence of standardized performance assessment complicate comparisons and generalizations due to the variability introduced by storm size, antecedent conditions, and pollutant concentrations.

To address these limitations, several innovations have been implemented in BMP systems. Media composition with iron-amended sands, alum, and biochar enhances nutrient sorption and facilitates microbial transformations. Studies have shown that the inclusion of biochar, pyrite, and alkaline solid waste improved nitrogen removal, particularly through denitrification under anoxic conditions. For instance, internal water storage designs amended with biochar or iron oxides demonstrate synergistic performance by extending retention times and providing reactive surfaces for phosphorus adsorption (Ali et al., 2021; Rodgers et al., 2024). These material-based innovations set the stage for a new generation of BMPs with improved consistency and multifunctionality, while offering scalable solutions, particularly in space-constrained urban environments.

Traditionally, geotextiles have been used as structural separators within infiltration trenches and permeable pavements, preventing subgrade mixing and stabilizing pavement layers. However, recent studies suggest that geotextiles, especially when chemically modified, could serve as reactive filters for nutrient retention and even potential recovery (Monrose et al., 2019; Tota-Maharaj & Paul, 2015). To evaluate the current state of research on geotextiles in stormwater BMPs, a systematic literature review was conducted using the keywords "geotextile," "stormwater," and "nutrient removal" across six major databases (ScienceDirect, SpringerLink, Scopus, Taylor & Francis, Web of Science, and Wiley Online Library). After removing duplicates, 147 records were screened. The first selection and eligibility criteria were based on title review, with only papers related to stormwater management performance included. A total of 69 papers were selected for further review. In the second stage, two eligibility criteria were applied: (1) the application of geotextile (Y/N classification—all papers discussing green structures incorporating geotextile were included), and (2) a focus on water parameter analysis (only papers reporting water quality parameters were considered). Based on these criteria, 30 papers were deemed eligible.

The initial review classified these studies according to the type of BMP where geotextiles were used. Among them, 14 focused on bioretention systems, four on permeable pavements, and three each on constructed wetlands and green roofs (Figure 17). This strong focus on bioretention, making up nearly half of all eligible studies, emphasizes the widespread acknowledgment of this system's flexibility and appropriateness for incorporating geotextile enhancements. However, the relatively small number of studies on permeable pavements, wetlands, and green roofs indicates that the use of geotextiles in these systems has received limited attention. These gaps suggest potential research opportunities, especially considering the increasing popularity of these BMPs in decentralized urban stormwater management. From an implementation perspective, the underrepresentation of modular BMPs, such as permeable pavements and green roofs, is particularly notable given their compatibility with geotextile integration and their use in retrofit projects.

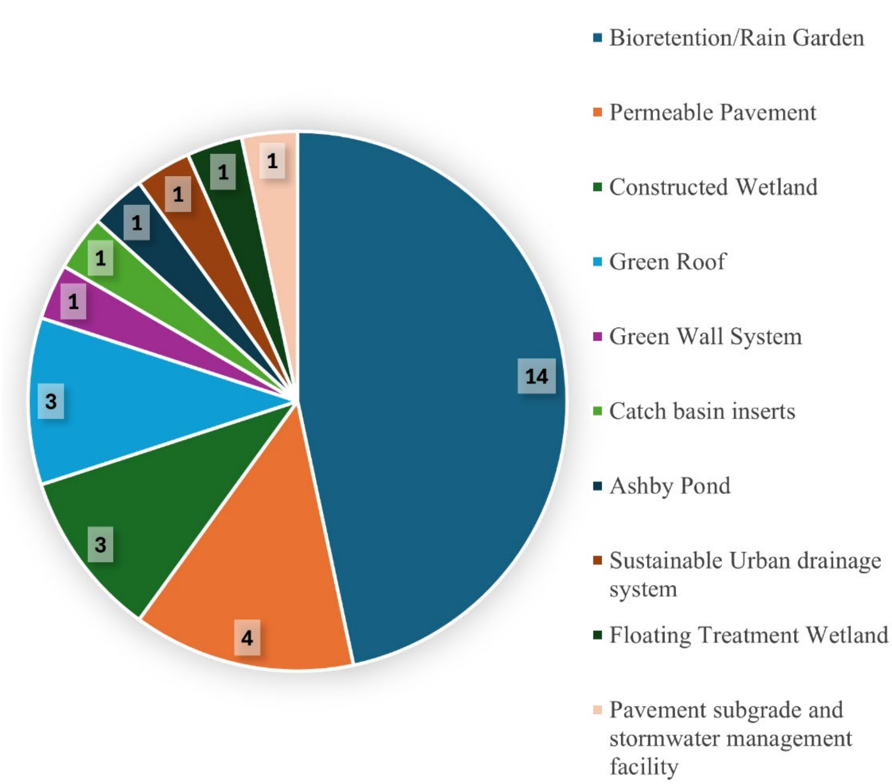

Figure 16. Overview of best management practice types applied for nutrient mitigation in stormwater runoff (n = 30 studies).

When examining how geotextiles were used across the reviewed studies, the most common application, reported in 14 papers, was as a layer separator to prevent subgrade contamination and minimize particle migration between media layers (Figure 18). This function aligns with traditional engineering practices, where geotextiles primarily serve to maintain the physical integrity of filtration systems and prevent clogging. However, only four studies explicitly investigated the use of geotextiles for pollutant removal, revealing their underused potential for improving water quality beyond conventional applications. Two studies employed geotextiles as biofilm support materials, suggesting possible roles in enhancing microbial transformation processes, particularly for nitrogen. Two additional uses were categorized under "other" uses, including hydraulic modification and runoff redirection strategies. Notably, eight papers did not clearly specify the geotextile's function, reflecting the need for more explicit reporting in BMP performance literature.

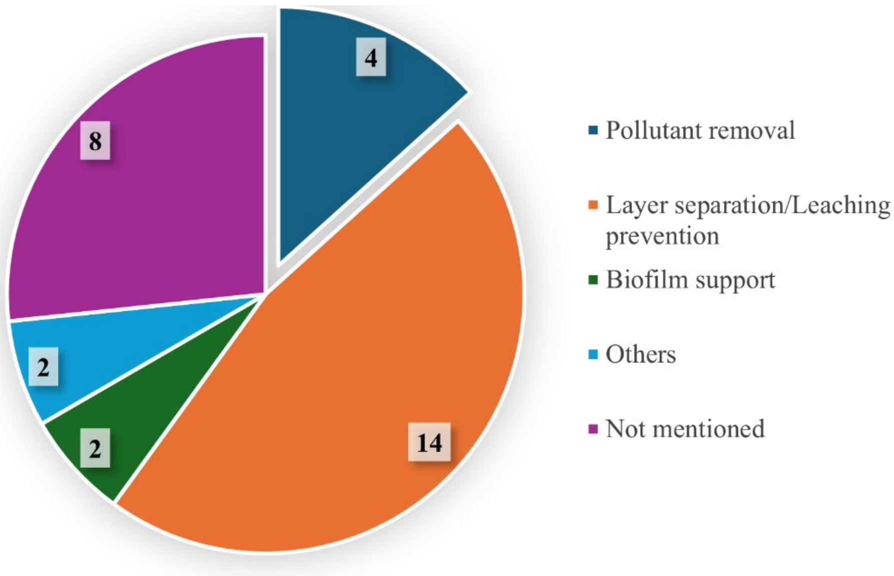

Figure 17. Geotextile function in best management practices (n = 30 studies).

While geotextiles have traditionally been applied in stormwater systems as structural components, an emerging body of research is reimagining their role as active treatment media. Recent studies, such as those by Bodus et al. (2024) and Li et al. (2024), explore membrane-embedded or chemically modified geotextiles designed to promote nutrient sorption, particularly for phosphorus and ammonium. These innovations represent a conceptual shift: from passive filtration barriers to reactive interfaces that enhance nutrient removal. In several configurations, geotextiles were strategically placed in the upper BMP layers to increase interaction with incoming runoff and maximize exposure to reactive additives, such as iron oxides or biochar. Despite these advances, most applications remain in early developmental phases, with limited assessment of long-term performance, saturation thresholds, or regeneration feasibility.

Addressing urban nutrient pollution requires integrated and adaptive management strategies. A single BMP rarely suffices to meet regulatory standards like Total Maximum Daily Loads (TMDLs), especially in highly urbanized catchments. Integrated watershed planning, which combines source control, spatial BMP allocation, and community engagement, offers a more sustainable and effective approach. For example, the Low Impact Development Handbook for Alabama underscores the importance of combining structural and non-structural practices to maximize pollutant removal and improve long-term performance (ADEM, 2014). Likewise, the Georgia Stormwater Management Manual emphasizes the effectiveness of treatment trains and multiple BMPs in series to achieve regulatory compliance (Georgia DNR & EPD, 2016). The USEPA offers tools, such as the National Stormwater Calculator, to simulate runoff and assess BMP configurations at the watershed level (USEPA, 2022). These tools and guidelines help municipalities and transportation agencies adopt adaptive, performance-based stormwater solutions (Lantin et al., 2019).

Policy and education also play essential roles. Public support for BMPs depends on awareness and perceived benefits. Maintenance incentives and clear performance standards can help ensure that systems work properly over the long term. Research by Sousa et al. (2021) indicates that the absence of broader education and performance-based evaluation criteria limits the effectiveness of BMPs in urban settings, particularly as climate change intensifies the frequency and severity of storm events. In a similar tropical urban context, (Batalini de Macedo et al., 2021) show that bioretention systems can greatly reduce runoff and support aquifer recharge. However, these systems are often used without structured monitoring or formal performance assessment. Innovative materials, such as modified geotextiles, which combine structural support with pollutant removal capabilities, are a valuable yet underutilized solution.

4.4. Iron-enriched materials for nutrient removal

Nutrient removal in stormwater treatment systems depends on physical, chemical, and biological processes within BMP components. Filtration plays a central role, especially for particulate-bound nutrients like phosphorus, which are physically retained as runoff infiltrates porous media (Francis & Yang, 2020). For dissolved phosphorus, chemical adsorption and precipitation are key mechanisms, often mediated by metal oxides such as iron and aluminum. In bioretention systems amended with metal-based adsorbents, these processes are enhanced through ligand exchange, a reaction in which phosphate ions replace hydroxyl or water molecules that are weakly bound to the metal oxide surface, and co-precipitation, where phosphate is immobilized as part of newly formed insoluble mineral complexes s (Jin et al., 2024; Liu et al., 2022). In contrast, nitrogen removal, particularly for nitrate, relies more heavily on microbial processes such as nitrification and denitrification. These transformations occur through alternating aerobic and anaerobic conditions, ultimately converting nitrate into inert nitrogen gas (Ali et al., 2021). The inclusion of saturated zones, organic substrates, and carbon-rich materials, such as compost or biochar, can enhance denitrification efficiency by supporting microbial activity and extending the residence time. Plant uptake may offer additional nutrient removal, although it is typically constrained by seasonal growth and nutrient availability (Moazzem et al., 2024).

The underlying chemistry of phosphate removal relies on iron's ability, particularly in its ferric (Fe^{3+}) form, to bind phosphate (PO_4^{3-}) through ligand exchange and precipitation, forming low-solubility iron-phosphate complexes. These reactions are most stable under aerobic conditions and moderate pH levels, where Fe^{2+} is oxidized and facilitates sustained phosphorus capture. As shown in Luo et al. (2020), iron hydroxides possess high surface areas and numerous reactive sites, making them especially effective in stormwater filters. However, the effectiveness of this mechanism is highly dependent on environmental conditions. Under acidified or anaerobic environments, these iron-phosphate bonds can become unstable, potentially releasing previously captured phosphorus back into the water column.

Studies investigating iron-enriched media in bioretention systems and infiltration filters used iron sources including iron filings, ferric chloride, iron-coated sands, and iron-modified biochar. Luo et al. (2020) found that biochar amended with ferric nitrate achieved up to 90%TP removal while maintaining favorable hydraulic performance. Similarly, Rodgers et al. (2024) demonstrated that adding 5–10% iron-based materials to bioretention media significantly improved phosphate adsorption compared to unmodified control systems, especially during high-flow events. Despite these performance benefits, a new challenge is the episodic nature of stormwater events. Sudden runoff surges can overwhelm conventional media, shortening contact times and decreasing phosphorus capture. Iron-rich filters mitigate this through high reaction rates and low solubility, maintaining high efficiency even during rapid inflow events.

Moreover, Ai et al. (2023) evaluated the long-term P removal efficiency of industrial iron shavings and found they maintained above 60% total phosphorus removal over 60 days in column experiments. The study also tested regeneration techniques, achieving phosphorus recovery rates of approximately 58% with NaOH treatment and up to 79.1% using induction heating. Li and Davis (2016) demonstrated that incorporating iron-enhanced media in bioretention systems can double phosphorus removal efficiency, increasing average TP removal to over 80%. Additionally, Yang et al. (2021) found that introducing an in a hydroxyaluminum and modified vermiculite sludge particle (HAVSP) (5-7% iron content) in bioretention columns, improved TP removal from 57% to 93% and total nitrogen removal from around 65% to over 80%, even under variable hydraulic loading. Liu et al. (2022) discussed how embedded iron oxides impart magnetic properties to the BMP, allowing for better recovery of removed components. Similarly, Shin et al. (2023) introduced a magnetic carbonaceous adsorbent synthesized via co-pyrolysis of spent coffee grounds and steel slags, where iron oxides (Fe_3O_4 and Fe_2O_3) played a central role in phosphate immobilization through electrostatic complexation and chemisorption. The embedded iron oxides' magnetic properties also enabled over 90% recovery of the adsorbent, highlighting a dual benefit for phosphate capture and material reuse.

While most applications have focused on granular media, the integration of iron into geotextiles introduces a novel configuration. These fabrics, typically composed of nonwoven polypropylene, can be coated with iron oxides or impregnated with fine iron particles to form reactive membranes. When placed near the surface or between infiltration layers, these modified geotextiles serve as immediate barriers to nutrient migration. Okaikue-Woodi et al. (2020) discussed the potential of engineered fabrics and other reactive materials to enhance phosphorus capture, highlighting their multifunctionality in removing multiple contaminants. This multifunctionality underscores the promise of reactive fabrics as scalable tools in integrated stormwater infrastructure.

However, iron-based systems are not without limitations. Over time, the saturation of reactive sites can reduce phosphorus retention, especially in regions experiencing frequent or intense rainfall events. Ali et al. (2021) emphasized that performance is closely linked to design parameters such as iron particle size, media thickness, contact time, and phosphorus speciation. Additionally, there is a need to monitor for potential iron leaching, particularly in acidic or anoxic environments where dissolved Fe^{2+} may mobilize. While concentrations are typically low, long-term use demands life-cycle assessments to evaluate trade-offs, including potential toxicity to aquatic life if released downstream. Moreover, coupling iron with biochar may help buffer pH shifts and extend adsorptive lifespan while simultaneously supporting nitrogen removal via microbial pathways (Moazzem et al., 2024).

Iron-enriched materials represent a significant advancement in nutrient-targeted BMPs. When used in infiltration systems, especially with modular, surface-level setups like iron-modified geotextiles, they deliver quick, stable, and space-efficient phosphorus removal. Chapter 5 expands on these findings by assessing a hybrid geotextile treated with iron for nutrient removal.

Chapter 5: Column Testing of Modified Geotextiles for Nutrient Removal from Stormwater Runoff

Building on the literature review of nutrient sources and treatment strategies presented in Chapter 4, Chapter 5 presents the results of laboratory column tests designed to evaluate the nutrient removal performance of geotextile materials modified with iron. The experimental setup aimed to simulate infiltration-based stormwater treatment and assess the removal of total nitrogen (TN) and total phosphorus (TP) across different configurations and application doses. This chapter describes the methodology, reports key findings, and discusses the implications of using engineered geotextiles in stormwater management systems.

5.1. Introduction

Nutrients like phosphorus (P) and nitrogen (N) are common pollutants in stormwater runoff. Their presence isn't limited to agricultural areas; in urban environments across the U.S., including residential, commercial, industrial, and mixed-use zones, median concentrations of total phosphorus and total nitrogen in runoff are around 0.2–0.3 mg/L and 1.2–1.7 mg/L, respectively, with higher values sometimes recorded (National Academies of Sciences, 2019; Pitt et al., 2018). Although these nutrients are vital for aquatic ecosystems, elevated levels can have harmful effects, particularly eutrophication.

Eutrophication is the process in which nutrient enrichment, primarily phosphorus and nitrogen, leads to excessive growth of algae and cyanobacteria. This rapid productivity can block sunlight, lower dissolved oxygen, and harm aquatic food webs, often leading to fish kills and biodiversity loss (Dodds et al., 2008; USEPA, 2025b). Fixing eutrophic water bodies is complicated and expensive, requiring management of nutrient sources and biological communities at the same time (Paerl et al., 2016).

Preventing nutrient pollution at its source is more effective than trying to fix it afterward. Urban stormwater runoff is a major way nutrients are transported, making the use of nature-based solutions like green infrastructure (GI) and best management practices (BMPs) essential (Kong et al., 2024; USEPA, 2025a). BMPs such as infiltration trenches, bioretention systems, and green roofs are commonly used to encourage infiltration and remove pollutants. However, traditional BMPs often have limited ability to remove dissolved nutrients, especially phosphorus, and in some cases, they may even cause nutrient leaching (Luo et al., 2020; Yang & Lusk, 2018).

This research explores a minimally invasive method to enhance existing BMPs by modifying only one layer—the filter fabric or geotextile—rather than redesigning the entire structure. Iron compounds are known for their strong affinity for phosphate, enabling both effective removal and potential recovery of phosphorus, a limited and geopolitically sensitive resource (Marvin et al., 2020; Withers et al., 2015). Incorporating this modified layer into existing systems without structural redesign supports cost-effective implementation and long-term scalability. Approaches to implementing iron-enriched media include integrating the modified geotextile as a replaceable layer within the surface treatment zone, embedding it between the soil media and drainage layer, or installing it as modular inserts in infiltration systems. These strategies allow for flexible deployment in bioretention areas, infiltration trenches, or green roof assemblies, supporting long-term performance and ease of maintenance without requiring major structural changes (Marvin et al., 2020; Withers et al., 2015).

In addition to improving retention, iron-based hybrid fabrics provide a potential secondary benefit. Since phosphorus is a limited resource, the ability to recover it from saturated filters supports current efforts to promote circular phosphorus management and reduce dependence on phosphate rock, which is becoming more scarce and geopolitically sensitive (Sarvajayakesavalu et al., 2018; U.S. Geological Survey, 2023). Laboratory column tests are an effective initial step for assessing the performance of these materials under controlled conditions that mimic field infiltration. The outcomes of these tests support early-stage design validation and guide future pilot-scale systems.

This study is part of the project "Non-woven hybrid geotextiles for urban stormwater nutrient management," a collaborative effort among Auburn University, the University of South Alabama, and Wake Forest University. The project aims to design, synthesize, and evaluate innovative geotextiles embedded with adsorptive materials to improve nutrient removal in stormwater BMPs. The need for better performance is urgent because traditional GI systems have sometimes acted as net exporters of nutrients, especially during early operation or under high loading conditions (Barrett, 2005). Therefore, this chapter presents the results of laboratory column tests comparing the performance of the hybrid geotextile, a standard commercial geotextile, and a no-fabric control setup in removing phosphorus and nitrogen from synthetic stormwater. By exposing these systems to both blank and nutrient-dosed stormwater, the experiment aims to quantify the effectiveness of modified geotextiles in removing nitrogen and phosphorus, and to provide evidence for their potential implementation in sustainable stormwater practices. The findings provide a foundation for future design iterations and field validation of iron-enriched fabrics for scalable use in urban stormwater management systems. The results will help develop improved BMP designs and guide future applications in engineered stormwater systems.

5.2. Materials and Methods

This section describes the materials, column design, and testing procedures used to evaluate the nutrient removal efficiency of standard and iron-modified geotextiles under controlled laboratory conditions. All tests were performed using synthetic stormwater with known nutrient concentrations to assess treatment performance across various dosing conditions. The methods were designed to mimic real-world infiltration scenarios while ensuring consistency and reproducibility.

5.2.1. Column Design and Material Composition

A series of laboratory mid-scale column tests was conducted to assess the capacity of geotextile-amended infiltration systems for removing nutrients from urban runoff. The columns were designed to simulate the vertical flow and material layering of infiltration trenches typically used in stormwater BMPs. The layer configuration followed the specifications outlined in the Georgia Department of Transportation Drainage Manual (GSMM, 2016). Each column was constructed using a 6-inch (15.24 cm) diameter PVC pipe with a height of 3 feet (91.4 cm), allowing for a representative media depth and sufficient detention volume.

Three column configurations were evaluated. Control column (no geotextile): layered with sand, pea gravel, and #57 gravel (Figure 19a); Standard geotextile column: same media layers as the control, with a commercial non-woven geotextile layer placed between the sand and pea gravel (Figure 19b); and Modified geotextile column: identical to the standard configuration but incorporating an iron-enriched geotextile developed by collaborators at the University of South Alabama (Figure 19b). The geotextile was dosed with iron at the University of South Alabama by submerging the fabric in a 0.25 M $FeCl_3$ solution at a 10:1 iron-to-material mass ratio and gently agitating it on a shaker table for 1.5 hours. To promote iron precipitation and fixation, 10 M NaOH was added slowly over a 3-hour period until the pH reached approximately 8.5–9.5. After dosing, the geotextile was air-dried for 4 to 7 days. This procedure allowed effective iron incorporation while maintaining the geotextile's structural integrity and permeability.

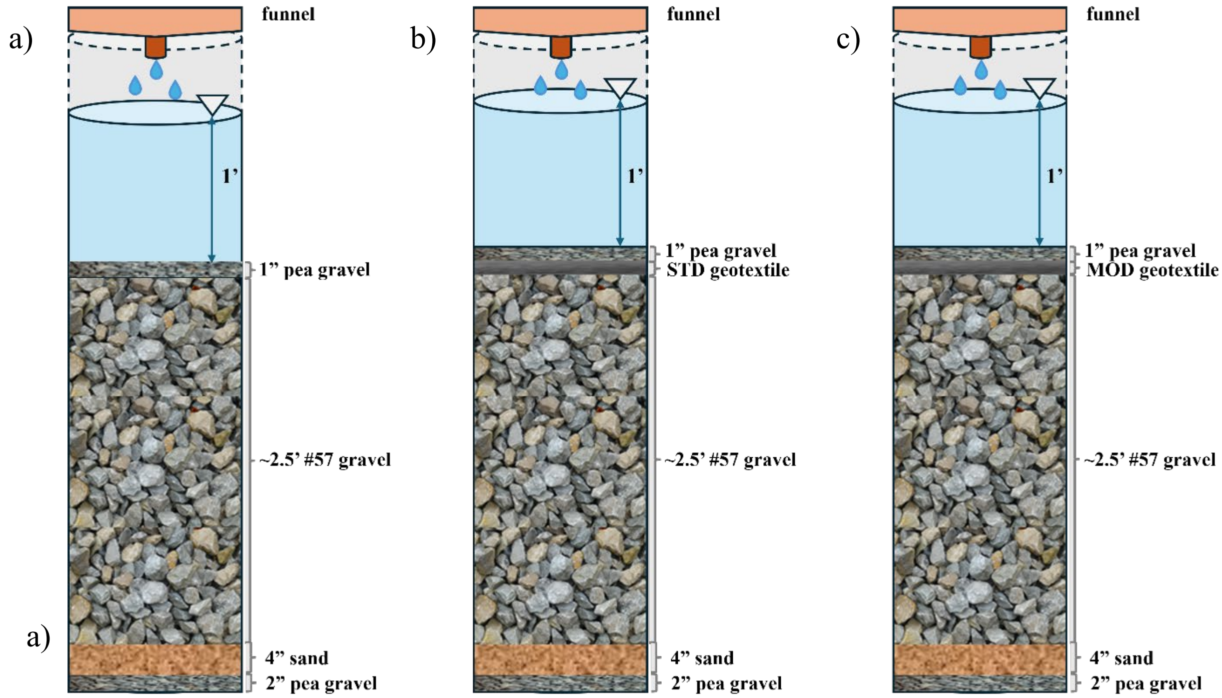

Figure 18. Infiltration Trench column test design: a)no geotextile, b)with the standard geotextile layer, and c) with iron-modified geotextile layer. Not drawn to scale.

The sand used in all columns was a commercial masonry-grade all-purpose sand (Quikrete®), while the pea gravel and #57 gravel were also sourced from Lowe's®. The standard geotextile employed was a non-woven, needle-punched polypropylene filter fabric (Super Geotextile®), selected for its high permeability and large specific surface area, which are advantageous for filtration and potential nutrient adsorption. Unlike woven alternatives, non-woven geotextiles allow for greater water flow and interaction with embedded media, making them suitable for stormwater applications requiring rapid drainage and contact with treatment layers. These fabrics are also known for their durability, UV resistance, and dimensional stability, which support long-term use under varying hydraulic conditions. To ensure a consistent flow and retention of fine media, all columns are equipped with an 80-mesh (0.18 mm pore size) screen at the base. All materials were packed uniformly, maintaining consistent thickness across the configurations. The resulting design reflects typical field-scale infiltration trench compositions while enabling controlled laboratory testing of nutrient removal performance.

Two sets of column tests were conducted to evaluate the influence of geotextile configuration on nutrient removal performance. The first test series used a single geotextile layer between sand and pea gravel. In this setup, the standard geotextile fabric was cut into strips to mimic the dimensions of the modified geotextile samples received from the University of South Alabama (Figure 20). Each configuration was tested under blank (non-dosed) and nutrient-dosed conditions, with three replicates conducted for each. The second and third test series incorporate a dual-layer geotextile configuration, consisting of the same base setup as the first series with an additional full layer of fabric placed above the first fabric layer. This arrangement aimed to maximize the contact surface area between the influent water and the modified geotextile material, enhancing nutrient adsorption (Figure 20).

Figure 19. Geotextile placement configurations used in the column tests: standard and modified geotextiles.

5.2.2. Experimental Setup: Blank and Dosed Conditions

The testing procedure was conducted in two phases: blank testing to assess baseline leaching from the column materials and dosed testing to evaluate nutrient removal performance under elevated concentrations representative of stormwater runoff.

In both phases, each column was flushed for 1 hour to clean and settle the material. This pre-flush procedure helped stabilize background nutrient contributions from media components, ensuring accurate baseline readings. For the test, columns were filled with a constant 1-foot head of water (approximately 7.2 L) and allowed to infiltrate under gravity. Between each test cycle, a two-day dry period was imposed to mimic natural drying and wetting conditions.

Under blank conditions, the columns were exposed only to tap water without simulated nutrient spikes (influent). For the nutrient dosing test, influent water was spiked with potassium phosphate monobasic (KH_2PO_4, molecular weight = 136.1 g/mol) as the phosphorus source and ammonium sulfate ($(NH_4)_2SO_4$, molecular weight = 132.14 g/mol) as the nitrogen source (Table 6). The final target concentrations were 0.4 mg/L of total phosphorus and 4.5 mg/L of total nitrogen. The third test set, with a high nutrient load, was prepared with a final target of 0.8 mg/L of total phosphorus and 6.0 mg/L of total nitrogen.

Table 6. Experimental setup for nutrient removal tests using geotextile columns

Test	Geotextile layer	Blank Test Duration	Blank TP conc. (mg/L as phosphate)	Blank TN conc. (mg/L as phosphate)	Dosed Test Duration	Dosed Test TP conc. (mg/L as phosphate)	Dosed Test TN con. (mg/L)
Test 1	1 layer	3 days	0.45 – 0.55	0.2-0.6	3 days	1.5	4.5
Test 2	2 layers	1 day	0.45 – 0.55	0.2-0.6	3 days	1.5	4.5
Test 3	2 layers	None	0.45 – 0.55	0.2-0.6	3 days	3	6

5.2.3. Sampling and Analytical Procedures

Effluent samples were collected at the base of each column after every infiltration event and analyzed for total nitrogen (TN) and total phosphorus (TP). These nutrients were quantified using colorimetric techniques based on Hach Test 'N Tube™ kits, following EPA-approved protocols. All analyses were performed using the Hach DR3900 VIS spectrophotometer for absorbance measurements, and digestion was conducted with the Hach DRB200 Reactor to ensure consistency in reaction temperatures.

The determination of total nitrogen was conducted using the Hach Method 10071. In this method, 2 mL of the sample was transferred into a Total Nitrogen digestion tube containing persulfate reagent. The tube was sealed and vigorously mixed by inversion. The digestion step involved heating the sample at 105 °C in the DRB200 Reactor for 30 minutes. After digestion, the tubes were left to cool to room temperature. One Total Nitrogen Reagent A pillow was then added to each tube, followed by gentle inversion and a 3-minute resting period. One pillow of Reagent B was then added, followed by gentle inversion and a 2-minute resting period. Subsequently, a 2 mL aliquot of the digested sample was transferred into a second tube containing Reagent C and mixed by inverting the tube ten times. After a 5-minute reaction period, the sample was wiped clean and placed into the DR3900 spectrophotometer, and the nitrogen concentration was recorded in mg/L.

The analysis of total phosphorus followed the Hach Method 8190. In this procedure, 5 mL of sample was added to a TP digestion vial along with a phosphorus persulfate reagent pillow. The contents were mixed and digested at 150 °C for 30 minutes in the DRB200 Reactor. After cooling, 2 mL of 1.54 N sodium hydroxide solution was added to neutralize the acidified sample. A PhosVer® 3 reagent pillow was then introduced to initiate the colorimetric reaction. The vial was mixed by inversion for 20 to 30 seconds, and the sample was allowed to react for two minutes at room temperature. The tube was then inserted into the DR3900 spectrophotometer, and the phosphorus concentration was measured as mg/L of phosphate (PO_4^{3-}).

In addition to nutrient measurements, general water quality parameters were monitored during each test cycle to assess the physicochemical conditions influencing nutrient transport and removal. Parameters including pH, electrical conductivity (EC), total dissolved solids (TDS), and temperature were measured using an Oakton® PCTSTestr™ 30 multiparameter probe, while turbidity was measured with an Oakton® Portable Turbidity Meter calibrated with standard solutions. These indicators were monitored before (Control/Influent) and after (Dose/Effluent) infiltration through each column configuration. The comparison of NO, STD, and MOD geotextile treatments provides insight into the passive effects of these materials on common stormwater quality parameters.

All samples were analyzed in triplicate to ensure statistical reliability. Nutrient removal efficiency was calculated as the percent difference between influent and effluent concentrations. The effect of geotextile configuration on nutrient attenuation was evaluated across treatment conditions and is discussed in detail in Section 5.3.2.

5.3. Results and Discussion

To evaluate the performance of modified and standard geotextiles for nutrient removal, multiple water parameters were monitored throughout the column tests. The results presented in the following sections include water quality indicators, nutrient concentrations, and removal efficiencies under different dosing and layering configurations.

5.3.1. Water Quality Parameters: pH, EC, TDS, Turbidity, and Temperature

The first set of analyses focused on background water quality parameters, pH, electrical conductivity (EC), total dissolved solids (TDS), turbidity, and temperature. These were evaluated separately for blank and dosed test conditions.

5.3.1.1. Blank test condition

In Test 1, blank tests were performed in triplicate for each geotextile configuration (NO, STD, MOD), while only one replicate was conducted per treatment to be a baseline if necessary for Tests 2 and 3. Across both tests, water quality parameters showed minimal deviations between influent and effluent conditions (after going to the column), indicating limited interaction between the media layers and the input solution under baseline loading.

In the blank test 1, pH values remained relatively stable across replicates, averaging 6.90 (STD/MOD – influent) to 7.05 (NO – influent), effluents showed a more concise value, ranging from 6.94 (STD – blank) to 7.02 (MOD – effluent) (Fig. 21a). Electrical conductivity decreased slightly in all treatments, with the NO geotextile condition dropping from 155.57 µS/cm in the influent to 100.63 µS/cm and the MOD geotextile condition dropping from 157.37 µS/cm to 85.53 µS/cm (Fig. 21b). Similarly, total dissolved solids decreased from approximately 115.67 mg/L (NO–influent) to 72.67 mg/L (NO–effluent) and from 144.7 (STD/MOD–influent) to 59.93 mg/L (STD – effluent) and 51.60 mg/L (MOD–effluent) (Fig. 21c).

The temperature was consistent across treatments, ranging from 19.7 °C to 20.7°C, reflecting the stability of the laboratory environment (Fig. 21d). Turbidity increased after the columns for all conditions, with the NO geotextile showing the greatest rise (+13.26 NTU compared to the influent). For the STD and MOD, the increases were 0.78 and 0.32, respectively (Fig. 21e).

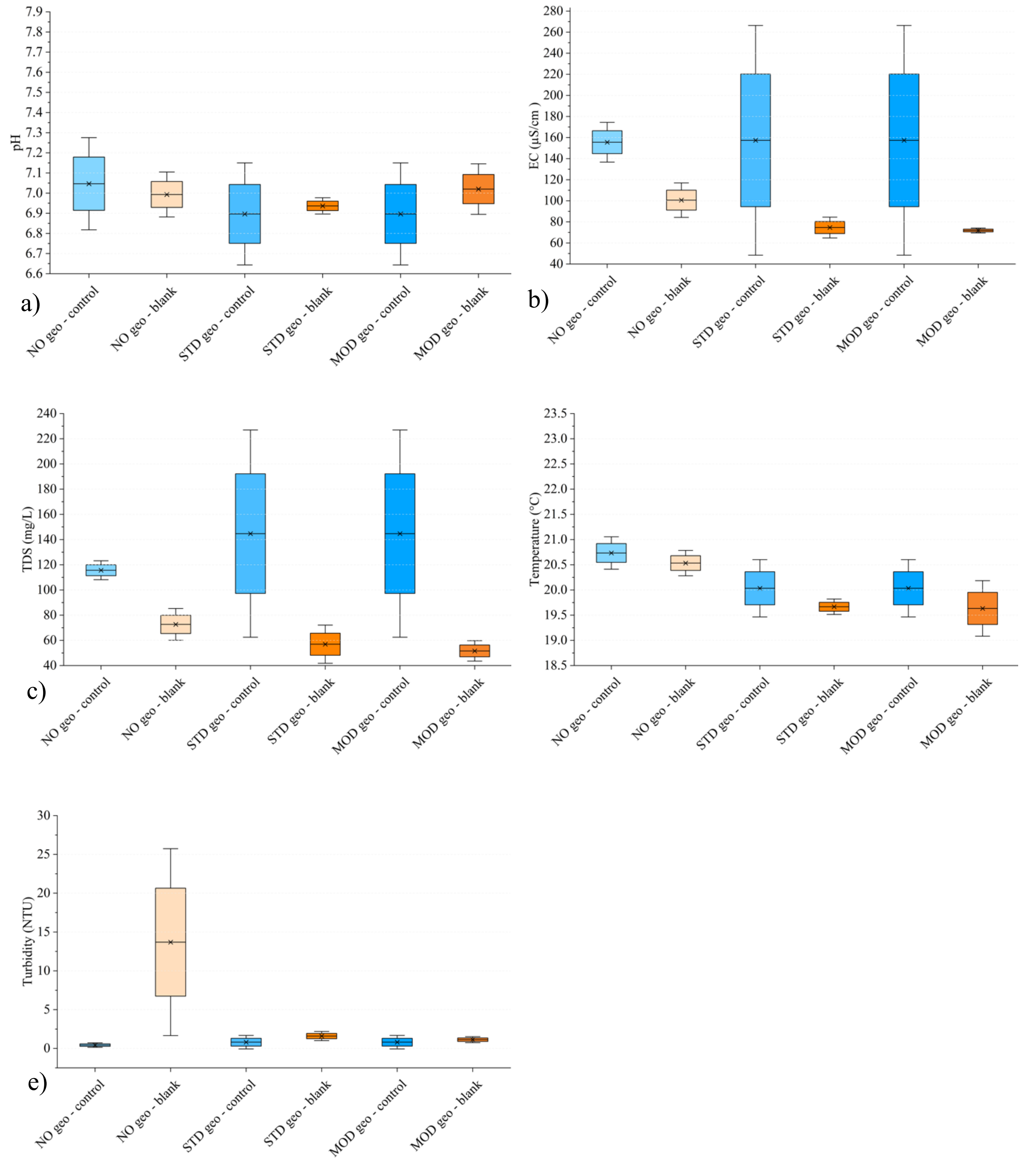

Figure 20. Water quality parameters for blank Test 1: a) pH, b) electrical conductivity (EC), c) total dissolved solids (TDS), d) temperature, and e) turbidity.

In Test 2, blank tests were conducted with only one replicate per configuration. Despite this limitation, results were generally consistent with those observed in Test 1. Effluent pH increased slightly across all treatments, ranging from 7.46 (NO) to 7.55 (MOD), compared to their respective influents. Electrical conductivity remained stable, with small variations (±2 µS/cm), and TDS followed a similar trend. Turbidity increased for all effluents, with the greatest rise present in the MOD (from 0.53 NTU to 9.96 NTU), suggesting possible leaching or particle mobilization from the media during initial wetting (Table 7). This effect may be attributed to entrapped fines in the iron-enriched fabric or incomplete flushing prior to testing. The temperature difference between the influent and effluent was lower than 2 °C.

Table 7. Water quality parameters (pH, electrical conductivity (EC), total dissolved solids (TDS), temperature, and turbidity) for blank test 2.

Parameter	NO geo – influent	NO geo – effluent	STD geo – influent	STD geo – effluent	MOD geo – influent	MOD geo – effluent
pH	7.39	7.46	7.44	7.52	7.48	7.55
EC (µS/cm)	119.8	121.9	121.9	119	117.4	121.8
TDS (mg/L)	85.8	87.5	87.5	84.5	82.4	87
Temp (°C)	18.5	16.6	16.6	16.5	16.1	16.4
Turbidity (NTU)	0.52	5.91	0.56	2.86	0.53	9.96

Overall, the blank tests confirm that under low-nutrient conditions, geotextile-modified infiltration columns have a limited influence on chemical parameters such as pH, EC, or TDS, but can meaningfully impact turbidity, depending on the configuration. The unexpected turbidity in MOD geo (Test 2) highlights the need to precondition the media to avoid transient leaching effects in early infiltration cycles; higher washing time may be required.

5.3.1.2. Dose test condition

Figure 22 presents the pH results for Test 1, Test 2, and Test 3, comparing influent (control) and effluent (dose) conditions across the three column configurations—NO geo (no geotextile), STD geo (commercial nonwoven geotextile), and MOD geo (iron-enriched geotextile). In Test 1, the NO geo column showed a slight decrease in pH from approximately 7.3 to 7.0, while in the STD geo column, the pH increased from 6.9 to 7.1. In the MOD geo column, the pH remained stable around 7.0. In Test 2, all treatments exhibited a shift toward higher pH values in the effluent. The NO geo column showed a modest increase from 7.45 to 7.55, and the STD geo column displayed a similar rise to 7.6. The MOD geo column again demonstrated the strongest buffering capacity, maintaining a stable pH of approximately 7.6. This increasing trend persisted in Test 3, where the MOD geo column showed the highest effluent pH at around 7.75. Overall, pH remained within the neutral range across all tests.

This pH behavior appears to be influenced by the interaction between the column media and the geotextile amendments. Interestingly, this trend contrasts with findings from other studies, where iron ochre deposits in geotextile and granular filter systems led to a pH decrease, likely due to mild acidification effects (Tophoff et al., 2024). In the present study, however, the iron-modified geotextile may have contributed to a buffering effect or cation exchange reactions that resulted in a slight elevation of pH. This is particularly relevant in the context of phosphorus removal, as elevated pH has been shown to enhance phosphate precipitation. For example, Christensen et al. (2022) reported that phosphorus removal rates exceeded 90% at pH 8.5 after the addition of calcium salts, highlighting the importance of pH control in nutrient treatment processes.

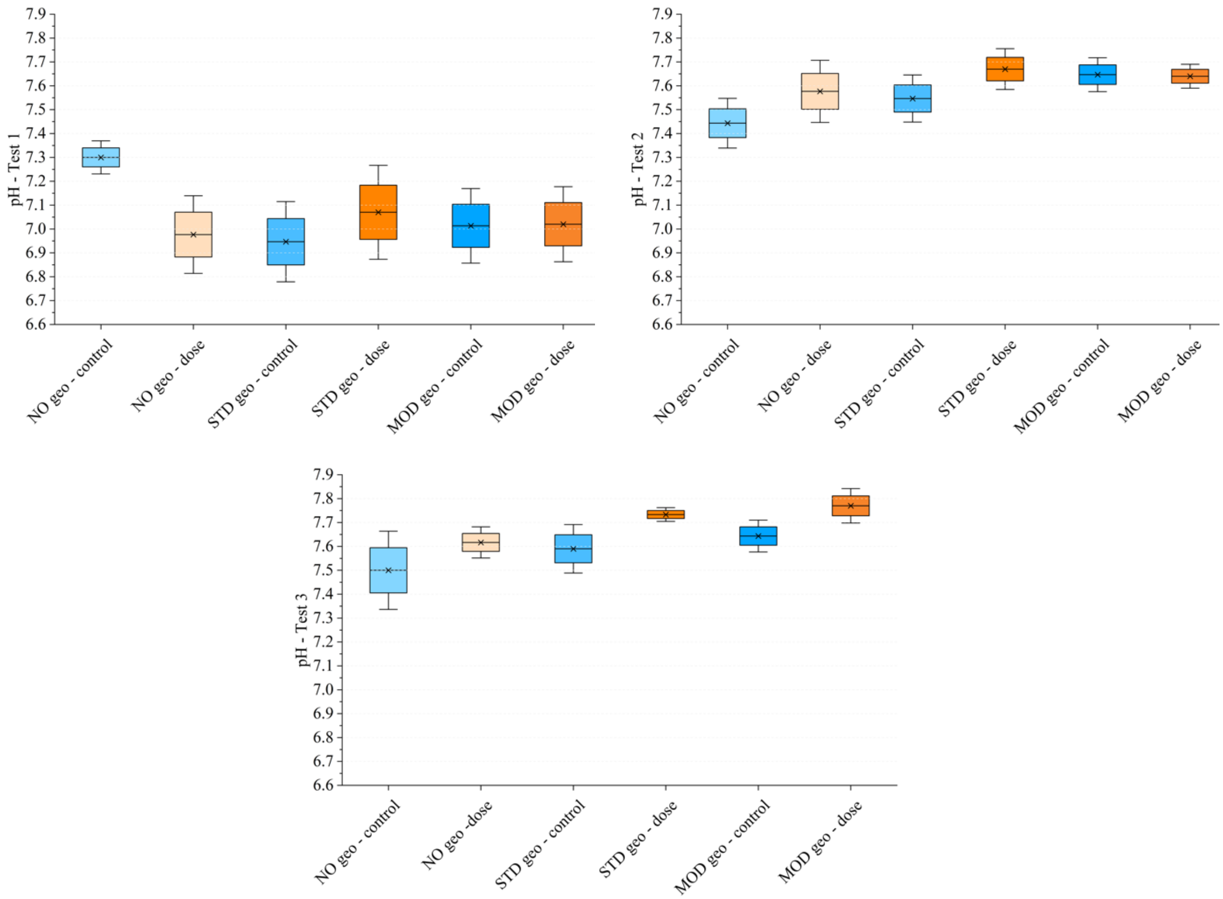

Figure 21. Influent and effluent pH for the dose Tests 1, 2, and 3.

Figure 23 presents the EC results for Test 1, Test 2, and Test 3. In Test 1, the EC of the effluent in the NO geo and STD geo setups was higher than the corresponding influent, indicating a release of ions during passage through the media. However, a reduction was observed in the MOD geotextile columns. The results suggest that all setups exhibited some degree of ionic retention or dilution. In Test 2, EC values were more stable across all configurations, with minimal differences between controls and doses. However, the MOD geo dose group exhibited an increase in variability, with a wider range of EC values and a slightly higher median compared to its control. This anomaly may indicate desorption or release of accumulated ions from the iron-enriched layer during prolonged exposure or under conditions approaching saturation. Despite this, the general similarity of EC levels across treatments suggests that most ions remained in solution without significant uptake or exchange. Test 3 presented greater variability in EC values overall, especially in the NO geo and STD geo configurations. The NO geo dose samples had a particularly wide interquartile range, possibly reflecting greater instability in the media without geotextile control. In contrast, the MOD geo system showed more uniform EC results between control and dose.

Altogether, while the overall EC reductions were not dramatic, the trends observed, support the interpretation that the iron-modified geotextile influenced ion exchange behavior, likely due to specific retention mechanisms. The EC reduction in the MOD geotextile in Tests 1 and 3, may indicate selective retention of specific anions, such as phosphate, through ligand exchange or electrostatic attraction, consistent with mechanisms reported in iron engineered media (Jin et al., 2024; Liu et al., 2022).

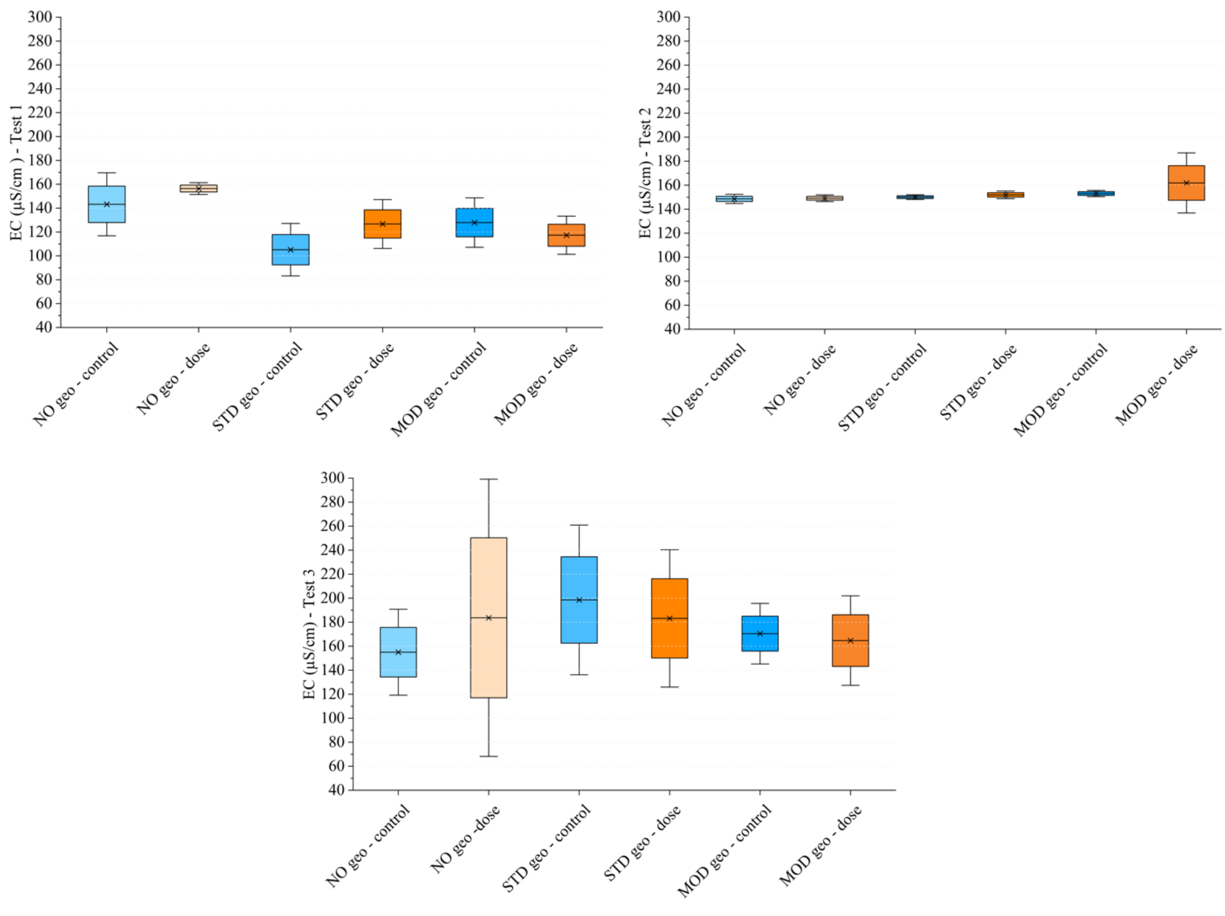

Figure 22. Influent and effluent electrical conductivity (EC) for the dose Tests 1, 2, and 3.

Figure 24 presents the TDS results for Test 1, Test 2, and Test 3. The results for TDS across the three tests followed trends closely aligned with EC, which is expected given their strong correlation. Tests 1 and 2 showed less variability in TDS values across influent and effluent, and across the different columns, compared to Test 3, possibly due to material dissolution or ion release under prolonged or repeated operation.

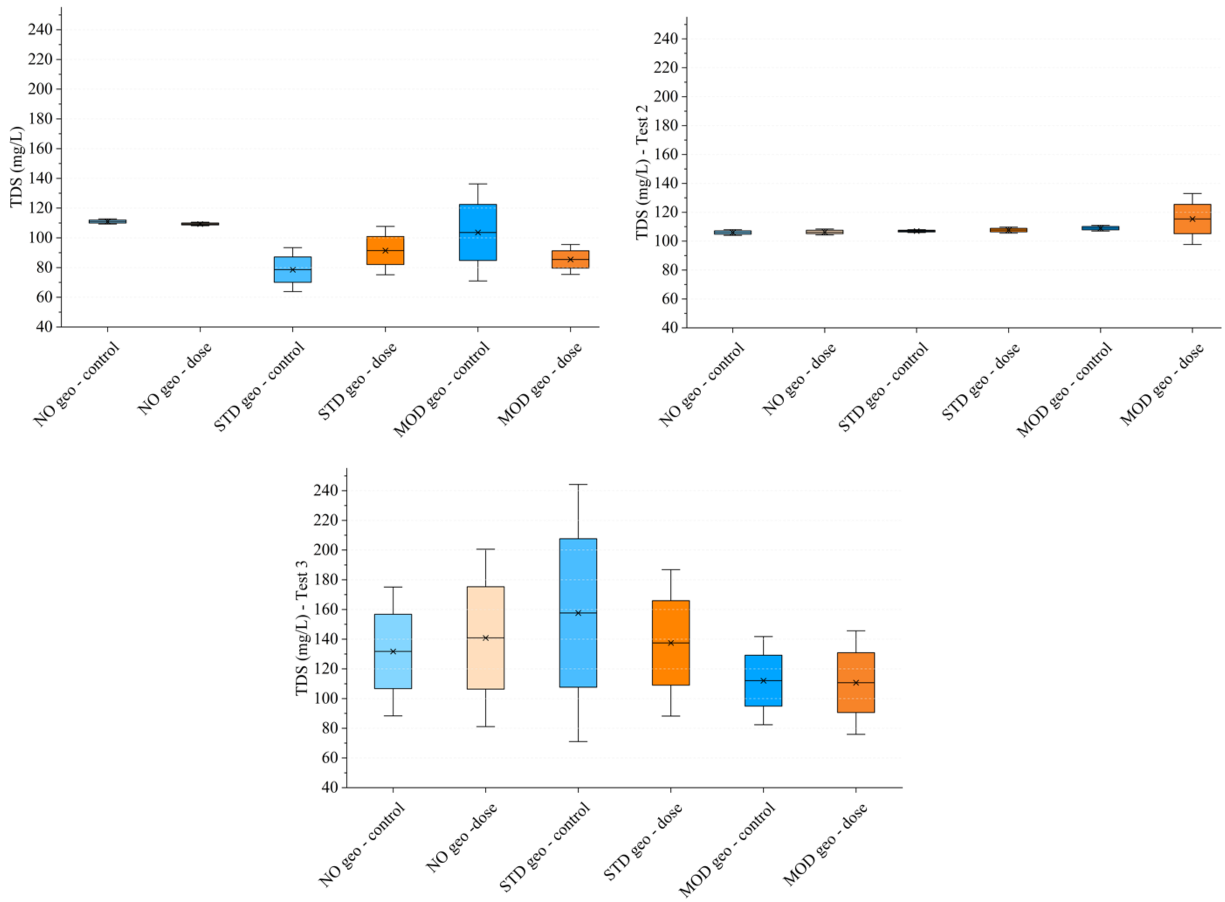

Figure 23 .Influent and effluent total dissolved solids (TDS) for the dose Tests 1, 2, and 3.

Figure 25 presents the temperature results for Test 1, Test 2, and Test 3. Water temperature ranged from 19 to 22.5 °C in Test 1, from 19.5 to 21.5 °C in Test 2, and from 20.2 to 22.5 °C in Test 3. It remained essentially constant across treatments, with values tightly clustered between 20.6 °C and 21.5 °C. Overall, the temperature in the effluent was slightly lower compared to the influent across all tests, probably due the heat loss through the column media.

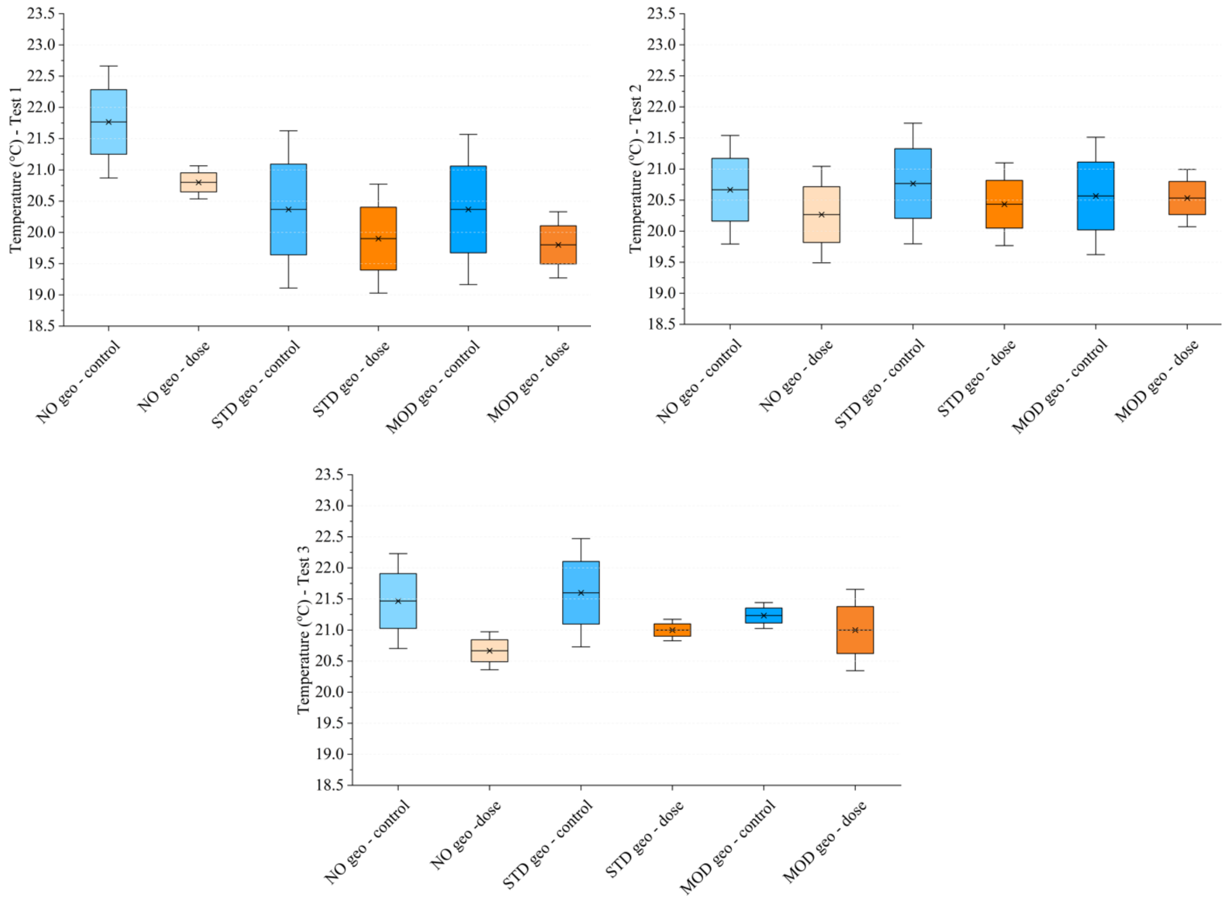

Figure 24 .Influent and effluent temperature for the dose Test 1, 2, and 3.

Figure 26 presents the turbidity results for Test 1, Test 2, and Test 3. Turbidity values across the three dosing tests revealed clear distinctions in performance among the different geotextile configurations. In Test 1, the NO geo condition showed a substantial increase in turbidity from the influent (0.4 NTU) to the effluent (13.5 NTU), indicating significant mobilization of particulates during percolation. In contrast, the STD geo and MOD geo treatments maintained considerably lower effluent turbidity levels, with averages of 2.9 NTU and 2.3 NTU, respectively. In Test 2, turbidity in the effluents also increased compared to the influents, with the highest value observed in the STD geo column, followed by NO geo and MOD geo. Test 3 featured overall lower turbidity across all treatments, with effluent means ranging between 2 and 4.3 NTU, suggesting reduced particulate loading or stabilization of the filter media over time. The increase in turbidity may be related to the disturbance of the media and the flushing of fine particles, trapped dust, or the release of fibers into the effluent.

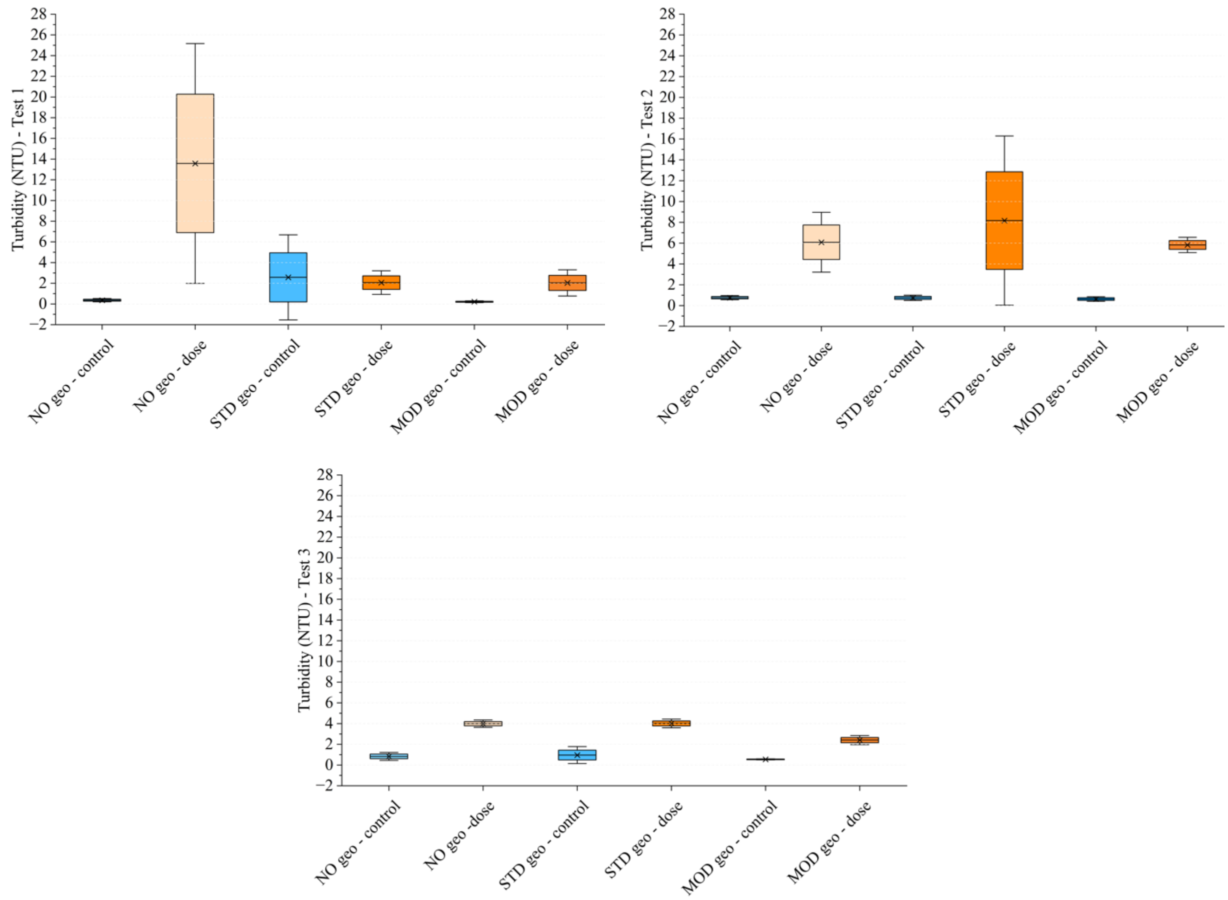

Figure 25: Influent and effluent turbidity for the dose tests 1, 2, and 3.

5.3.2. Performance on Phosphorus and Nitrogen removal

To evaluate the nutrient removal ability of the tested geotextiles, phosphorus and nitrogen levels were measured in the effluent under both blank and dosed conditions. The following sections present the results, starting with the blank tests, which establish a baseline for assessing treatment effectiveness without nutrient dosing.

5.3.2.1. Blank test condition

The blank test offers insight into the media's background behavior and helps identify potential leaching or nutrient interactions before exposing the system to higher loading conditions. In Blank Test 1 (Figs. 27a and 27b), phosphorus removal varied among treatments and over time. MOD geo showed the highest TP removal on Day 6 (~56%), followed closely by STD geo (~55%) on the same day. NO geo removal peaked on Day 3 (~32%), with all treatments demonstrating improved performance over time. These results suggest that some level of conditioning or media activation may have occurred with repeated dosing, particularly in the presence of geotextile.

Nitrogen behavior, however, followed a different trend. NO geo showed high TN removal at Day 0 (~55%), followed by MOD geo (~30%). All treatments experienced a decrease in TN removal over time. STD geo consistently released nitrogen throughout the test, with the lowest value on Day 6 (–20%). MOD geo displayed variable TN performance, with positive values early on but shifting to negative removal by Day 6. These trends suggest that nitrogen leaching from the media or geotextile may have occurred without external nutrient loading, especially after repeated applications.

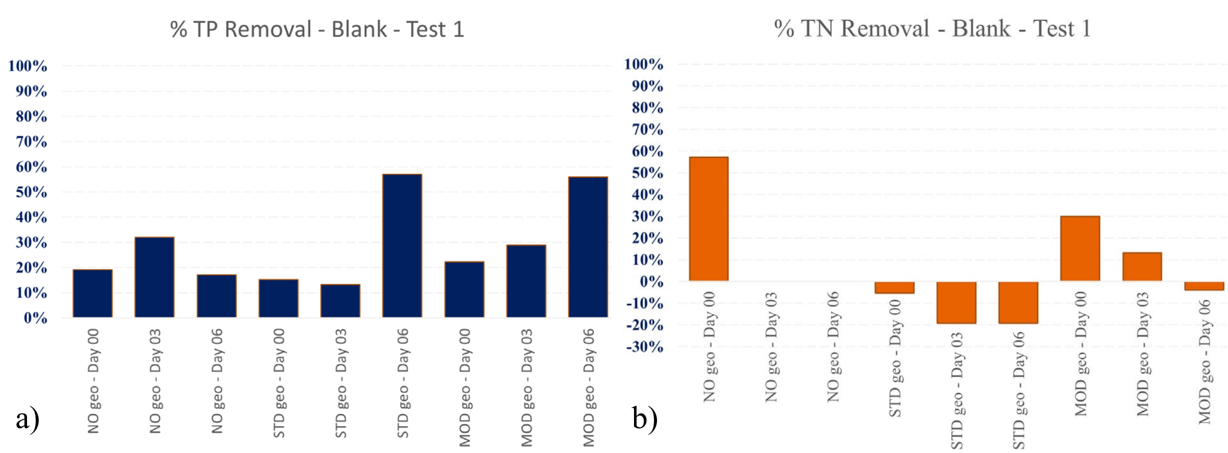

Figure 26. Nutrient removal performance over time for a) total phosphorus (TP) and b)total nitrogen (TN) in Blank Test 1.

In Blank Test 2, only one influent application was used per column. With the same initial concentrations (~0.5 mg/L P and ~0.1 mg/L N), phosphorus removal was lower than in the first test: NO geo achieved 13.8%, STD geo 10.9%, and MOD geo only 1.9%. All treatments again showed net nitrogen release.

These results emphasize the importance of early media stabilization, as initial contact with clean water can promote nitrogen desorption or mobilization from previously saturated or reactive surfaces. The findings indicate that the media and fabrics may release residual nitrogen compounds during initial flushing, and that phosphorus removal was mainly due to the native capacity of the underlying media. This preliminary assessment highlights the need to adjust geotextile installation and layering before conducting tests with synthetic stormwater containing controlled nutrient concentrations.

5.3.2.2. Dose test condition

Phosphorus removal varied notably across treatments and over time in the first dose application (Test 1). NO geo exhibited the highest TP removal, with values increasing from approximately 53% on Day 0 to 58% on Day 3, and decreasing to 39% on Day 6 (Figure 28a). MOD geo showed consistent intermediate performance, with 29% removal on Days 0 and 3, followed by a slight decline to 25% by Day 6. STD geo presented the lowest and most stable values, ranging from 23% to 20% throughout the test. The pronounced performance of NO geo suggests that the native media had available binding sites for phosphate, while the lower removal in treatments with geotextile may be associated with early installation issues. In this initial configuration, geotextile strips allowed water to bypass the fabric and flow through the space between the geotextile and the column wall, reducing contact efficiency. To mitigate this, a second layer of geotextile was added in the following tests to improve water-media interaction.

Nitrogen removal, however, followed a different trend. NO geo started with positive TN removal (~45%) on Day 0 but declined to 20% on Day 3 and showed net nitrogen release (–17%) by Day 6 (Figure 28b). STD geo had poor performance, ranging from 12% removal on Day 0 to –27% by Day 6. MOD geo exhibited variable results, beginning at ~18%, decreasing to 12% on

Day 3, and then becoming negative (–16%) by Day 6. These patterns indicate early-stage leaching of nitrogenous compounds from the media or geotextile, reinforcing the importance of media stabilization before applying synthetic stormwater. These results are consistent with the literature, where initial leaching is often observed in BMPs before stabilization is achieved (Akther et al., 2021; Batalini de Macedo et al., 2021).

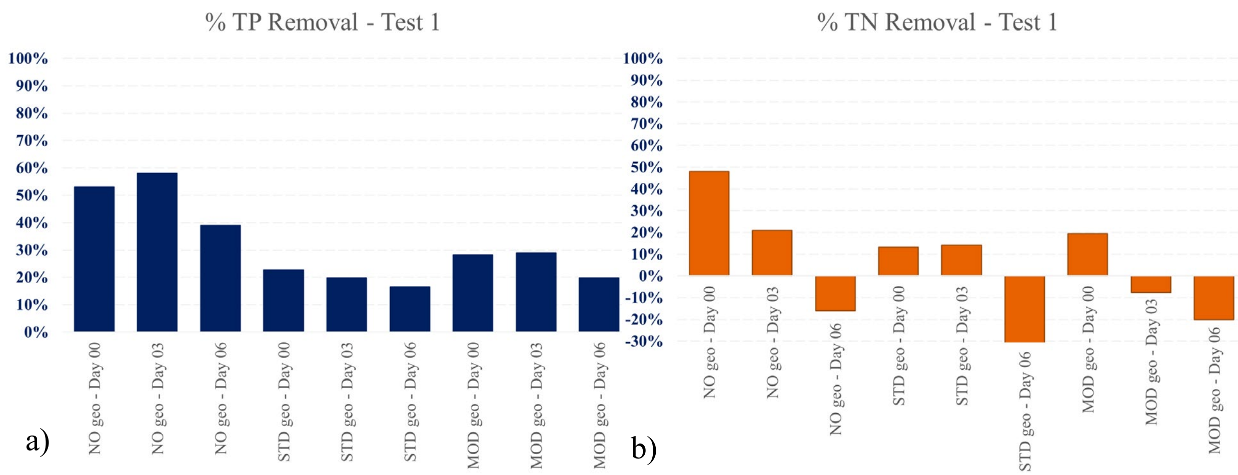

Figure 27. Nutrient removal performance over time for a) total nitrogen (TN) and b) total phosphorus (TP) in Test 1 for NO geo, STD geo, and MOD geo treatments.

In Test 2, after improving the geotextile layering, phosphorus removal efficiency remained significantly different across treatments (Figure 29a). MOD geo demonstrated the highest removal, starting at 49% on Day 0 and maintaining consistent performance at 45% on Day 3 and 42% on Day 6. NO geo followed with 35% removal on Day 0, a slight increase to 37% on Day 3, and a decline to 30% on Day 6. STD geo had the lowest values, ranging from 21% to 28% during the test. The improved performance of MOD geo suggests that the modified material stabilized after the first test, increasing its phosphate-binding capacity, likely due to increased surface affinity and ligand exchange mechanisms, which are dominant in iron-based substrates under slightly acidic to neutral pH conditions (Jin et al., 2024; Liu et al., 2022). The observed consistency also suggests a more effective interaction between the synthetic runoff and the media, likely due to the installation of the second geotextile layer.

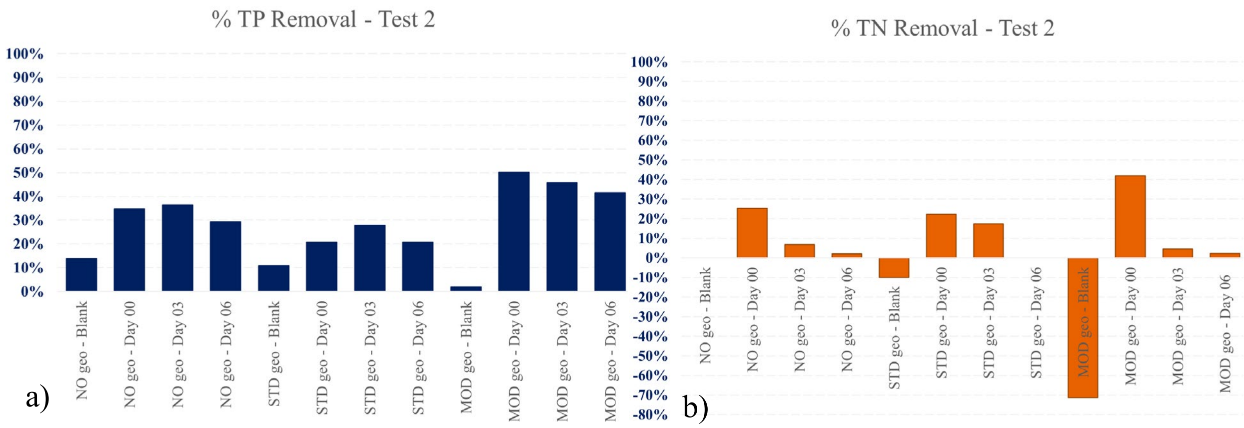

Figure 28. Nutrient removal performance over time for a) total nitrogen (TN) and b) total phosphorus (TP) in Test 2 for NO geo, STD geo, and MOD geo treatments.

For Test 3, phosphorus removal remained highest in the MOD geo treatment, with values of 43% on Day 0 and 3, followed by a decline to 34% on Day 6 (Figure 30a). NO geo started at 26%, peaked at 37% on Day 3, and returned to 26% by Day 6, showing a similar cyclic trend to previous tests. STD geo ranged from 24% on Day 0 to 28% on Day 3, declining to 19% on Day 6. The overall decrease in TP removal in this final test suggests progressive saturation of binding sites, particularly in the standard and unmodified configurations. MOD geo retained superior performance, indicating that the iron-enriched layer continued to provide reactive surfaces for phosphate capture despite repeated dosing. This behavior is consistent with sorption dynamics observed in iron-based media, where adsorption efficiency declines after a critical loading threshold is reached unless regeneration or layer renewal occurs (Ai et al., 2023; Jin et al., 2024).

TN removal in Test 3 showed differences across treatments, although overall values remained low. MOD geo achieved the highest removal, with 18% on Day 0, decreasing to 14% on Day 3 and 10% on Day 6 (Figure 30b). STD geo fluctuated slightly, from 7% to near-zero values across the three days. NO geo, however, showed minimal removal, with negative values on Day 3 (–5%) and near-zero on the other days. These results reflect the limited nitrogen retention capacity of the media and suggest that physical filtration and adsorption alone are not sufficient for TN removal. The improved retention in MOD geo may indicate the gradual establishment of microbial processes or continued filtering by the modified matrix, as seen in other studies where time and conditioning enhance denitrification potential (Kong et al., 2024).

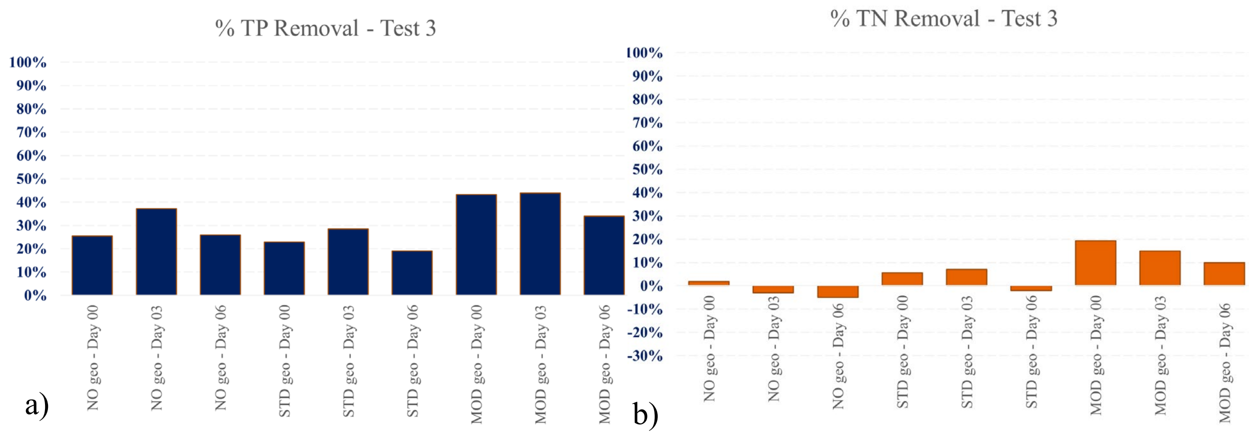

Figure 29. Nutrient removal performance over time for a) total nitrogen (TN) and b) total phosphorus (TP) in Test 3 for NO geo, STD geo, and MOD geo treatments.

5.4 Statistical and Comparative Evaluation

Nutrient removal performance varied notably across treatments and over time. The three column tests were conducted sequentially on the same setup, allowing for the observation of potential reductions in treatment efficiency due to material saturation of removal sites. Comparisons between NO geo, STD geo, and MOD geo treatments revealed differences in both total nitrogen (TN) and total phosphorus (TP) removal across tests.

For TP removal, NO geo showed the highest average TP removal (~50%), while STD and MOD treatments removed approximately 20% and 30%, respectively (Figure 31). One-way ANOVA indicated statistically significant differences between treatments ($p = 0.0031$), with pairwise comparisons confirming that NO geo outperformed both geotextile configurations. For TN removal, efficiency was low across all treatments, with negative values observed for both STD and MOD geotextiles, and no significant differences were detected ($p = 0.5912$). These results suggest that the first test may have primarily flushed out nitrogen rather than promoted its retention, possibly due to initial saturation or mobilization of nitrogen compounds present in the media. It is essential to note that, in this initial test, the geotextile was installed in strips, which allowed water to flow through the space between the geotextile and the inner wall of the column. This may partially explain the lower efficiency observed in the presence of geotextile. To address this issue, an additional geotextile layer was added in subsequent tests to prevent bypass flow and improve contact between the influent and the media.

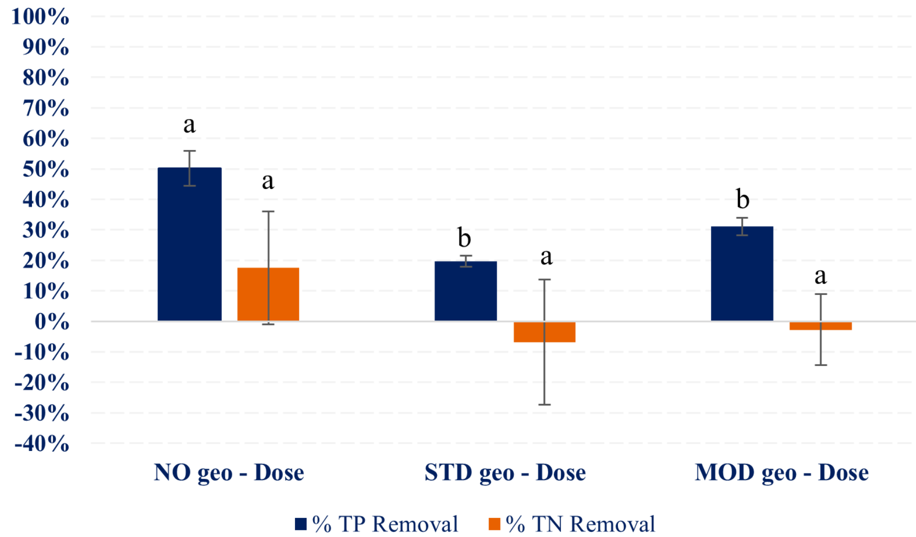

Figure 30. Overall total nitrogen and total phosphorus removal for NO geo, STD geo, and MOD geo treatments in Test 1. Different lowercase letters indicate statistically significant differences between groups ($p < 0.05$).

Adding an extra geotextile layer may have enhanced the contact area and duration between the hybrid geotextile and water. As a result, in Test 2, phosphorus removal still showed a significant difference between treatments ($p = 0.0012$). MOD geo achieved the highest average TP removal (about 46%), followed by NO geo (33%) and STD geo (16%) (Figure 32). The steady performance of MOD geo in this test indicates improved phosphorus retention, possibly due to stabilization of the modified media after initial leaching. For TN, all treatments had low and statistically similar removal efficiencies ($p = 0.9284$), averaging around 13%. These findings suggest that nitrogen removal either was not yet active or had not been significantly affected by the media at this stage.

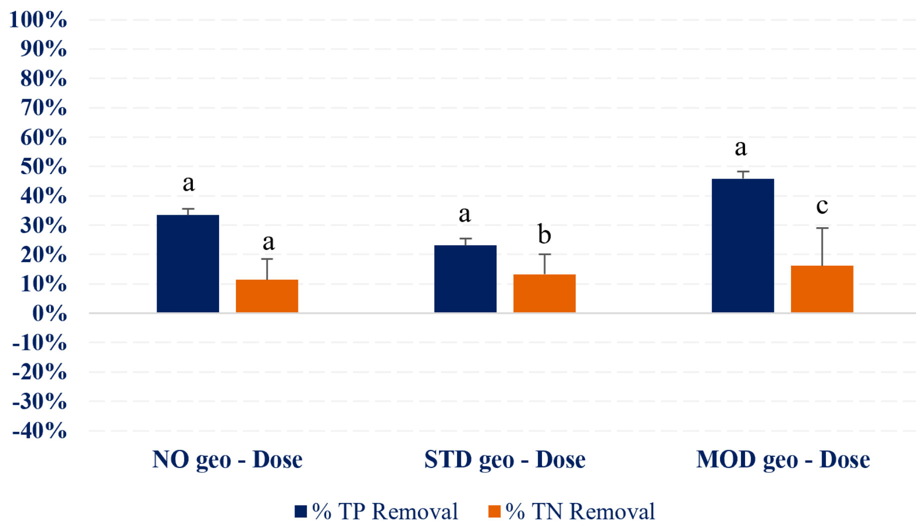

Figure 31. Overall total nitrogen and total phosphorus removal for NO geo, STD geo, and MOD geo treatments in Test 2. Different lowercase letters indicate statistically significant differences between groups ($p < 0.05$).

In Test 3, both TN and TP removal showed statistically significant differences among treatments ($p = 0.0099$ and $p = 0.0308$, respectively, as determined by one-way ANOVA). For TP, MOD geo again exhibited the highest removal (~40%), followed by NO geo (~29%) and STD geo (~24%) (Figure 33). The less pronounced differences in TP removal suggest a partial decline in overall phosphorus retention across the columns, potentially due to the saturation of binding sites after repeated dosing. MOD geo also achieved the highest TN removal (~14%), while NO geo exhibited negative removal, indicating continued leaching of nitrogen from the media. STD geo showed variable performance, with overall TN removal of 4%. The overall significant difference in TN removal suggests that MOD geo developed an improved capacity to retain nitrogen by the third test, potentially due to microbial activity or cumulative filtering effects.

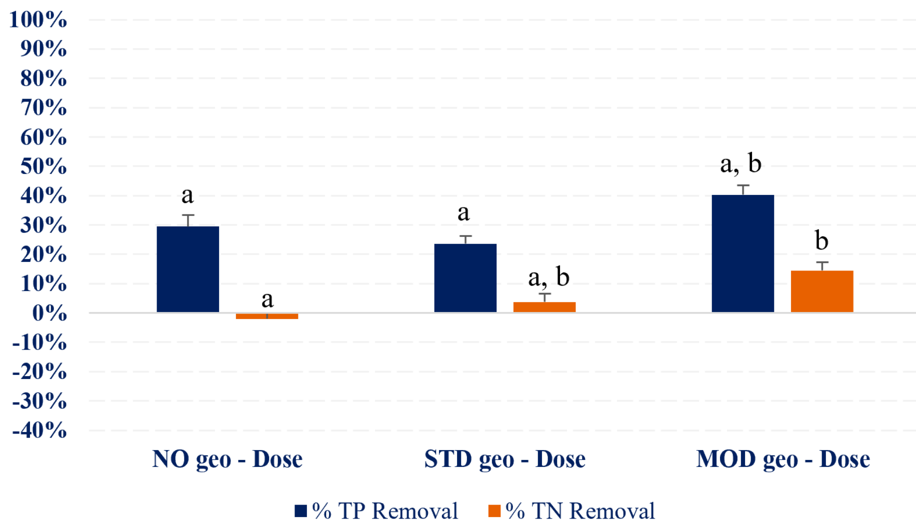

Figure 32. Overall total nitrogen and total phosphorus removal for NO geo, STD geo, and MOD geo treatments in Test 3. Different lowercase letters indicate statistically significant differences between groups ($p < 0.05$).

Phosphorus removal in this system aligns with removal mechanisms widely reported in recent literature. Shin et al. (2023) reported 23 mg/g phosphate adsorption with 90% magnetic separability of the media (carbonaceous adsorbent embedded with metal oxides, including Fe_3O_4 and Fe_2O_3). Similarly, Erickson et al. (2012) demonstrated up to 85% phosphate removal in sand filters amended with 5% iron filings. Ai et al. (2023) further showed that industrial iron shavings achieved over 60% phosphate retention over 60 days without compromising permeability. These findings are consistent with Jin et al. (2024) and Liu et al. (2022), who reviewed iron-based media such as ferrihydrite, goethite, and Fe–Mn oxides and reported adsorption capacities ranging from 4.3 to 33 mg P/g depending on environmental pH, media crystallinity, and competing anions.

Bioretention systems with integrated saturation zones and specialized media generally outperform surface systems, such as the geotextile, in both phosphorus and nitrogen removal. For example, Luo et al. (2020) reported TP removal ranging from 85% to 92% and TN removal between 57% and 74% in their strengthened bioretention column containing zeolite, volcanic rock, and sponge iron. Yang et al. (2021) found similarly high removal efficiencies, 93% for TP, 83% for NO_3^--N, and 78% for NH_4^+-N in a bioretention column system amended with hydroxy-aluminum and iron-modified media. Kong et al. (2024) achieved 80 to 95% TP and 64 to 86% TN removal using a multimedia combination of pyrite, woodchips, and biochar, where each component contributed to targeted pollutant removal through precipitation, denitrification, and adsorption.

These values highlight the superior performance of more complex or saturated BMP designs. However, they also require deeper excavation, plant establishment, long-term maintenance, and in some cases, active flow management to maintain saturated conditions. In contrast, the geotextile examined in this study, while reaching only 30–50% TP removal, was applied at the surface level, required no excavation or structural alteration, and showed no loss in permeability, an advantage noted in other studies evaluating textile-based filters (Tophoff et al., 2024; Tota-Maharaj & Paul, 2015). This makes it especially useful in retrofitting infiltration trenches, roadside swales, or permeable pavements.

Nitrogen removal remains more challenging in geotextile-based systems due to the solubility and mobility of nitrate, as well as the lack of sustained anoxic zones required for denitrification. Initial tests in this study revealed limited TN removal, which improved to less than 20%. Hopkins et al. (2017) found that distributed stormwater systems led to long-term reductions in nitrate export as microbial communities stabilized. Ruiz-Cosgaya et al. (2024) also emphasized the potential for ion-exchange-based columns to remove over 90% of ammonium and phosphate during regenerative cycles in centralized wastewater systems, highlighting the importance of combining chemical and biological processes for sustained nutrient control.

Traditional stormwater BMPs vary significantly in effectiveness. According to Yu et al. (2013), vegetated swales remove only 10–30% of TP and 4.5 to 11.5% of TN, while constructed wetlands achieve over 60% removal of TP. Infiltration trench performance was 23.3% for TP and 23.1% for TN. Barrett (2005) in a comparative review of field systems, noted that nitrate removal occurred in 12 of the 39 storms analyzed in swales; load reduction was also observed in wet basins and extended detention. However, nitrate and orthophosphate were sometimes net released in several BMPs, such as strips. These benchmarks place the hybrid geotextile in the middle to upper range of performance for phosphorus removal, despite its low-profile design and simpler installation.

In conclusion, although the hybrid geotextile does not outperform the most advanced BMPs in terms of nutrient removal efficiency (Table 8), it offers a compelling combination of design flexibility, low maintenance, and modular deployment. Its implementation could serve as an effective enhancement for stormwater retrofits, infiltration trenches, and green infrastructure in space-limited or maintenance-sensitive environments, especially where phosphorus loading is a concern and where integrating deeper media is impractical.

Table 8. Nutrient removal performance by BMP

BMP Type	TP Removal (%)	TN Removal (%)	Reference
Hybrid Geotextile (NO geo) Test 1	50	0	Present Study
Hybrid Geotextile (STD geo) Test 1	20	-5	Present Study
Hybrid Geotextile (MOD geo) Test 1	30	-3	Present Study
Hybrid Geotextile (NO geo) Test 2	33	13	Present Study
Hybrid Geotextile (STD geo) Test 2	16	12	Present Study
Hybrid Geotextile (MOD geo) Test 2	46	14	Present Study
Hybrid Geotextile (NO geo) Test 3	29	-2	Present Study
Hybrid Geotextile (STD geo) Test 3	24	4	Present Study
Hybrid Geotextile (MOD geo) Test 3	40	14	Present Study
Bioretention with Iron/Aluminum Media	85	74	Luo et al., 2020; Yang et al., 2021
Bioretention with Pyrite/Biochar/Woodchip	80	86	Kong et al., 2024
Constructed Wetlands	60	60	Yu et al., 2013
Vegetated Swales	10	4.5	Yu et al., 2013
Infiltration Trenches	23.3	23.1	Yu et al., 2013

5.5. Conclusion

This ongoing study evaluated the nutrient removal performance of an iron-enriched hybrid geotextile in comparison to a standard commercial geotextile and a no-fabric control using laboratory-scale column tests. Under conditions with phosphorus and nitrogen, the modified geotextile consistently demonstrated better phosphorus removal efficiency, exceeding 40% even after repeated loading. These findings support the idea that surface-placed, iron-modified fabrics can enhance phosphate capture at the inflow point, providing a minimally invasive alternative to more complex BMP retrofits. Unlike traditional systems that require deep excavation or vegetation-based uptake, the hybrid geotextile remained effective while maintaining infiltration capacity and minimizing media disturbance.

Nitrogen removal, however, remained a challenge throughout the tests. Although MOD geo achieved some TN retention (~14%) by the third test, earlier trials showed net leaching across all treatments. These findings align with broader studies that highlight the need for carbon supplementation or redox manipulation to support microbial denitrification in stormwater systems. The gradual improvement observed in MOD geo over time suggests that microbial development or media stabilization may enhance nitrogen removal, but further investigation is needed to clarify these mechanisms.

Overall, the results establish a foundation for further development of iron-modified fabrics as an improvement to infiltration-based stormwater systems. Their modularity and efficiency make them ideal for space-limited urban environments. However, the hybrid geotextile should undergo additional testing under different field conditions, and alternative configurations, such as incorporating biochar or carbon amendments, should be explored to enhance nitrogen removal. Additionally, future research should consider the potential of phosphorus recovery, which could become an innovative feature of this hybrid geotextile. The findings here contribute to an expanding body of work aimed at optimizing stormwater BMPs for nutrient control, promoting more resilient and sustainable urban water infrastructure.

6. Concluding Remarks and Perspectives

This thesis explored two major challenges in stormwater management: the emerging concern of tire-derived pollutants such as 6-PPDq and the persistent issue of nutrient pollution in urbanized stormwater runoff. Although these pollutants differ in origin, behavior, and regulatory recognition, both are transported by stormwater runoff and remain insufficiently addressed by conventional infrastructure. In response, this research focused on low-impact, scalable interventions, both nature-based and engineered, to advance decentralized stormwater treatment practices.

To address these challenges, the study was guided by two central research objectives: (1) to evaluate the tolerance and phytoremediation potential of plant species exposed to 6-PPDq, and (2) to assess the effectiveness of modified geotextiles for nutrient removal in BMPs. The first part of the work examined the response of three plant species, *R. hirta*, *R. crispus*, and *T. pratense,* to 6-PPDq exposure across a range of concentrations. Results showed that *R. hirta* maintained high germination rates and biomass production even at elevated concentrations, while *T. pratense* exhibited consistent growth and no significant phytotoxic effects under long-term exposure. These findings represent some of the first evidence of terrestrial plant tolerance to 6-PPDq and help fill a critical knowledge gap in its potential phytoremediation. This insight is particularly relevant to vegetated BMPs, where plant species are often selected for aesthetics or climate resilience rather than contaminant tolerance. As 6-PPDq gains increasing regulatory scrutiny, such as its inclusion on the USEPA's Contaminant Candidate List, incorporating tolerant species into green infrastructure may offer a cost-effective and ecologically beneficial mitigation strategy.

The second part of the thesis examined the role of geotextile materials in enhancing nutrient removal within infiltration systems. By incorporating an iron-modified nonwoven fabric into column setups, the study demonstrated improvements in phosphorus retention compared to standard and unmodified designs. Therefore, the application of functionalized geotextiles represents a promising advancement in BMP design, enabling multifunctional infrastructure that offers both structural support and water quality treatment. In addition, these materials can be integrated into existing systems or utilized in space-limited urban areas to enhance the performance of traditional BMPs.

This research underscores the value of integrated, adaptable, and low-maintenance strategies in urban runoff management. The combined use of tolerant vegetation and engineered filtration fabrics illustrates how relatively small design modifications can generate meaningful improvements in stormwater runoff treatment. From a regulatory perspective, these solutions align with federal and state-level initiatives promoting green infrastructure and pollutant load reduction.

Future research should build upon these findings by:

- Expanding phytotoxicity studies to include uptake, translocation to the leaves, bioaccumulation, and transformation pathways for 6-PPDq and similar contaminants;
- Investigating long-term geotextile performance, including saturation thresholds and regeneration potential;
- Testing the combined application of vegetation and functionalized materials under real-world stormwater flow conditions.

7. References

ADEM, Alabama Cooperative Extension System, & Auburn University. (2014). *Low Impact Development Handbook for the State of Alabama.* https://adem.alabama.gov

Ai, H., Zhang, K., Penn, C. J., & Zhang, H. (2023). Phosphate removal by low-cost industrial byproduct iron shavings: Efficacy and longevity. *Water Res*, *246*, 120745. https://doi.org/10.1016/j.watres.2023.120745

Akther, M., He, J., Chu, A., & van Duin, B. (2021). Nutrient leaching behavior of green roofs: Laboratory and field investigations. *Sci Total Environ*, *754*, 141841. https://doi.org/10.1016/j.scitotenv.2020.141841

Ali, W., Takaijudin, H., Yusof, K. W., Osman, M., & Abdurrasheed, A. S. i. (2021). The Common Approaches of Nitrogen Removal in Bioretention System. *Sustainability*, *13*(5). https://doi.org/10.3390/su13052575

Aryal, M. (2024). Phytoremediation strategies for mitigating environmental toxicants. *Heliyon*, *10*(19), e38683. https://doi.org/10.1016/j.heliyon.2024.e38683

Barrett, M. E. (2005). Performance comparison of structural stormwater best management practices. *Water Environ Res*, *77*(1), 78-86. https://doi.org/10.2175/106143005x41654

Batalini de Macedo, M., Pereira de Oliveira, T. R., Halmenschlager Oliveira, T., Nobrega Gomes Junior, M., Teixeira Brasil, J. A., Ambrogi Ferreira do Lago, C., & Mendiondo, E. M. (2021). Evaluating low impact development practices potentials for increasing flood resilience and stormwater reuse through lab-controlled bioretention systems. *Water Sci Technol*, *84*(5), 1103-1124. https://doi.org/10.2166/wst.2021.292

Bodus, B., O'Malley, K., Dieter, G., Gunawardana, C., & McDonald, W. (2024). Review of emerging contaminants in green stormwater infrastructure: Antibiotic resistance genes, microplastics, tire wear particles, PFAS, and temperature. *Sci Total Environ*, *906*, 167195. https://doi.org/10.1016/j.scitotenv.2023.167195

Bohara, K., Timilsina, A., Adhikari, K., Kafle, A., Basyal, S., Joshi, P., & Yadav, A. K. (2024). A mini review on 6PPD quinone: A new threat to aquaculture and fisheries. *Environ Pollut*, *340*(Pt 2), 122828. https://doi.org/10.1016/j.envpol.2023.122828

Botelho, M. T., Militao, G. G., Brinkmann, M., & Umbuzeiro, G. A. (2023). Toxicity and mutagenicity studies of 6PPD-quinone in a marine invertebrate species and bacteria. *Environ Mol Mutagen*, *64*(6), 335-341. https://doi.org/10.1002/em.22560

Brinkmann, M., Montgomery, D., Selinger, S., Miller, J. G. P., Stock, E., Alcaraz, A. J., Challis, J. K., Weber, L., Janz, D., Hecker, M., & Wiseman, S. (2022). Acute Toxicity of the Tire Rubber-Derived Chemical 6PPD-quinone to Four Fishes of Commercial, Cultural, and Ecological Importance. *Environmental Science & Technology Letters*, *9*(4), 333-338. https://doi.org/10.1021/acs.estlett.2c00050

Cai, S., Zhao, X., & Yan, X. (2025). Towards precise nitrogen fertilizer management for sustainable agriculture. *Earth Critical Zone*, *2*. https://doi.org/10.1016/j.ecz.2025.100026

Cakaj, A., Hanć, A., Lisiak-Zielińska, M., Borowiak, K., & Drapikowska, M. (2023). Trifolium pratense and the Heavy Metal Content in Various Urban Areas. *Sustainability*, *15*(9). https://doi.org/10.3390/su15097325

Calarnou, L., Traikia, M., Leremboure, M., Malosse, L., Dronet, S., Delort, A. M., Besse-Hoggan, P., & Eyheraguibel, B. (2023). Assessing biodegradation of roadway particles via complementary mass spectrometry and NMR analyses. *Sci Total Environ*, *900*, 165698. https://doi.org/10.1016/j.scitotenv.2023.165698

Cao, G., Wang, W., Zhang, J., Wu, P., Zhao, X., Yang, Z., Hu, D., & Cai, Z. (2022). New Evidence of Rubber-Derived Quinones in Water, Air, and Soil. *Environ Sci Technol*, *56*(7), 4142-4150. https://doi.org/10.1021/acs.est.1c07376

Cao, G. D., Wang, W., Zhang, J., Wu, P. F., Qiao, H., Li, H. K., Huang, G. F., Yang, Z., & Cai, Z. W. (2023). Occurrence and Fate of Substituted p-Phenylenediamine-Derived Quinones in Hong Kong Wastewater Treatment Plants. *Environmental Science & Technology*, *57*(41), 15635-15643. https://doi.org/10.1021/acs.est.3c03758

Castan, S., Sherman, A., Peng, R. T., Zumstein, M. T., Wanek, W., Hüffer, T., & Hofmann, T. (2023). Uptake, Metabolism, and Accumulation of Tire Wear Particle-Derived Compounds in Lettuce. *Environmental Science & Technology*, *57*(1), 168-178. https://doi.org/10.1021/acs.est.2c05660

CDC, U. S. Center for Disease Control aand Prevention (2024). *Summary Report – One Health Harmful Algal Bloom System (OHHABS), United States, 2022*. CDC. https://www.cdc.gov/ohhabs/data/summary-report-united-states-2020.html

Chen, X., He, T., Yang, X., Gan, Y., Qing, X., Wang, J., & Huang, Y. (2023). Analysis, environmental occurrence, fate and potential toxicity of tire wear compounds 6PPD and 6PPD-quinone. *Journal of Hazardous Materials*, *452*, 131245.

Christensen, M. L., Cvitanich, C., Quist-Jensen, C. A., Thau, M., & Malmgren-Hansen, B. (2022). Precipitation and recovery of phosphorus from the wastewater hydrolysis tank. *Sci Total Environ*, *813*, 151875. https://doi.org/10.1016/j.scitotenv.2021.151875

Collins, K. A., Hunt, W. F., & Hathaway, J. M. (2008). Hydrologic and Water Quality Comparison of Four Types of Permeable Pavement and Standard Asphalt in Eastern North Carolina. *Journal of Hydrologic Engineering*, *13*(12), 1146-1157. https://doi.org/https://doi.org/10.1061/(ASCE)1084-0699(2008)13:12(1146)

Cordell, D., Drangert, J.-O., & White, S. (2009). The story of phosphorus: Global food security and food for thought. *Global Environmental Change*, *19*(2), 292-305. https://doi.org/10.1016/j.gloenvcha.2008.10.009

Deng, C., Huang, J., Qi, Y., Chen, D., & Huang, W. (2022). Distribution patterns of rubber tire-related chemicals with particle size in road and indoor parking lot dust. *Sci Total Environ*, *844*, 157144. https://doi.org/10.1016/j.scitotenv.2022.157144

Di, S., Liu, Z., Zhao, H., Li, Y., Qi, P., Wang, Z., Xu, H., Jin, Y., & Wang, X. (2022). Chiral perspective evaluations: Enantioselective hydrolysis of 6PPD and 6PPD-quinone in water and enantioselective toxicity to Gobiocypris rarus and *Oncorhynchus mykiss*. *Environ Int*, *166*, 107374. https://doi.org/10.1016/j.envint.2022.107374

Dixon, S., & Goh, C.-Y. (2022). Tire-driven stormwater toxicity and salmon mortality from 6PPD-quinone. *Trends, Aug*, *28*, 2022-2023.

Dodds, W. K., Bouska, W. W., Eitzmann, J. L., Pilger, T. J., Pitts, K. L., Riley, A. J., & Schloesser, J. T. (2008). Eutrophication of U.S. freshwaters: Analysis of potential economic damages. *Environmental Science & Technology*, *43*(1), 12-19. https://doi.org/10.1021/es801217q

Erickson, A. J., Gulliver, J. S., & Weiss, P. T. (2012). Capturing phosphates with iron enhanced sand filtration. *Water Res*, *46*(9), 3032-3042. https://doi.org/10.1016/j.watres.2012.03.009

Fohet, L., Andanson, J. M., Charbouillot, T., Malosse, L., Leremboure, M., Delor-Jestin, F., & Verney, V. (2023). Time-concentration profiles of tire particle additives and transformation products under natural and artificial aging. *Sci Total Environ*, *859*(Pt 1), 160150. https://doi.org/10.1016/j.scitotenv.2022.160150

Francis, O. P., & Yang, L. (2020). *Stormwater Drainage Design and Best Management Practices With Applications to Roadways and Climate Change*. P. S. R. U. T. Center.

Ge, Y. C., Liu, J. Z., Shi, R. Y., Li, X., Zeb, A., Wang, Q., Wang, J. L., Zhao, Y. X., Yu, M., Yin, C., Xiong, H. X., & Liu, W. T. (2024). Environmental concentrations of 6PPD and 6PPD-Q cause oxidative damage and alter metabolism in *Eichhornia crassipes. Science of the Total Environment*, *951*, 8, Article 175736. https://doi.org/10.1016/j.scitotenv.2024.175736

Georgia DNR, G. D. o. N. R., & EPD, E. P. D. (2016). Georgia Stormwater Management Manual. In *Volume 2: Technical Handbook*.

Giechaskiel, B., Grigoratos, T., Mathissen, M., Quik, J., Tromp, P., Gustafsson, M., Franco, V., & Dilara, P. (2024). Contribution of Road Vehicle Tyre Wear to Microplastics and Ambient Air Pollution. *Sustainability*, *16*(2). https://doi.org/10.3390/su16020522

Grasse, N., Seiwert, B., Massei, R., Scholz, S., Fu, Q., & Reemtsma, T. (2023). Uptake and biotransformation of the tire rubber-derived contaminants 6-PPD and 6-PPD quinone in the zebrafish embryo (Danio rerio). *Environmental Science & Technology*, *57*(41), 15598-15607.

Greer, J. B., Dalsky, E. M., Lane, R. F., & Hansen, J. D. (2023). Tire-Derived Transformation Product 6PPD-Quinone Induces Mortality and Transcriptionally Disrupts Vascular Permeability Pathways in Developing Coho Salmon. *Environ Sci Technol*, *57*(30), 10940-10950. https://doi.org/10.1021/acs.est.3c01040

GSMM. (2016). *Georgia Stormwater Management Manual* (Vol. 2).

Halle, L. L., Palmqvist, A., Kampmann, K., & Khan, F. R. (2020). Ecotoxicology of micronized tire rubber: Past, present, and future considerations. *Sci Total Environ*, *706*, 135694. https://doi.org/10.1016/j.scitotenv.2019.135694

Hammer, Ø., Harper, D. A. T., & Ryan, P. D. (2001). Past: Paleontological Statistics Software Package For Education And Data Analysis. *Palaeontologia Electronica*.

Hiki, K., Asahina, K., Kato, K., Yamagishi, T., Omagari, R., Iwasaki, Y., Watanabe, H., & Yamamoto, H. (2021). Acute Toxicity of a Tire Rubber-Derived Chemical, 6PPD Quinone, to Freshwater Fish and Crustacean Species. *Environmental Science & Technology Letters*, *8*(9), 779-784. https://doi.org/10.1021/acs.estlett.1c00453

Hiki, K., & Yamamoto, H. (2022). Concentration and leachability of N-(1,3-dimethylbutyl)-N'-phenyl-p-phenylenediamine (6PPD) and its quinone transformation product (6PPD-Q) in road dust collected in Tokyo, Japan. *Environ Pollut*, *302*, 119082. https://doi.org/10.1016/j.envpol.2022.119082

Hildebrandt, A., Hu, X., Germeau, H., Gonzalez, M., Yih, F., Rideout, C., & Kolodziej, E. P. (2024). *Evaluation of 6PPD-Quinone Sorption to Treatment Media and Engineered Soil Mixtures*. WA Department of Ecology . https://www.ezview.wa.gov/Portals/_1962/Documents/6ppd-bmp/FINAL%20Ecologyreview%20_Sorption_Report_020324%20(2).pdf

Hopkins, K. G., Loperfido, J. V., Craig, L. S., Noe, G. B., & Hogan, D. M. (2017). Comparison of sediment and nutrient export and runoff characteristics from watersheds with centralized

versus distributed stormwater management. *J Environ Manage*, *203*(Pt 1), 286-298. https://doi.org/10.1016/j.jenvman.2017.07.067
Hu, X., Zhao, H. N., Tian, Z., Peter, K. T., Dodd, M. C., & Kolodziej, E. P. (2023). Chemical characteristics, leaching, and stability of the ubiquitous tire rubber-derived toxicant 6PPD-quinone. *Environ Sci Process Impacts*, *25*(5), 901-911. https://doi.org/10.1039/d3em00047h
Hua, X., Feng, X., Liang, G., Chao, J., & Wang, D. (2023a). Long-term exposure to 6-PPD quinone reduces reproductive capacity by enhancing germline apoptosis associated with activation of both DNA damage and cell corpse engulfment in *Caenorhabditis elegans*. *J Hazard Mater*, *454*, 131495. https://doi.org/10.1016/j.jhazmat.2023.131495
Hua, X., Feng, X., Liang, G., Chao, J., & Wang, D. (2023b). Long-term exposure to tire-derived 6-PPD quinone causes intestinal toxicity by affecting functional state of intestinal barrier in *Caenorhabditis elegans*. *Sci Total Environ*, *861*, 160591. https://doi.org/10.1016/j.scitotenv.2022.160591
Hua, X., & Wang, D. (2023). Tire-rubber related pollutant 6-PPD quinone: A review of its transformation, environmental distribution, bioavailability, and toxicity. *J Hazard Mater*, *459*, 132265. https://doi.org/10.1016/j.jhazmat.2023.132265
Ihenetu, S. C., Xu, Q., Khan, Z. H., Kazmi, S., Ding, J., Sun, Q., & Li, G. (2024). Environmental fate of tire-rubber related pollutants 6PPD and 6PPD-Q: A review. *Environ Res*, *258*, 119492. https://doi.org/10.1016/j.envres.2024.119492
ITRC, Interstate Technology Regulatory Council (2023). *6PPD and 6PPD-Quinone: Overview and Guidance.* ITRC. https://6ppd.itrcweb.org/3-chemical-properties/
Jiang, N., Li, M., Wang, Z., Hao, X., Guo, Z., Guo, J., Zhang, R., Zhang, H., Chen, J., & Geng, N. (2024). P-phenylenediamines (PPDs) and 6PPD-quinone in tunnel PM(2.5): From the perspective of characterization, emission factors, and health risks. *J Hazard Mater*, *480*, 136269. https://doi.org/10.1016/j.jhazmat.2024.136269
Jiang, Y., Wang, C., Ma, L., Gao, T., & Wāng, Y. (2024). Environmental profiles, hazard identification, and toxicological hallmarks of emerging tire rubber-related contaminants 6PPD and 6PPD-quinone. *Environment International*, *187*, 108677.
Jin, X., Guo, J., Hossain, M. F., Lu, J., Lu, Q., Zhou, Y., & Zhou, Y. (2024). Recent advances in the removal and recovery of phosphorus from aqueous solution by metal-based adsorbents: A review. *Resources, Conservation & Recycling*, *204*, 107464. https://doi.org/10.1016/j.resconrec.2024.107464
Johannessen, C., Helm, P., Lashuk, B., Yargeau, V., & Metcalfe, C. D. (2022). The tire wear compounds 6PPD-quinone and 1, 3-diphenylguanidine in an urban watershed. *Archives of environmental contamination and toxicology*, 1-9.
Jurczak, T., Wagner, I., Wojtal-Frankiewicz, A., Frankiewicz, P., Bednarek, A., Łapińska, M., Kaczkowski, Z., & Zalewski, M. (2019). Comprehensive approach to restoring urban recreational reservoirs. Part 1 – Reduction of nutrient loading through low-cost and highly effective ecohydrological measures. *Ecological Engineering*, *131*, 81-98. https://doi.org/10.1016/j.ecoleng.2019.03.006
Keener, B. R., A.R. Diamond, T.W. Barger, L.J. Davenport, P.G. Davison, S.L. Ginzbarg, C.J. Hansen, D.D. Spaulding, J.K. Triplett, and M. Woods. (2025a). *Rudbeckia hirta var. hirta*. University of West Alabama. Retrieved June 10, 2025 from https://www.floraofalabama.org/

Keener, B. R., A.R. Diamond, T.W. Barger, L.J. Davenport, P.G. Davison, S.L. Ginzbarg, C.J. Hansen, D.D. Spaulding, J.K. Triplett, and M. Woods. (2025b). *Rumex crispus*. University of West Alabama.

Keener, B. R., A.R. Diamond, T.W. Barger, L.J. Davenport, P.G. Davison, S.L. Ginzbarg, C.J. Hansen, D.D. Spaulding, J.K. Triplett, and M. Woods. (2025c). *Trifolium pratense*. University of West Alabama.

Klauschies, T., & Isanta-Navarro, J. (2022). The joint effects of salt and 6PPD contamination on a freshwater herbivore. *Sci Total Environ*, *829*, 154675. https://doi.org/10.1016/j.scitotenv.2022.154675

Kole, P. J., Lohr, A. J., Van Belleghem, F., & Ragas, A. M. J. (2017). Wear and Tear of Tyres: A Stealthy Source of Microplastics in the Environment. *Int J Environ Res Public Health*, *14*(10). https://doi.org/10.3390/ijerph14101265

Kolomijeca, A., Parrott, J., Khan, H., Shires, K., Clarence, S., Sullivan, C., Chibwe, L., Sinton, D., & Rochman, C. M. (2020). Increased Temperature and Turbulence Alter the Effects of Leachates from Tire Particles on Fathead Minnow (Pimephales promelas). *Environ Sci Technol*, *54*(3), 1750-1759. https://doi.org/10.1021/acs.est.9b05994

Kong, Z., Song, Y., Xu, M., Yang, Y., Wang, X., Ma, H., Zhi, Y., Shao, Z., Chen, L., Yuan, Y., Liu, F., Xu, Y., Ni, Q., Hu, S., & Chai, H. (2024). Multi-media interaction improves the efficiency and stability of the bioretention system for stormwater runoff treatment. *Water Res*, *250*, 121017. https://doi.org/10.1016/j.watres.2023.121017

Kuo, L. J., Tietsort, J., Bolton, J. L., Gates, J. B., Langness, M., Carey, A., O'Neill, S., & Schultz, I. R. (2025). Analysis of 6PPD-Q in finfish, shellfish, and marine mammal tissues. *Chemosphere*, *379*, 144418. https://doi.org/10.1016/j.chemosphere.2025.144418

Lane, R. F., Kelly L. Smalling, Paul M. Bradley, Justin B. Greer, Stephanie E. Gordon, John D. Hansen, Dana W. Kolpin, Andrew R. Spanjer, & Masoner, J. R. (2024). Tire-derived contaminants 6PPD and 6PPD-Q: Analysis, sample handling, and reconnaissance of United States stream exposures. *Chemosphere*, *363*. https://doi.org/https://doi.org/10.1016/j.chemosphere.2024.142830

Lantin, A., Larsen, L., Vyas, A., Barrett, M., Leisenring, M., Koryto, K., & Pechacek, L. (2019). *Approaches for Determining and Complying with TMDL Requirements Related to Roadway Stormwater Runoff*. https://doi.org/10.17226/25473

Lapointe, M., Rochman, C. M., & Tufenkji, N. (2022). Sustainable strategies to treat urban runoff needed. *Nature Sustainability*, *5*(5), 366-369.

Li, J., & Davis, A. P. (2016). A unified look at phosphorus treatment using bioretention. *Water Research*, *90*, 141-155. https://doi.org/https://doi.org/10.1016/j.watres.2015.12.015

Li, Y., Tang, Y., Wu, Q., He, Y., Liu, Z., Yuan, S., Cheng, Q., Lian, X., Tan, Y., Su, Y., & Chen, Y. (2024). Synergism of nitrogen removal and greenhouse gases emission reduction in pyrite/biochar-based bioretention system coupled with microbial fuel cell: Performance and mechanism. *Journal of Cleaner Production*, *434*, 140420. https://doi.org/https://doi.org/10.1016/j.jclepro.2023.140420

Liu, B., Gai, S., Lan, Y., Cheng, K., & Yang, F. (2022). Metal-based adsorbents for water eutrophication remediation: A review of performances and mechanisms. *Environ Res*, *212*(Pt B), 113353. https://doi.org/10.1016/j.envres.2022.113353

Liu, J., Yu, M., Li, X., Ge, Y., Shi, R., Bao, Y., Liu, J., & Liu, W. (2024). Phytotoxicity of 6PPD and its oxidized product 6PPD ‐ Q on pakchoi (Brassica rapa L. ssp. chinensis). *Land Degradation & Development*.

Liu, J., Yu, M., Shi, R., Ge, Y., Li, J., Zeb, A., Cheng, Z., & Liu, W. (2024). Comparative toxic effect of tire wear particle-derived compounds 6PPD and 6PPD-quinone to Chlorella vulgaris. *Science of the Total Environment*, *951*, 175592. https://doi.org/10.1016/j.scitotenv.2024.175592

Liu, W., Feng, Q., Chen, W., & Deo, R. C. (2020). Stormwater runoff and pollution retention performances of permeable pavements and the effects of structural factors. *Environmental Science and Pollution Research*, *27*(24), 30831-30843. https://doi.org/10.1007/s11356-020-09220-2

Luo, H., Guan, L., Jing, Z., He, B., Cao, X., Zhang, Z., & Tao, M. (2020). Performance Evaluation of Enhanced Bioretention Systems in Removing Dissolved Nutrients in Stormwater Runoff. *Applied Sciences*, *10*(9). https://doi.org/10.3390/app10093148

Maji, U. J., Kim, K., Yeo, I. C., Shim, K. Y., & Jeong, C. B. (2023). Toxicological effects of tire rubber-derived 6PPD-quinone, a species-specific toxicant, and dithiobisbenzanilide (DTBBA) in the marine rotifer Brachionus koreanus. *Mar Pollut Bull*, *192*, 115002. https://doi.org/10.1016/j.marpolbul.2023.115002

Marín, C., El Bachawati, M., & Pérez, G. (2023). The impact of green roofs on urban runoff quality: A review. *Urban Forestry & Urban Greening*, *90*. https://doi.org/10.1016/j.ufug.2023.128138

Marvin, J. T., Passeport, E., & Drake, J. (2020). State-of-the-Art Review of Phosphorus Sorption Amendments in Bioretention Media: A Systematic Literature Review. *Journal of Sustainable Water in the Built Environment*, *6*(1). https://doi.org/10.1061/jswbay.0000893

McIntyre, J. K., Spromberg, J., Cameron, J., Incardona, J. P., Davis, J. W., & Scholz, N. L. (2023). Bioretention filtration prevents acute mortality and reduces chronic toxicity for early life stage coho salmon (*Oncorhynchus kisutch*) episodically exposed to urban stormwater runoff. *Science of the Total Environment*, *902*, 165759. https://doi.org/10.1016/j.scitotenv.2023.165759

Mihalakakou, G., Santamouris, M., Kolokotsa, D., & Synnefa, A. (2023). Green roofs as a nature-based solution for improving urban sustainability: Progress and perspectives. *Renewable and Sustainable Energy Reviews*, *175*, 113172. https://doi.org/10.1016/j.rser.2023.113306

Miles, L. J., & Parker, G. R. (1979). Heavy Metal Interaction for Andropogon scoparius and Rudbeckia hirta Grown on Soil from Urban and Rural Sites with Heavy Metals Additions. *Journal of Environmental Quality*, *8*(4), 443-449. https://doi.org/10.2134/jeq1979.00472425000800040001x

Mitchell, C. J., & Jayakaran, A. D. (2024). Mitigating tire wear particles and tire additive chemicals in stormwater with permeable pavements. *Science of the Total Environment*, *908*, 168236. https://doi.org/10.1016/j.scitotenv.2023.168236

Moazzem, S., Bhuiyan, M., Muthukumaran, S., Fagan, J., & Jegatheesan, V. (2024). A Critical Review of Nature-Based Systems (NbS) to Treat Stormwater in Response to Climate Change and Urbanization. *Current Pollution Reports*, *10*(2), 286-311. https://doi.org/10.1007/s40726-024-00297-8

Monrose, J., Tota-Maharaj, K., & Mwasha, A. (2019). Assessment of the physical characteristics and stormwater effluent quality of permeable pavement systems containing recycled materials. *Road Materials and Pavement Design*, *22*(4), 779-811. https://doi.org/10.1080/14680629.2019.1643397

Mosley, O. E., Gios, E., Close, M., Weaver, L., Daughney, C., & Handley, K. M. (2022). Nitrogen cycling and microbial cooperation in the terrestrial subsurface. *ISME J*, *16*(11), 2561-2573. https://doi.org/10.1038/s41396-022-01300-0

National Academies of Sciences, E., and Medicine. (2019). *Approachs for Determining and Complying with TMDL Requirements Related to Roadway Stormwater*. T. N. A. Press.

Nicomel, N. R., & Li, L. Y. (2023). Review of 6PPD-quinone environmental occurrence, fate, and toxicity in stormwater. *Ecocycles*, *9*(3), 33-46. https://doi.org/10.19040/ecocycles.v9i3.347

Okaikue-Woodi, F. E. K., Cherukumilli, K., & Ray, J. R. (2020). A critical review of contaminant removal by conventional and emerging media for urban stormwater treatment in the United States. *Water Res*, *187*, 116434. https://doi.org/10.1016/j.watres.2020.116434

Paerl, H. W., Gardner, W. S., Havens, K. E., Joyner, A. R., McCarthy, M. J., Newell, S. E., Qin, B., & Scott, J. T. (2016). Mitigating cyanobacterial harmful algal blooms in aquatic ecosystems impacted by climate change and anthropogenic nutrients. *Harmful Algae*, *54*, 213-222. https://doi.org/10.1016/j.hal.2015.09.009

Philibert, D., Stanton, R. S., Tang, C., Stock, N. L., Benfey, T., Pirrung, M., & de Jourdan, B. (2024). The lethal and sublethal impacts of two tire rubber-derived chemicals on brook trout (*Salvelinus fontinalis*) fry and fingerlings. *Chemosphere*, *360*, 142319. https://doi.org/10.1016/j.chemosphere.2024.142319

Pilon-Smits, E. (2005). Phytoremediation. *Annu Rev Plant Biol*, *56*, 15-39. https://doi.org/10.1146/annurev.arplant.56.032604.144214

Pitt, R., Maestre, A., & Clary, J. (2018). *The National Stormwater Quality Database (NSQD), Version 4.02*.

Rauert, C., Charlton, N., Okoffo, E. D., Stanton, R. S., Agua, A. R., Pirrung, M. C., & Thomas, K. V. (2022). Concentrations of Tire Additive Chemicals and Tire Road Wear Particles in an Australian Urban Tributary. *Environ Sci Technol*, *56*(4), 2421-2431. https://doi.org/10.1021/acs.est.1c07451

Razzaghmanesh, M., & Borst, M. (2019). Long-term effects of three types of permeable pavements on nutrient infiltrate concentrations. *Sci Total Environ*, *670*, 893-901. https://doi.org/10.1016/j.scitotenv.2019.03.279

Revitt, D. M., Shutes, R.B.E., Jones, R.H., Forshaw, M., & Winter, B. (2004). The performances of vegetative treatment systems for highway runoff during dry and wet conditions. *Science of the Total Environment*, *334-335*, 261–270. https://doi.org/10.1016/j.scitotenv.2004.04.046

Rodgers, T. F. M., Spraakman, S., Wang, Y. R., Johannessen, C., Scholes, R. C., & Giang, A. (2024). Bioretention Design Modifications Increase the Simulated Capture of Hydrophobic and Hydrophilic Trace Organic Compounds. *Environmental Science & Technology*, *58*(12), 5500-5511. https://doi.org/10.1021/acs.est.3c10375

Rout, S., Abhilash, Meshram, P., & Zhang, P. (2023). A Comprehensive Review on Occurrence and Processing of Phosphate Rock Based Resources- Focus on REEs. *Mineral Processing and Extractive Metallurgy Review*, *45*(4), 368-388. https://doi.org/10.1080/08827508.2022.2161537

Ruiz-Cosgaya, L., Izquierdo, W. A., Martinez-Guijarro, R., Serralta, J., & Barat, R. (2024). Ion exchange columns. A promising technology for nitrogen and phosphorus recovery in the main line of a wastewater treatment plant. *J Environ Manage*, *370*, 122719. https://doi.org/10.1016/j.jenvman.2024.122719

Sarvajayakesavalu, S., Lu, Y., Withers, P. J. A., Pavinato, P. S., Pan, G., & Chareonsudjai, P. (2018). Phosphorus recovery: a need for an integrated approach. *Ecosystem Health and Sustainability*, *4*(2), 48-57. https://doi.org/10.1080/20964129.2018.1460122

Seiwert, B., Nihemaiti, M., Troussier, M., Weyrauch, S., & Reemtsma, T. (2022). Abiotic oxidative transformation of 6-PPD and 6-PPD quinone from tires and occurrence of their products in snow from urban roads and in municipal wastewater. *Water Research*, *212*, Article 118122. https://doi.org/10.1016/j.watres.2022.118122

Sharma, R., Kumar, R., Hajam, Y. A., & Rani, R. (2022). Role of biotechnology in phytoremediation. In M. Y. e. al. (Ed.), *Phytoremediation - Biotechnological Strategies for Promoting Invigorating Environs* (pp. 437-454). Elsevier. https://doi.org/https://doi.org/10.1016/B978-0-323-89874-4.00021-2

Shen, D., Shi, Q., Zhang, J., Sy, N. D., Yates, R., Wang, W., & Gan, J. (2025). Transformations of 6PPD and 6PPD-quinone in soil under redox-driven conditions: Kinetics, product identification, and environmental implications. *Environ Int*, *200*, 109532. https://doi.org/10.1016/j.envint.2025.109532

Sherman, A., Hämmerle, L. E., Ben Mordechay, E., Chefetz, B., Hüffer, T., & Hofmann, T. (2024). Uptake of tire-derived compounds in leafy vegetables and implications for human dietary exposure. *Frontiers in Environmental Science*, *12*, Article 1384506. https://doi.org/10.3389/fenvs.2024.1384506

Shin, J., Kwak, J., Kim, S., Son, C., Lee, Y.-G., Kim, J., Bae, S., Park, Y., Lee, S.-H., & Chon, K. (2023). Highly selective recovery of phosphate ions using a novel carbonaceous adsorbent synthesized via co-pyrolysis of spent coffee grounds and steel slags: A potential phosphatic fertilizer. *Chemical Engineering Journal*, *451*. https://doi.org/10.1016/j.cej.2022.138978

Smith, V. H. (2003). Eutrophication of Freshwater and Coastal Marine Ecosystems: A Global Problem. *Environmental Science & Pollution Research*, *10*(2), 126-139. https://doi.org/10.1065/esor2002.12.142

Sommer, F., Dietze, V., Baum, A., Sauer, J., Gilge, S., Maschowski, C., & Gieré, R. (2018). Tire Abrasion as a Major Source of Microplastics in the Environment. *Aerosol and Air Quality Research*, *18*(8), 2014-2028. https://doi.org/10.4209/aaqr.2018.03.0099

Sousa, B. J. d. O., Filho, H. C. P., Taffarello, D., Souza, F. A. A., Hassanzadeh, E., Mendiondo, E. M., & de Oliveira, P. T. S. (2021). Citizens' viewpoints on stormwater Beneficial Management Practices (BMPs) in Brazil. *Journal of Cleaner Production*, *328*. https://doi.org/10.1016/j.jclepro.2021.129569

Spomer, L. A. (1985). Techniques for measuring plant water. *HortScience*, *20*(6).

Tian, Z., Zhao, H., Peter, K. T., Gonzalez, M., Wetzel, J., Wu, C., Hu, X., Prat, J., Mudrock, E., Hettinger, R., Cortina, A. E., Biswas, R. G., Kock, F. V. C., Soong, R., Jenne, A., Du, B., Hou, F., He, H., Lundeen, R.,…Kolodziej, E. P. (2022). A ubiquitous tire rubber–derived chemical induces acute mortality in coho salmon. *Science*, *371*, 185-189.

Tophoff, L., Finklenburg, B., Schriewer, E.-L., Schüttrumpf, H., & Heimbecher, F. (2024). Assessment of the functionality of geotextile and granular filter systems in hydraulic engineering in case of iron ochre clogging tendency. *Geotextiles and Geomembranes*, *52*(4), 465-478. https://doi.org/10.1016/j.geotexmem.2024.01.002

Tota-Maharaj, K., & Paul, P. (2015). Investigating the influence of geotextile layers as biofilm granular filters to treat stormwater. *Urban Water Journal*, *12*(7), 559-569. https://doi.org/10.1080/1573062x.2014.916726

USDA NRCS, U.S. Department of Agriculture, Natural Resources Conservation Service (2008). *Plant guide: Trifolium pratense L. (Red clover)*. U.S. Department of Agriculture, Natural Resources Conservation Service. Retrieved June 09 from https://plants.usda.gov/plantguide/pdf/pg_trpr2.pdf

USDA NRCS, U.S. Department of Agriculture, Natural Resources Conservation Service (2024a). *Rudbeckia hirta L. blackeyed Susan: Plant profile*. U.S. Department of Agriculture. Retrieved June, 09 from https://plants.usda.gov/plant-profile/RUHI2

USDA NRCS, U.S. Department of Agriculture, Natural Resources Conservation Service (2024b). *Rumex crispus L. – curly dock: Plant profile*. U.S. Department of Agriculture. Retrieved June, 09 from https://plants.usda.gov/plant-profile/RUCR

U.S. Geological Survey. (2023). *Phosphate Rock* (Mineral Commodity Summaries, Issue.

USEPA, United States Environmental Protection Agency (1996). Ecological Effects Test Guidelines. In *OPPTS 850.4200 Seed Germination/Root Elongation Toxicity Test*: EPA.

USEPA, United States Environmental Protection Agency (2012). Ecological Effects Test Guidelines. In *OCSPP 850.4800: Plant Uptake and Translocation Test*: USEPA.

USEPA, United States Environmental Protection Agency (2022). *National Stormwater Calculator (SWC)*. Retrieved from https://www.epa.gov/water-research/national-stormwater-calculator

USEPA, United States Environmental Protection Agency (2024a). *FY 2025-2028 6PPD/6PPD-quinone Action Plan*. USEPA

USEPA, United States Environmental Protection Agency (2024b). *Nonpoint Source - Urban Areas*. USEPA.

USEPA, United States Environmental Protection Agency (2025a). *Green Infrastructure*. Retrieved from https://www.epa.gov/green-infrastructure

USEPA, United States Environmental Protection Agency (2025b). *Nutrient Pollution*. https://www.epa.gov/nutrientpollution

Vangronsveld, J., Herzig, R., Weyens, N., Boulet, J., Adriaensen, K., Ruttens, A., Thewys, T., Vassilev, A., Meers, E., Nehnevajova, E., van der Lelie, D., & Mench, M. (2009). Phytoremediation of contaminated soils and groundwater: lessons from the field. *Environ Sci Pollut Res Int*, *16*(7), 765-794. https://doi.org/10.1007/s11356-009-0213-6

Varshney, S., Gora, A. H., Siriyappagouder, P., Kiron, V., & Olsvik, P. A. (2022). Toxicological effects of 6PPD and 6PPD quinone in zebrafish larvae. *J Hazard Mater*, *424*(Pt C), 127623. https://doi.org/10.1016/j.jhazmat.2021.127623

Wagner, S., Huffer, T., Klockner, P., Wehrhahn, M., Hofmann, T., & Reemtsma, T. (2018). Tire wear particles in the aquatic environment - A review on generation, analysis, occurrence, fate and effects. *Water Res*, *139*, 83-100. https://doi.org/10.1016/j.watres.2018.03.051

Wahdan, S. F. M., Heintz-Buschart, A., Sansupa, C., Tanunchai, B., Wu, Y.-T., Schädler, M., Noll, M., Purahong, W., & Buscot, F. (2021). Targeting the Active Rhizosphere Microbiome of *Trifolium pratense* in Grassland Evidences a Stronger-Than-Expected Belowground Biodiversity-Ecosystem Functioning Link. *Frontiers in Microbiology*, *12*. https://doi.org/10.3389/fmicb.2021.629169

Wan, X., Liang, G., & Wang, D. (2024). Potential human health risk of the emerging environmental contaminant 6-PPD quinone. *Sci Total Environ*, *949*, 175057. https://doi.org/10.1016/j.scitotenv.2024.175057

Wang, C., Huang, C., Zhang, S., Zhang, L., Li, T., Peng, J., & Zhang, L. (2023). Research Progress on Nitrogen and Phosphorus Loss in Small Watersheds: A Regional Review. *Water*, *15*(16). https://doi.org/10.3390/w15162894

Wang, J. X., Zhang, Y., Hu, J., Li, Y. F., Egorovich, K. V., Nikolaevna, P. N., Vasilevich, M. V., Zhang, Z. F., & Tang, Z. H. (2024). Metabolomics combined with physiology reveal how white clover (Trifolium repens L.) respond to 6PPD stress. *Science of the Total Environment*, 176121. https://doi.org/10.1016/j.scitotenv.2024.176121

Withers, P. J. A., Elser, J. J., Hilton, J., Ohtake, H., Schipper, W. J., & van Dijk, K. C. (2015). Greening the global phosphorus cycle: how green chemistry can help achieve planetary P sustainability. *Green Chemistry*, *17*(4), 2087-2099. https://doi.org/10.1039/c4gc02445a

Yamauchi, T., Colmer, T. D., Pedersen, O., & Nakazono, M. (2018). Regulation of Root Traits for Internal Aeration and Tolerance to Soil Waterlogging-Flooding Stress. *Plant Physiol*, *176*(2), 1118-1130. https://doi.org/10.1104/pp.17.01157

Yan, A., Wang, Y., Tan, S. N., Mohd Yusof, M. L., Ghosh, S., & Chen, Z. (2020). Phytoremediation: A Promising Approach for Revegetation of Heavy Metal-Polluted Land. *Frontiers in Plant Science*, *11*. https://doi.org/10.3389/fpls.2020.00359

Yang, R., Zheng-Rong, F., Man-Ying, M., & Xian, L. (2021). Enhancing nitrate and phosphorus removal from stormwater in a fold-flow bioretention system with saturated zones. *Water Sci Technol*, *84*(8), 2079-2092. https://doi.org/10.2166/wst.2021.403

Yang, Y.-Y., & Lusk, M. G. (2018). Nutrients in Urban Stormwater Runoff: Current State of the Science and Potential Mitigation Options. *Current Pollution Reports*, *4*(2), 112-127. https://doi.org/10.1007/s40726-018-0087-7

Yu, H., Luo, L., Wu, B., He, J., Wang, H., Chen, R., Ji, M., Yang, Q., Zeng, G., Wu, W., & Sun, D. (2025). Efficient catalytic degradation and detoxification of 6PPD-quinone by the multifunctional enzyme system of phanerochaete chrysosporium. *J Hazard Mater*, *494*, 138634. https://doi.org/10.1016/j.jhazmat.2025.138634

Yu, J., Yu, H., & Xu, L. (2013). Performance evaluation of various stormwater best management practices. *Environ Sci Pollut Res Int*, *20*(9), 6160-6171. https://doi.org/10.1007/s11356-013-1655-4

Yu, W. Y., Tang, S. Y., Luo, Z. J., Li, Z. R., Zhu, M. H., Yin, H., Thai, P. K., & Niu, J. F. (2024). Degradation and detoxification of 6PPD-quinone in water by ultraviolet-activated peroxymonosulfate: Mechanisms, byproducts, and impact on sediment microbial community. *Water Research*, *263*, Article 122210. https://doi.org/10.1016/j.watres.2024.122210

Zeng, L., Li, Y., Sun, Y., Liu, L. Y., Shen, M., & Du, B. (2023). Widespread Occurrence and Transport of p-Phenylenediamines and Their Quinones in Sediments across Urban Rivers, Estuaries, Coasts, and Deep-Sea Regions. *Environ Sci Technol*, *57*(6), 2393-2403. https://doi.org/10.1021/acs.est.2c07652

Zhang, R., Zhao, S., Liu, X., Thomes, M. W., Bong, C. W., N. D. Samaraweera, D., Priyadarshana, T., Zhong, G., Li, J., & Zhang, G. (2023). Fates of Benzotriazoles, Benzothiazoles, and p-Phenylenediamines in Wastewater Treatment Plants in Malaysia and Sri Lanka. *Acs Es&T Water*, *3*(6), 1630-1640. https://doi.org/10.1021/acsestwater.2c00410

Zhang, Y., Yan, L., Wang, L., Zhang, H., Chen, J., & Geng, N. (2024). A nation-wide study for the occurrence of PPD antioxidants and 6PPD-quinone in road dusts of China. *Sci Total Environ*, *922*, 171393. https://doi.org/10.1016/j.scitotenv.2024.171393

Zhang, Y., Yang, H., Wang, Y., Tang, C., Liu, C. E., Zhao, Y., Li, S., & Duan, C. (2020). Ecological differentiation in Rumex crispus L. natural populations in metal mining areas. *Research Square Platform LLC*. https://dx.doi.org/10.21203/rs.3.rs-15476/v1